Synthesis of Acid Leached Diatomaceous Earth/ Amine-Functionalized Activated Carbon Composite and its Potential Application in Oily Wastewater Treatment

A Full Masters Dissertation submitted in fulfilment of the academic requirements for the Master's Degree in Environmental Sciences in the Faculty of Engineering, Science and Agriculture, Department of Geography and Environmental Sciences, University of Venda.

By

Mabidi Thinawanga Jennifer

(16014691)

Supervisor: Prof. W.M. Gitari

Co-Supervisor: Dr. R Mudzielwana

Co-Supervisor: Dr. O.U. Izevbekhai

Declaration

I, Mabidi Thinawanga Jennifer, hereby declare that "Synthesis of Acid leached Diatomaceous Earth/ Amine Functionalized activated Carbon Composite and its potential application for Oily Wastewater Treatment" is my work in design and execution and it has never been submitted to any other university and that all reference materials and resources have been duly acknowledged.

Full names: Mabidi Thinawanga Jennifer

Signature: …… Date: 12 October 2023 ……

Acknowledgement

Firstly, I would like to thank **God** and my **Ancestors** for making everything possible for me.

I want to convey my honest and sincere appreciation to my supervisors, **Prof. Gitari W.M**, **Dr. Mudzielwana R** and **Dr. Izevbekhai O.U** for their dedicated guidance, facilitation, and solid assistance throughout this study.

I would like to thank my parents from the bottom of my heart**, Mr Thilivhali Reckson Mabidi** and **Mrs Shonisani Letticia Mabidi and** all my siblings (**Mulalo, Nyawasedza, Tshinanne, Muelelwa, Mavhuthu, Mudzunga and Mokgadi Mabidi**) for their moral support, prayers, and words of encouragement. To my partner, **Edzani Khwashaba,** I thank you for all the role you play in my life, and the love and emotional support you give me.

I would also like to thank the financial assistance from **NRF-Sasol Foundation"** and **Prof Gitari's research Incentives.**

Lastly, to my fellow "**Environmental Remediation and Nanoscience Research"** group members for their support and the funny moments we shared, I thank you.

Dedication

This work is dedicated to my parents, siblings and my partner for standing firm by me throughout my studies and for your sacrifice, support, encouragement, and prayers.

Abstract

Due to the expanding worldwide oil exploration, a significant amount of oily wastewater is being produced. Oily wastewater lowers the diversity of aquatic life and plants by changing the structure of aquatic communities and food chains, among other ecological disturbances. Therefore, the overall aim of this project is to synthesize acid-leached diatomaceous earth (DE) and amine-functionalized activated carbon composite adsorbent for the treatment of oily wastewater. Acid leached diatomaceous earth was synthesized by leaching the raw diatomaceous step-wisely in a 120 mL volume of 2.2 M Nitric acid (HNO_3) for three hours on a hotplate set to 60°C at a speed of 300 rpm. Thereafter, the mixture was filtered and the residue was washed with 1.5 L of deionized water. The residue was oven-dried at 50°C for 12 hours. The acid leached DE was then ground with mortar and pestle and then kept in a zip lock bag for further use in oily wastewater treatment. Activated carbon was synthesized from raw macadamia nutshell using of Orthophosphoric acid (H_3PO_4). Response surface methodology was used to determine the optimum conditions for synthesizing activated where 3 parameters (activation time, impregnation ratio, and activation temperature) were varied. Furthermore, 13 runs were completed at diverse conditions from the response surface methodology. To modify the synthesized activated carbon, hydroxylamine hydrochloride was used as a chemical agent to enhance the adsorption efficiency on the surface of the activated carbon and the amine-functionalized activated carbon was used in the removal of oil from oily wastewater. Lastly, a composite was prepared using both the synthesized acid leached diatomaceous earth and amine functionalized activated carbon and further evaluate its adsorption capacity and oil removal efficiency. All the synthesized adsorbents were applied in oily wastewater treatment and response surface methodology was used to optimize the variable parameters (adsorbent dosage, initial oil concentration and contact time) and to determine the optimum conditions for the oil removal efficiency. Therefore, this study was divided into 3 sections of results as discussed below.

The first section of results is focused on the preparation of acid leached diatomaceous earth and its application in oily wastewater treatment. The results showed that acid treatment does not alter the physical structure of the diatomaceous earth significantly although there was an increase of silica content, its surface area, and pore volume from 78.98 to 91.57%, 15.02 to 22.40 m^2/g, and 60.88 to 68.71 Å, respectively. The maximum adsorption capacity of 124.16 mg/g and oil removal efficiency of 78.55% were achieved at initial oil concentration of 3229.69 using 0.05 g adsorbent dosage and 119.20 mins contact time. The adsorption kinetics data fitted

better to pseudo-second order model (R^2=0.98) of reaction kinetics indicating that adsorption occurred through chemisorption. The adsorption isotherms were descried better by the Freundlich isotherms model (R^2=0.87) indicating that adsorption occurred in a heterogeneous and multilayer surface.

The second section focused on the synthesis of amine functionalized activated carbon for oily wastewater treatment. Activated carbon was prepared from macadamia nutshells (MNS) using H_3PO_4 as activating agent and further modified with amine groups using hydroxylamine hydrochloride. Amine-functionalization increases the adsorption capacity and removal efficiency due to expansion of the adsorbent's particles. The oil removal experiment using amine-functionalized activated carbon showed a maximum percentage removal of 82.93% with adsorption capacity of 167.96 mg/g when initial oil concentration of 10 000 mg/L, adsorbent dosage of 0.1 g adsorbent dosage and contact time of 60 mins were used. The adsorption kinetics data fitted to pseudo-second order model (R^2=0.92) of reaction kinetics indicating that adsorption occurred via chemisorption. The adsorption isotherm data fitted Freundlich adsorption isotherms (R^2=1) model indicating that adsorption took place on heterogeneous and multilayer surface.

The last section of the study focused on the preparation of the acid leached diatomaceous earth/amine-functionalized activated carbon composite adsorbent and its application in treatment oily wastewater. Due to challenges associated with synthesizing an ideal adsorbent for oily wastewater treatment, this composite adsorbent was synthesized to overcome the activated carbon drawbacks which include low thermal conductivity affecting the regeneration efficiency leading to a reduced adsorption capacity after being used for a certain period. Consequently, the advantages of the diatomaceous earth which include excellent heat resistance and its high porosity can improve the physicochemical properties such as surface area and thermal conductivity on the composite adsorbent. The SEM micrographs showed the presence of pores and rough surface with some particles of varying sizes on the surface of the composite material due to the addition of some functional groups which allowed the transfer of the oil molecules into the inner surface of the composite adsorbent. The prepared composite adsorbent showed a maximum oil removal percentage of 90.02% with maximum adsorption capacity of 416.67 mg/g at initial oil concentration of 5250 mg/L, an adsorbent dosage of 0.3 g, and contact time of 60 mins. The adsorption kinetics data showed a better fit to the pseudo-second order model (R^2=0.98) showing that adsorption took place via chemisorption.

Freundlich adsorption isotherm model descried the adsorption better showing that adsorption occurred on a heterogeneous and multilayer surface.

Based on these findings, both materials prepared in this study has potential for use in treatment of oily wastewater. However, the composite displayed higher affinity towards treatment of oily wastewater compared to the acid leached diatomaceous earth and amine-functionalized activated carbon. Based on the conclusions, the main recommendations made from this study were to: 1) test the feasibility of adsorbent in field application and 2) conduct the cost-benefit analysis for this adsorbent.

Keywords: *Activated Carbon; Acid leached diatomaceous earth; Diatomaceous Earth, Composite; Functionalization; Macadamia Nutshells; Oily Wastewater treatment.*

Academic Output

Conference presentation:

- **Jennifer T. Mabidi**, Wilson M. Gitari, Rabelani Mudzielwana, Oisaemi U. Izevbekhai, and Ayinde W. Babatunde, **Preparation and Characterization of Acid Leached Diatomaceous Earth for Application in Treatment of Oily Wastewater.** The 23rd WaterNet/WARFSA/GWP-SA on Integrated Water Resources Management for Sustainable Development in Eastern and Southern Africa. 19th -21st of October 2022, Sun City Resort, North West, South Africa. Oral Presentation.

Submitted review:

- **Jennifer T. Mabidi**, Wilson M. Gitari, Rabelani Mudzielwana and Oisaemi U. Izevbekhai, and Ayinde W. Babatunde, **Preparation and Characterization of Acid Leached Diatomaceous Earth for Application in Treatment of Oily Wastewater.** Journal of Physics and Chemistry of the Earth. Status: **Under Review.**

Manuscripts to be prepared:

- **Jennifer T. Mabidi**, Wilson M. Gitari, Rabelani Mudzielwana and Oisaemi U. Izevbekhai, **Preparation of amine-functionalized macadamia nutshell derived activated carbon for the treatment of oily Wastewater.**
- **Jennifer T. Mabidi**, Wilson M. Gitari, Rabelani Mudzielwana and Oisaemi U. Izevbekhai **Preparation and Characterization of Acid Leached Diatomaceous Earth and Amine-Functionalized Activated Carbon Composite Adsorbent for Application in Treatment of Oily Wastewater.**

Table of Contents

List of Figures

List of Tables

Chapter 1: INTRODUCTION

1.1. Background

Water is a valuable resource to human and other living organisms (Mohammed & Tanweer, 2018). However, owing to anthropogenic activities, producing potable water for domestic use has become a difficult task in various parts of the world. Industrialization, oil exploration, and agricultural activities are the main anthropogenic activities affecting water quality through discharging various pollutants such as oils, solvents, fungicides, antibiotics, and herbicides into water bodies (Firdous et al., 2018, Zhou et al., 2018).

Oily wastewater is wastewater that contains various types and concentrations of oils including hydrocarbons, petroleum fractions (e.g., kerosene, gasoline, and diesel oil), and lipids (Sanaa et al., 2015). Surface waters and groundwater resources are contaminated by oils through the discharge of industrial oily wastewater into aquatic ecosystems. Whereas human and aquatic resources may be endangered by oily wastewater, the atmospheric environment and natural landscapes can also suffer the same fate (Huang et al., 2018). Several techniques have been used for the removal of oil pollutants from wastewater prior to these pollutants entering and contaminating water bodies. These techniques include but are not limited to electrochemical enhanced oxidation techniques and membrane filtration (Dickhout et al., 2017, Moreira et al., 2017), reverse osmosis (Makisha, 2020), coagulation-flocculation (Zhao et al., 2020), evaporation (Han et al., 2019), ion exchange (Comstock and Boyer, 2014), and adsorption (Sohaimi et al., 2017).

Owing to their outstanding properties including simplicity of design, low start-up costs, ease of operation, superior contaminant-removal efficiency, and sensitivity to lethal contaminants, adsorption-based techniques have attracted attention for the treatment of oily wastewaters (Danish et al., 2016, Kuyukina et al., 2020). To this end, several adsorbents such as rice husk (Angelova et al., 2011), sawdust (Ismail, 2015), sugar cane bagasse (Samsuir et al., 2016), and vegetable fibres (Annunciado et al., 2005), fly ash (Agarwal et al., 2020), activated carbon (Anifa et al., 2022) and diatomaceous earth (Bandura et al., 2017) have been used for the treatment of oily wastewaters. Highly porous activated carbon produced by heating agricultural waste under inert conditions has gained specific attention owing to its superior adsorption efficiency (Gummas & Okpeke, 2015). Moreover, addition of oxidizing agents or other chemicals during preparation of activated carbon has enabled the generation of a very fine

powdery form of this material leading to a further improvement of its physicochemical properties and enhancement of its adsorption efficiency (Omri, 2002, Djilani et al., 2015).

At the same time, the application of activated carbon in adsorption is limited by its heat conductivity (Fu et al., 2020). Since adsorption is a thermodynamic process, the heat generated during this process is not quickly dissipated making the adsorbent to overheat and thus affect its performance (Su et al., 2012). Consequently, activated carbon-based adsorbents have lower rate of regeneration, making them unsuitable for industrial application (Pan et al., 2011). When activated carbon is not properly recycled, its adsorption capability is significantly reduced over time eventually resulting in the activated carbon being transformed into solid waste with inevitable potential for secondary environmental pollution (Zhang et al., 2016). In addition, the absence of active functional groups serves as surface-based adsorption sites of carbon-based adsorbents. In the end, the absence of the requisite functional groups negatively impacts the stability of the adsorption process (Liu et al., 2022). Functional groups such as amines can therefore be used to alter the surface of activated carbon with a view to amplify its potential for adsorption (Lekene et al., 2021). Owing to their strong affinity for toxicants, amine groups are frequently used as effective functional groups for removing contaminants from water (Yang et al., 2022).

Diatomaceous earth (also called diatomite) is a siliceous sedimentary rock that contains between 80 and 90% amorphous hydrated silica ($SiO_2.nH_2O$) and impurities such as clay minerals, iron oxides, carbonate minerals, silica sand, and organic matter (Akafu et al., 2019). The presence of impurities in the diatomaceous earth affects the uptake of toxicants from aqueous solutions thus resulting in low adsorption capacity of the diatomaceous earth towards the toxicant (Bello et al., 2014). As a result, Abdellaoui et al. (2018) acid leached diatomaceous earth with nitric acid to eliminate Ca, Mg and Fe impurities. Acid leaching is known to increase the pore diameters and surface area of the diatomaceous earth, leading to an improvement of the adsorption of the material. Furthermore, acid-leached diatomaceous earth has excellent heat resistance which is directly linked to its physical structure (Benkacem et al., 2018, Aivalioti et al., 2010, Bandura et al., 2017).

Therefore, it is envisaged that blending acid-leached diatomaceous earth with amine-functionalized activated carbon will yield an adsorbent with improved adsorption effectiveness and regeneration potential. The improved properties of the new adsorbent stem largely from the combined physicochemical properties of the activated carbon (i.e., large

sorption capacity and high porosity) and the diatomaceous earth (i.e., excellent heat resistance). In this study, a composite adsorbent composed of acid-leached diatomaceous earth and amine-functionalized activated carbon will be fabricated before its adsorption capacity and removal efficiency for oil is evaluated.

1.2. Problem statement

The rapid growth in global oil pollution caused by industrial development in the shipping, petrochemical, oil and gas, pharmaceutical and food industries is an increasingly serious environmental problem (Jernelov, 2010). Oily wastewater generated by these industries contain toxic substances that have the potential to change the structure of aquatic communities and food chains, among other ecological disturbances (Kuwahara et al., 2010). For instance, toxins and carcinogens that accumulate at the base of the food chain that are consumed by humans have a serious adverse impact on human health. Furthermore, atmospheric pollution through evaporation of oil, gas and hydrocarbons coupled with spillages of oil containing hazardous elements have negative effects on the immediate environment (Han et al., 2019).

To reduce the impact of oily wastewaters on the environment and ecosystem at large, it is important to develop technologies that are capable of effective treatment of these wastewaters prior to discharge into water bodies and/or the environment (Ardejani et al., 2007). The challenge faced by many researchers involves synthesizing oily wastewater treatment materials that are effective in terms of cost of production and oil removal efficiency. Activated carbon appears to be a cheaper and effective material for use in adsorption of oils since it is prepared from readily available biomass such as macadamia nutshells (Musapatika, 2010), rice husks (Vlaev et al., 2011) and banana peels (Tripathy et al., 2021), amongst others. However, a need still exists to address the problems associated with activated carbon, namely lack of adequate regeneration and disposal options as well as secondary pollution emanating from the use of such materials (Zhang et al., 2016, Musapatika, 2010). It suffices to say that regeneration and disposal of the adsorbent have a direct bearing on the cost of the adsorbent.

In a quest to address the cost and regeneration problems associated with commercial activated carbon, this project sought to develop more stable activated carbon based-adsorbent by synthesizing acid-leached diatomaceous earth-amine-functionalized activated carbon composite for application in the treatment of oily wastewater. Activated carbon was synthesized from macadamia nutshells. South Africa is the leading macadamia nut producer in the world, with over 700 macadamia nut farmers mostly located in Limpopo, Mpumalanga and

KwaZulu-Natal provinces and sprinkle of growers also found in the Eastern and Western Cape. macadamia nutshells are regarded as an abundant agricultural waste in the country (SAMAC, 2023).

1.3. Aims and objectives

The aim of this study is to synthesize acid-leached diatomaceous-amine-functionalized activated carbon composite adsorbent for application in treatment of oily wastewater.

To accomplish the aim of this study, the following specific objectives were pursued:

- Prepare and characterize acid-leached diatomaceous earth for application in treatment of oily wastewater.
- Prepare and characterize amine-functionalized macadamia nutshell-derived activated carbon for the treatment of oily wastewater.
- Prepare and characterize acid-leached diatomaceous earth-amine-functionalized activated carbon composite for application in the treatment of oily wastewater and further evaluate the regeneration potential of the synthesized composite.

1.4. Significance of the study

In light of South Africa being the leading producer of macadamia nuts in the world, this study will contribute towards reducing the environmental load arising from the disposal of macadamia nutshell wastes in the country (Poinern et al., 2011). Furthermore, this study will also contribute meaningful technical and research knowledge for developing advanced and cost-effective technologies for the removal of contaminants from oily wastewater streams. It is envisaged that such endeavours will lead to improved water quality and production of safer drinking water. According to DWAF (1998), the National Water Act (NWA; Act 36 of 1998) requires that water is protected, used, conserved, developed, managed, and controlled sustainably and equitably for the benefit of all persons. Lastly, this study will promote the Sustainable Development Goals (SDGs), goal 6 which calls for clean water and sanitation, thus ensuring availability and sustainable management of water, and sanitation for all" (UNDP, 2015). SDG 6 includes eight targets with target 6.3 involving the treatment and reuse of wastewater, and ambient water quality.

1.5. Dissertation layout

The structure of this dissertation is illustrated in Figure 1.1.

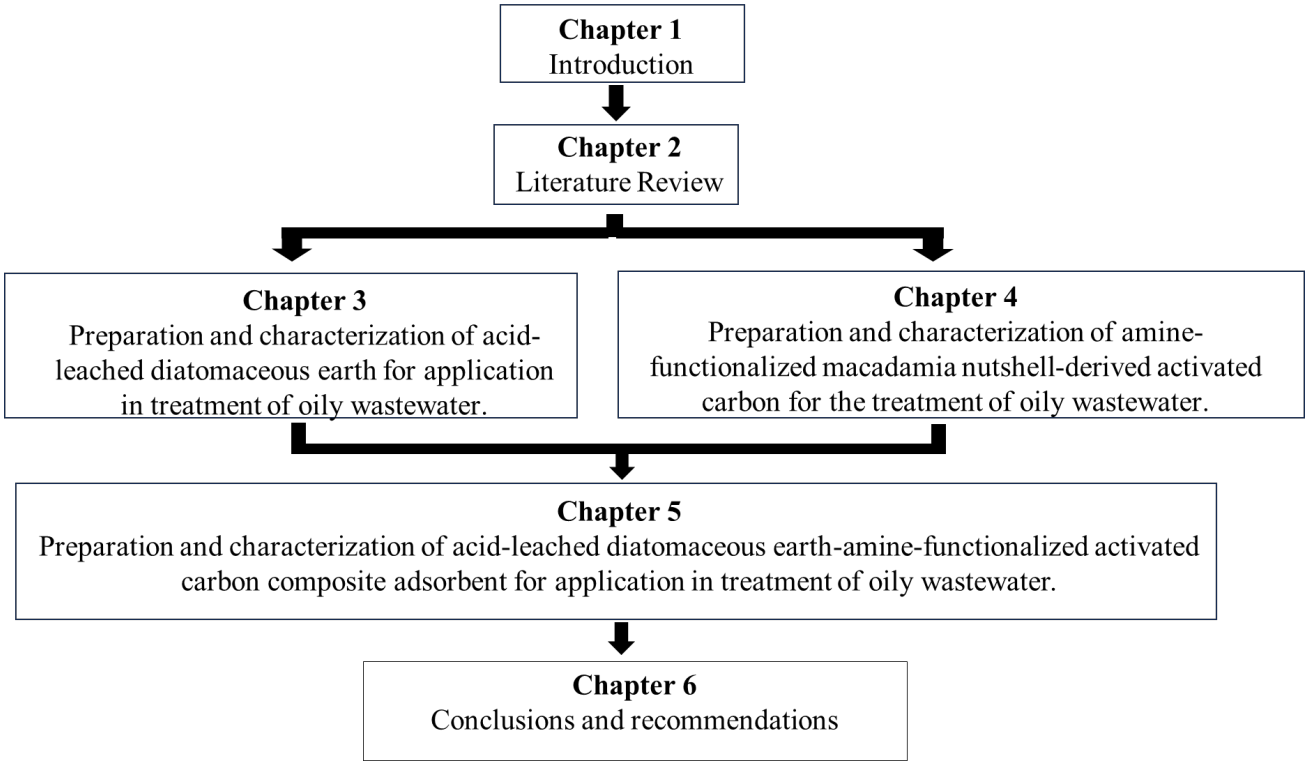

Figure 1.1: An illustration of the layout of the dissertation.

References

Abdellaoui, I., Islam, M. M., Sakurai, T., Hamzaoui, S & Akimoto, K. 2018. Impurities removal process for high-purity silica production from diatomite. *Hydrometallurgy,* 179, 207-214.

Agarwal, A., Samanta, A., Nandi, B. K & Mandal, A. (2020). Synthesis, characterization and performance studies of kaolin-fly ash-based membranes for microfiltration of oily waste water. *Journal of Petroleum Science and Engineering*, *194*, 107475.

Aivalioti, M., Vamvasakis, I & Gidarakos, E. 2010. Btex and mtbe adsorption onto raw and thermally modified diatomite. *Journal of Hazardous Materials,* 178, 136-143.

Akafu, T., Chimdi, A & Gomoro, K. 2019. Removal of fluoride from drinking water by sorption using diatomite modified with aluminum hydroxide. *Journal of analytical methods in chemistry*, *2019*.

Angelova, D., Uzunov, I., Uzunova, S., Gigova, A & Minchev, L. 2011. Kinetics of oil and oil products adsorption by carbonized rice husks. *Chemical Engineering Journal,* 172, 306-311.

Anifa, E. M., Ariani, I. K., Hatati, R. N & Nugraha, S. A. 2022. Adsorption of oil and grease in wastewater using activated carbon derived from sewage sludge *IOP Conference Series: Earth and Environmental Science,* 1098(1), 012043.

Annunciado, T., Sydenstricker, T & Amico, S. 2005. Experimental investigation of various vegetable fibers as sorbent materials for oil spills. *Marine Pollution Bulletin,* 50, 1340-1346.

Ardejani, F. D., Badii, K., Limaee, N. Y., Shafaei, S. Z & Mirhabibi, A. R. 2007. Numerical modelling and laboratory studies on the removal of direct red 23 and direct red 80 dyes from textile effluents using orange peel, a low-cost adsorbent. *Dyes and Pigments,* 73, 178-185.

Bandura, L., Woszuk, A., Kolodynska, D & Franus, W. 2017. Application of mineral sorbents for removal of petroleum substances: A review. *Minerals,* 7(3), 37.

Bello, O. S., Adegoke, K. A & Oyewole, R. O. 2014. Insights into the adsorption of heavy metals from wastewater using diatomaceous earth. *Separation Science and Technology,* 49, 1787-1806.

Benkacem, T., Hamdi, B., Chamayou, A., Balard, H & Calvet, R. (2016). Physicochemical characterization of a diatomaceous upon an acid treatment: a focus on surface properties by inverse gas chromatography. *Powder Technology*, *294*, 498-507.

Comstock, S. E. H & Boyer, T. H. 2014. Combined magnetic ion exchange and cation exchange for removal of doc and hardness. *Chemical Engineering Journal,* 241, 366-375.

Danish, M., Ahmad, T., Hashim, R., Hafiz, M. R., Ghazali, A., Sulaiman, O & Hiziroglu, S. 2016. Characterization and adsorption kinetic study of surfactant treated oil palm (Elaeis guineensis) empty fruit bunches. *Desalination and Water Treatment,* 57(20), 9474-9487.

Dickhout, J. M., Moreno, J., Biesheuvel, P. M., Boels, L., Lammertink, R. G. H & De Vos, W. M. 2017. Produced water treatment by membranes: A review from colloidal perspectives. *Journal of Colloid and Interface Science.,* 487, 523-534.

Djilani, C., Zaghdhoudi, R., Djazi, F., Bouchekima, B., Lallam, A., Modarresi, A & Rogalski, M. 2015. Adsorption of dyes on activated carbon prepared from apricot stones and commercial activated carbon. *Journal of Taiwan Institute of Chemical Engineers,* 53, 112-121.

DWAF 1998. No. 36 of 1998: National Water Act, 1998. Cape Town, South Africa: South African government.

Firdous, S., Jin, W., Shahid, N., Bhatti, Z. A., Igbal, A., Mahmood, Q & Ali, A. 2018. The performance of microbial fuel cells treating oil industrial wastewater. *Environmental and Technology Innovation,* 10, 143-151.

Fu, L., Zhu, J., Huang, W., Fang, J., Sun, X., Wang, X & Liao, K. 2020. Preparation of nano-porous carbon-silica composites and its adsorption capacity to volatile organic compounds. *Processes,* 8(3), 372.

Gummas, R. H & Okpeke, I. 2015. Production of activated carbon and characterization from snail shell waste (helix pomatia). *Advances in Chemical Engineering and Science,* 5, 51-61.

Han, M., Zhang, J., Chu, W., Chen, J & Zhou, G. 2019. Research progress and prospects of marine oily wastewater treatment: A review. *Water Air and Soil Pollution,* 11(12), 2517.

Huang, S., Ras, R. H. S & Tian, X. 2018. Antifouling membranes for oily wastewater treatment: Interplay between wetting and membrane fouling. *Current Opinion in Colloid and Interface Science,* 36, 90-109.

Ismail, A. S. 2015. Preparation and evaluation of fatty-sawdust as a natural biopolymer for oil spill sorption. *Chemistry Journal,* 5, 80-85.

Jamaly, S., Giwa, A., & Hasan, S. W. 2015. Recent improvements in oily wastewater treatment: Progress, challenges, and future opportunities. *Journal of Environmental Sciences*, 37, 15-30.

Jernelov, A. 2010. The threats from oil spills: Now, then, and in the future. *Ambio,* 39, 353-366.

Kuwahara, Y., Ohmichi, T., Kamegawa, T., Mori, K & Yamashita, H. 2010. A novel conversion process for waste slag: Synthesis of a hydrotalcite-like compound and zeolite from blast furnace slag and evaluation of adsorption capacities. *Journal of Materials Chemistry,* 20, 5052-5062.

Kuyukina, M.S., Krivoruchko, A.V. & Ivshina, I.B., 2020. Advanced bioreactor treatments of hydrocarbon-containing wastewater. *Applied Sciences,* 10, 831–849.Lekene, R. B. N., Kouotou, D., Ankoro, N. O., Sone Kouoh, A. P.-M., Ndi, J. M & Ketcha, J. M. 2021. Development and tailoring of amino-functionalized activated carbon based Cucumerupsi manni Naudin seed shells for the removal of nitrate ions from aqueous solution. *Journal of Saudi Chemical Society,* 25(10), 101316.

Liu, Y., Zhou, S., Liu, R., Chen, M., Xu, J., Liao, M., Mei, J & Yang, L. 2022. Study on amino-directed modification of oil sludge-derived carbon and its adsorption behavior of bisphenol a in water *Separation and Purification Technology,* 298, 121625.

Makisha, N. 2020. Research of oily wastewater treatment by means of membrane methods. *Earth and Environmental Science,* 459(4), 042015.

Mohammed, D & Tanweer, A. 2018. A review on utilization of wood biomass as a sustainable precursor for activated carbon production and application. *Renewable and Sustainable Energy Reviews,* 87, 1-21.

Moreira, F. C., Boaventura, R. A. R., Brillas, E & Vilar, V. J. P. 2017. Electrochemical advanced oxidation processes: A review on their application to synthetic and real wastewaters. *Applied. Catalysis. B: Environmental.,* 202, 217-261.

Musapatika, T. E. 2010. *Use of low-cost adsorbents to treat industrial wastewater.* Master of Science in Engineering. University of the Witwatersrand.

Omri 2002. Activated carbon processing in natural organic standard board technical advisory panel reviews, USDA National Organic Program.

Pan, N., Su, Z., Mo, J., Xi, H., Xia, Q & Li, Z. 2011. Preparation of novel composite activated carbon with high applicability to microwave and its regeneration under microwave radiation. *Journal of Chemical Engineering,* 62, 111-118.

Poinern, G. E. J., Senanayake, G., Shah, N., Thi-Le, X. N., Parkinson, G. M & Fawcett, D. 2011. Adsorption of the aurocyanide, complex on granular activated carbons derived from macadamia nut shells—a preliminary study. *Minerals Engineering,* 24, 1694-1702.

SAMAC (South African Macadamia Growers' Association), 2023. Macadamia South Africa NPC. Statistics on the Southern African Macadamia Industry. 〈https://www.samac.org.za/industry-statistics/〉 (accessed 01 April 2023).

Samsuir, A. A., Ismail, N & Ghazi, R. M. 2016. Optimization of oil removal by sugarcane bagasse using response surface methodology. *Journal of Tropical Resources and Sustainable science,* 4, 82-87.

Sohaimi, K. S. A., Ngadi, N., Mat, H., Inuwa, I. M & Wong, S. 2017. Synthesis, characterization and application of textile sludge biochars for oil removal. *Journal of Environmental Chemical Engineering,* 5, 122-135.

Su, Z., Pan, N., Zhao, W., Mo, J & Xi, H. 2012. Preparation and properties of activated carbons with high thermal conductivity. *Chemical Engineering Journal,* 40, 14-18.

Tripathy, A., Mohanty, S., Nayak, S. K., & Ramadoss, A. (2021). Renewable banana-peel-derived activated carbon as an inexpensive and efficient electrode material showing fascinating supercapacitive performance. *Journal of Environmental Chemical Engineering*, *9*(6), 106398.

UNDP 2015. Goal 6: Clean water and sanitation.

Vlaev, L., Petkov, P., Dimitrov, A & Genieva, S. 2011. Cleanup of water polluted with crude oil or diesel fuel using rice husks ash. *Journal of the Taiwan Institution of Chemical Engineers,* 42, 957-964.

Yang, Y., Jiang, X., Liu, H., Ai, G., Shen, L., Feng, X., Ye, F., Zhang, Z., Yuan, H & Mi, Y. 2022. Diethylenetriamine modified biological waste for disposing oily wastewater *Environmental Research,* 212, 113395.

Zhang, Y., Jiang, C & Zhang, H. 2016. Research of absorbent materials for volatile organic compounds. *Safe, Health and Environment,* 16, 1-6.

Zhao, C., Zhou, J., Yan, Y., Yang, L., Xing, G., Li, H., Wu, P., wang, M. & Zeng, H. 2020. Application of coagulation/flocculation in oily wastewater treatment: A review. *Science of the Total Environment*, 765, 142795.

Zhou, R., Yu, H., Yuan, P., Fan, J., Chen L., Li, Y., Ma, F & Zhang, X. 2018. Heterologous expression and characterization of three laccases obtained from Pleurotus ostreatus HAUCC 162 for removal of environmental pollutants. *Journal of Hazardous Materials,* 344, 499-510.

Chapter 2: LITERATURE REVIEW

2.1. Introduction

This chapter presents a general overview of oily wastewater, wastewater treatment techniques, application of activated carbon in oily wastewater treatment, diatomaceous earth, acid-leached diatomaceous, amine-functionalization, macadamia nutshells as a waste and response surface methodology.

2.2. Oily wastewater

Oily wastewater is composed of wastewater with different types of oil at various concentration levels. One of the main components of wastewater discharged by industries is oily wastewater. Oily wastewater can contain lipids, hydrocarbons, and petroleum fractions such as gasoline, diesel and kerosene oils (Jamaly et al., 2015). The food and beverage industry produces significant amounts of oily wastewaters, however, the bulk of the oil that finds its way into water bodies comes from the petrochemical and metal processing industries. Oil refineries are significant sources of pollution because they use a great deal of oil and water, which results in the production of loads of wastewaters (Yu et al., 2013). Oily wastewaters vary according to the production processes used in the various industries. It is nevertheless characterized by high levels of total suspended solids (Diya'udeen et al., 2011), biochemical oxygen demand (Al Zarooni & Elshorbagy, 2006), chemical oxygen demand (Tobiszewski et al., 2012) as well as sulphides, ammonia, total organic carbon, and total petroleum hydrocarbon content (Adetunji & Olaniran, 2021). Due to inadequate reporting, sensitivity, and lack of public availability of wastewater data, previous South African studies have identified loopholes in wastewater data and wastewater generation., With that being said, Cloete et al. (2010) assert that, in South Africa, 26% of wastewater is generated by the petroleum industry.

2.2.1. Sources of oily wastewater

Oil refineries, the petrochemical sector, processes for the production of crude oil, metal processing, oil extraction processes, condensates from a compressor, lubricants, and car washings are some of the sources of oily wastewater (Lan et al., 2009). Two refineries exist in South Africa (Ratshomo & Nembahe, 2018). These are the Engen refinery, which is located in Durban and has a crude refining capacity of 110,000 barrels per day, and a crude oil refinery near Cape Town. The oil extraction sector produces the most oily wastewater due to oil extraction procedures in oil mills and mill effluents, such as palm oil mill effluents, which have a concentration of grease and oil of between 4000 and 6000 mg/L (Ahmad et al., 2005a).

Untreated domestic wastewater consists of 50 to 100 mg/L of grease and oil (Abass et al., 2011). However, Friedler (2004) reported kitchen greywater as being the highest source of oil and grease in domestic wastewater. Also, oily wastewater is produced in the metalworking and finishing sectors where coolants and lubricants are used for cooling machine tools to prevent friction and tool wear (Wu et al., 2017). The concentration of hydraulic, lubricating, and fuel oils in bilge water is extremely reliant on the manner of operation of the ship (Tasker et al., 2018a). Lastly, kitchen greywater is said to provide the most oil and grease to home wastewater and is often used for irrigation purposes (Travis et al., 2008). Figure 2.1 shows the various sources of oily wastewater.

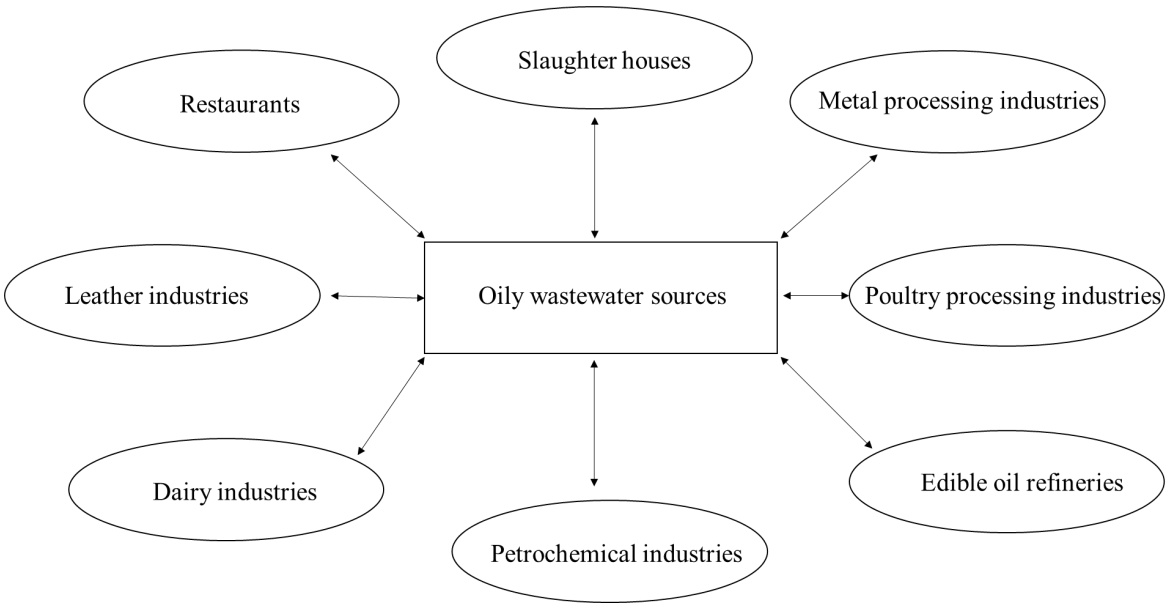

Figure 2.1: A depiction of the various sources of oily wastewater (Adetunji and Olaniran, 2021)

2.2.2 Environmental impacts of oily wastewater

Globally, water bodies are becoming more polluted by oily water and the impacts can be irreversible for aquatic lives (Kuyukina et al., 2020). Furthermore, these impacts can be transferred to humans since humans are part of the ecosystem and are at the top of the food chain (Abass et al., 2011). Oil in water bodies can cause an oil layer to form, which significantly pollutes the water body environment by reducing light penetration and photosynthesis (Abass et al., 2011). Furthermore, the oil layer hinders oxygen from being transmitted from the atmosphere to the aqueous medium leading to a superficial dissolved oxygen content in the water that is accompanied by a detrimental consequence on aquatic life (Bakke et al., 2013). In July 2019, about 200 to 400 litres of oil spilled in the Port of Ngqura 20 km north east of Gqeberha (formerly called Port Elizabeth) while a vessel was being refuelled (Che, 2019). Over

100 penguins and other seabirds were affected by the spill. A month later, oil spillage was also reported in Pietermaritzburg (Duzi Disaster Fund, 2019). This around 1.6 million litres of oil were spilled from the Willowton oil factory into the Msunduzi River where almost all the aquatic life that run along the river were killed. Figure 2.2 shows (a) the impact of the oil spillage on the Msunduzi River aquatic life and (b) oil-slicked penguins that were rescued following the oil spillage in Post Elizabeth, the coast of South Africa.

Figure 2.2: (a) Dead aquatic life caused by the oil spillage in the Msunduzi River in South Africa, Pietermaritzburg (Duzi Disaster Fund, 2019) and (b) Oil-slicked penguins that were rescued after a spill off in the coastal city of Gqeberha, South Africa (Che, 2019).

2.3. Conventional treatment techniques for oily wastewater

Conventional methods of wastewater treatment combine physical, chemical, and biological processes to get rid of particles, organic materials, and occasionally nutrients from wastewater. The amount of oil used has increased due to industrial growth (Yu et al., 2013). Oily wastewater sources range from processes related to production, refining, storage, transportation, and the petrochemical industry (Ahmed et al., 2007, Yu et al., 2013). Conventional methods for treating wastewater contaminated with oil are discussed in the sections that follow.

2.3.1. Coagulation

Coagulation is a well-known physicochemical method which is widely applied in oily wastewater treatment (Ahmad, 2006). The process involves two steps, namely coagulation and flocculation (Lee et al., 2012). Coagulation is the initial step where coagulants decrease the electrical double-layer of the colloid's repulsive force. Thereafter, larger particles called flocs

gradually aggregate from microparticles—this is the flocculation step (Elimelech et al., 2013). This procedure aids in lowering the turbidity of the water and removing heavy metals, organic matter, macromolecules, bacteria, viruses, and nutrients that contribute to the eutrophication of waterbodies (You et al., 2018). Due to its quick response time and affordability, poly-aluminum chloride (PACl) is frequently employed as an inorganic coagulant for the pre- or post-treatment of oily wastewater. Coagulation has gained popularity as a technique for lowering the total dissolved solids and total suspended solids of the wastewater, reducing the amount of time required for solids to settle naturally, and assisting smaller colloidal particles and mineral impurities to settle (You et al., 2018). Even so, the main disadvantage of this techniques is that coagulation typically requires the addition of chemicals which produces sludge. The sludge contains toxic chemicals and ultimately requires disposal especially in the case of South Africa where lad disposal is the preferred disposal option. Moreover, land disposal poses a serious risk to the environment and water bodies, and the disposal costs often increase based on the amount and toxicity of the sludge as well as the difficulties associated with dewatering it (Yu et al., 2013).

2.3.2. Flotation

Flotation includes the separation of suspended particles by having them stick to the surface of ascending bubbles (Zouboulis & Avranas, 2000). This technique is employed for the removal of lipids, dissolved ions, oils, fatty acids, suspended water solids, and biomolecules. Flotation is dependent on the surface chemistry of separating the material. Flotation impeller and dissolved air flotation are the two basic flotation methods for removing oil from wastewater (Yu et al., 2013). The procedure of "dissolved air flotation" involves bringing a layer of particles on the liquid's surface, dissolving the air in a saturator at high pressure, and then releasing water under atmospheric pressure to create microbubbles in the flotation cell (Al-Shamrani et al., 2002).

To increase their durability and enable them to rise to the surface, the microbubbles become linked to the surface (Al-Shamrani et al., 2002). Alternative flotation methods such as induced air flotation and electrolytic flotation are not employed often (Zouboulis & Avranas, 2000). Al-Shamrani et al. (2002) studied the “dissolved air flotation” to separate oil and water and discovered that the oil base may be extracted by flotation even at modest working pressure and recycling ratio during the dilution of oil droplets using aluminum sulphate. Flotation is useful for primary classification

The flotation systems are generally highly effective when removing lighter particles such as algae which under normal circumstances are difficult to settle. Apart from being efficient in the removal of suspended solids, greases, oils, and metals and allowing low effluent turbidity to be obtained, flotation systems have an added advantage of being not too sensitive to extreme temperatures. Furthermore, this system can be used as an integrated physicochemical process (Crini & Lichtfouse, 2018). This system is however time consuming and energy intensive. Device manufacturing and repairing problems have also been reported (Yu et al., 2013).

2.3.3. Biological treatment

By utilizing microbial metabolism, biological treatment procedures are affordable and effective ways to handle oily wastewater from the industry. Water is dissolved and the colloidal organic contaminants are stabilized as harmless compounds (Jou & Huang, 2003, Kriipsalu et al., 2007). The use of biological treatment is common in activated sludge and biological filtering techniques (Yu et al., 2013). A state vector purifies the microbes via adsorption and then focuses on the activated sludge microbes to break down organic matter which makes up sludge that has been activated in aeration tanks. The microorganisms are connected to the filter where wastewater is discharged from the upper part via the surface of the filter throughout the sorption of organic contaminants and degradation by organisms, and they are killed throughout these processes (Yu et al., 2013).

Santo et al. (2013) explored the biological treatment provided by activated sludge for effluent from petroleum refineries. The results showed that total suspended particles, chemical oxygen demand, and total organic carbon had been removed, respectively, by 94–95%, 85-87%, and 98–99%. The rate of degradation was also calculated using the pseudo-first-order of the kinetic model with and without recycling of the sludge, and the resulting rate constants were 0.055 and 0.959 mg/L, respectively. Biological treatment is effective removal of suspended solids and biochemical oxygen demand, produces less waste sludge, and is easy to operate (Izanloo et al., 2007). This being a biological process, the advantage of this system is that it requires active management and maintenance of the microorganisms, has poor decolorization (activated sludge), and possible sludge bulking and foaming (Crini and Lichtfouse, 2018).

2.3.4. Membrane separation technology

The membrane separation method makes use of a unique permeable material that was created for the physical elimination of a specific kind of the trapped pollutants' particle sizes (Lin et al., 2006). Reverse osmosis (Zhang et al., 2006), ultrafiltration, and microfiltration (Dickhout

et al., 2017) are the three main types of this technology. Oil-water emulsion separation has received a lot of attention lately thanks to membrane separation technologies (Pan et al., 2007). The characteristics of membrane separation technology include waste oil permeability with special attention being given to the particle size and membrane molecular weight cut-off (Arkhangelsky et al., 2012). The process, generally, has no phase alteration but a direct application of oil-water separator (Arkhangelsky et al., 2012).

Song et al. (2006) studied the usage of a low-cost, extruded tubular carbon matrix that is suitable for treating oily wastewater. This carbon matrix is generated by carbonization microfiltration. While treating oil-contaminated water, the optimum parameters were 1 m/s pore size, 0.10 MPa pressure, and 0.1 m/s flow rate. The findings revealed up to 97% oil removal efficiency with an oil concentration of lower than 10 mg/L. Advantages of membrane separation technology include efficient removal rates, chemical-free additives, absence of phase transitions, being economical, and practical friendliness. However, this technology is limited by severe membrane fouling and expensive preparation costs.

2.3.5. Adsorption

Adsorption employs the use of solid adsorption resources with high specific surface area and good porosity to adsorb oil molecules on the surface with the aim of separating oil from water (Han et al., 2019). Liquid-solid intermolecular attraction forces make solute particles from the solution to be concentrated at the solid surface when the solution encounters a highly porous-surfaced structure.

Among the most efficient methods to treat oily wastewater is adsorption, especially when a proper adsorbent is used (Wang et al., 2014). High lipophilicity, low hydrophobicity, high adsorption capacity, recyclable material, and environmental friendliness are all desirable characteristics of an ideal adsorbent (Dong et al., 2012). Several natural adsorbents, including rice husk, sawdust, sugar cane bagasse, vegetable fibres, and carbonized peat bagasse, have been utilized for oil sorption, along with inorganic substances such as fly ash, activated carbon, and zeolites (Ma et al., 2018).

The use of rice husk-based activated carbon in the removal of spilled oil, oil wastes, or bilge water was studied by Vlaev et al. (2011). According to this study, rice husk-based activated carbon has a higher capacity for adsorption at 298 K, where 6.22 g/g of crude oil and 5.02 g/g of diesel fuel were adsorbed. The obtained results demonstrated that the investigated adsorbent

has a high adsorption capacity, is reasonably priced, and can be successfully employed as an adsorbent to clean up bilge water and oil-produced spills in water basins.

2.3.5.1. Adsorbents used in oil removal

Acetic anhydride was used by Nwadiogbu et al. (2016) to enhance the hydrophobicity and sorption efficiency of corncobs. With a sorption capacity of 2500 mg/g, results of the study revealed that acetylated corncobs are good sorbents with potential for management of oil spills. To increase the hydrophobicity of the acetylated bagasse, Sun et al. (2004) used N-bromo succinimide in a solvent-free process as a catalyst under mild conditions in a solvent free system. Machine oil was removed from water using the sorbent and a sorption capacity range of 13.5–20.2 g/g was achieved.

To increase the hydrophobicity and oil absorption of banana fibre, Teli and Valia (2013) investigated the acetylation of the banana fibre. Using the raw and acetylated fibres to remove the oil from water, sorption capacities of 2.10 g/g and 11.86-18.37 g/g were achieved, respectively. To remove diesel oil from oily wastewater, Cai et al. (2019) impregnated crab shells with potassium hydroxide to create activated biochar, and an adsorption capacity of 93.9 mg/g was achieved. Sulyman et al. (2018) synthesized textile fibres from used tyres as an affordable static adsorbent for the removal of crude oil and used cooking oil from wastewater. The adsorption capacities for the crude oil and used cooking oil were found to be 14.4 g/g and 17 g/g, respectively. Khader et al. (2021) employed combined adsorbents (i.e., zeolite, silica gel, and commercial activated carbon) in the reduction of chemical oxygen demand (an indirect indication of the number of organic pollutants present in a water sample) and remediation of oily water. Mixed adsorbents had elevated sorption capacities of 96.4 mg/g for chemical oxygen demand and 108.38 mg/g for oil.

Several advantages of adsorption are known, and these include design simplicity, ease of operation, and cost effectiveness. However, this technology requires relative high capital costs and the spent adsorbents may be considered hazardous waste.

2.4. Application of activated carbon in oily wastewater treatment

Due to its extensive pore volume and surface area, activated carbon has been used in adsorption. Activated carbon is an amorphous carbonaceous material with a highly developed porous structure that is primarily composed of carbon atoms organized in disordered arrangements to form macropores bigger than 50 nanometers, mesopores between 2 and 50 nanometers, and micropores less than 2 nanometers of radius (Djilani et al., 2015). There are

three main steps for manufacturing activated carbon, namely: (i) raw material preparation, (ii) low-temperature carbonization, and (iii) activation.

Activation by physical and chemical procedures is commonly used for fabricating activated carbon from biomass precursors (Antal & Gronli, 2003). To improve conventional techniques for the fabrication of activated carbon, hydrothermal carbonization (Jain et al., 2016) and microwave heating (Ao et al., 2018) were developed. Moreover, combining physical and chemical activation is thought to improve the textural qualities and provide highly ordered porosity. Table 2.1 summarises studies involving the application of activated carbon-based adsorbents in oily wastewater treatment.

Table 2.1. Activated carbon-based adsorbents in oily wastewater treatment.

Adsorbent	Oil Studied	Oil Removal efficiencies (%)	Reference (s)
Macadamia nutshell-based activated carbon	BTEX (benzene, toluene, ethylbenzene, and xylene) compounds	58,90%, 70.40%, 78.49%, and 85.56%.	(Melaphi et al., 2023)
Plum pit shell-based activated carbon	Hexane-band chloroform-extracted oil	95.5%	(Yessenbek et al., 2023)
oil sludge-derived activated carbon	Oily wastewater	94%	(Amari et al., 2023)
Sewage sludge-based activated carbon	Oil and grease	77%	(Anifa et al., 2022)
Corn cobs activated carbon	Oil and grease	60.38%	(Igwegbe et al., 2020)
Palm kernel shells	Oil and grease	99.89%	(Ramli & Ghazi, 2020)
Rice husk-based activated carbon	BTEX (benzene, toluene, ethylbenzene, and xylene) compounds	22%, 33%, 58%, and 18.8%.	(Yakout & Daifullah, 2013)

2.5. Amine-functionalization

The adsorbent-adsorbate relationship is greatly influenced by the surface characteristics of the adsorbent. To increase the stability, adsorption capacity, and adsorptive properties of porous materials for improved water treatment, surface modification through amine-functionalization has been examined in depth (Bouazizi et al., 2022). The negatively charged surfaces of inorganic adsorbents' hydroxyl groups (-OH) and saturated oxygen render them unstable and limit their adsorption effectiveness (Nabil et al., 2019).

2.5.1. Amine-functionalization of carbon-based adsorbents

Activated carbons, graphene, carbon nanotubes, and biochar are the most popular types of carbon-based adsorbent (Ghalib et al., 2020). Due to their high surface area, pore volume, superior electrical conductivity, surface chemical inertness, and outstanding mechanical conductivity, carbon materials have demonstrated excellent performance in the treatment of water (Rashidi and Yusup, 2016). Owing to their mechanical stability and high nitrogen content, various amines such as polyethyleneimine (PEI) and tetraethylenepentamine (TEPA) can be employed to improve the performance of an adsorbent (Zhao et al., 2021). The amine content put within the material's pores is influenced by the overall volume of the adsorbents' pores. As a result, the pore structure of the carrier material determines how well the amine-modified adsorbent captures particles. For the amine species to aggregate on the surface of the carrier material, the amine-based adsorbent needs to be in powdery form (Zhao et al., 2021). Figure 2.3 illustrates the synthesis of amine-derived solid adsorbent using PEI.

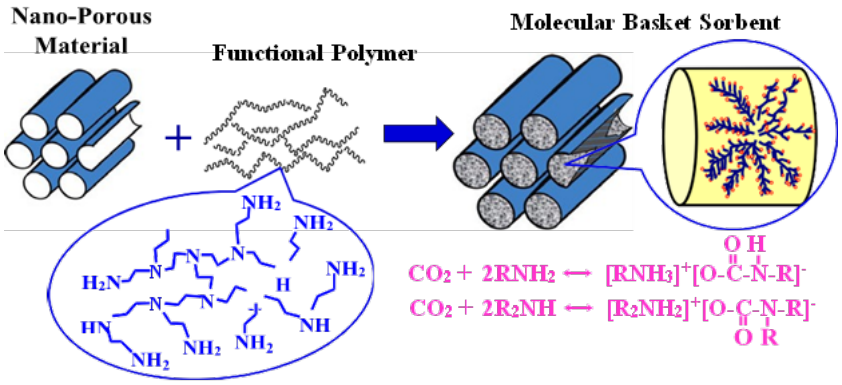

Figure 2.3: Graphic illustration of the synthesis of amine-derived solid adsorbent using PEI (Wang et al., 2013).

2.5.2. Importance of amine-functionalization of adsorbents

Amine-functionalization of adsorbents has been reported to generate activated sites and improve the surface properties of inorganic adsorbents for water treatment (Bouazizi et al.,

2022). Furthermore, amine functionalization is also known to increase the stability of the adsorbent thus resulting in an increase in the stability and reusability of the amine-functionalized adsorbent (Bouazizi et al., 2022). The addition of organic moieties bearing chelating groups reduces aggregation of adsorbent particles (Azzouz et al., 2015). Amine groups are widely considered as effective functional groups for the adsorption of various contaminants (Yang et al., 2022). This was evident in a study by Liu et al. (2022) which sought to synthesize modified oil sludge-derived carbon using polyethyleneimine (PEL) for the adsorption of bisphenol-A in water. The study reported a respective adsorption capacity and removal efficiency of 393.2 mg/g and 95% after a contact time of 1 hour.

Wang et al. (2018) prepared recyclable amine-functionalized magnetic nanoparticles for efficient demulsification of crude oil-in-water emulsions. Their results showed demulsification efficiency of 99.7% and 95% after six cycles of testing. Ye et al. (2022) reported oily wastewater treatment and its demulsification mechanism using amine-functionalized cellulose. The results, which confirmed the great application potential of wastepaper in industrial large-scale oily wastewater treatment, revealed an excellent demulsification performance of 99.16%.

2.6. Macadamia nutshells

Macadamia nuts are commercially grown in Limpopo, Mpumalanga and KwaZulu-Natal provinces and sprinkle of growers also found in the Eastern and Western Cape. South Africa is the leading macadamia nut producer in the world, with over 700 macadamia nut farmers mostly located in Limpopo, are regarded as an abundant agricultural waste in the country (SAMAC, 2023). The ever-increasing output growth, disposal of macadamia nut shells has become a significant challenge for the sector. This agricultural waste stream results in a significant environmental load caused by the nutshells (Poinern et al., 2011). Owing to their high carbon content, macadamia nutshells were utilized for the production of biochar and activated carbon (Dao et al., 2021). The physical characteristics of macadamia nutshells include hardness and brittleness (Nekhavhambe, 2021). Macadamia nutshells consists of carbon, hydrogen, nitrogen, oxygen, and sulphur with lignin, cellulose, hemicellulose being the main components (Pakade et al., 2017).

Literature on the application of macadamia nutshell-based activated carbon in oily wastewater treatment is scant. However, activated carbons derived from macadamia nut shells have shown great promise as adsorbents for the removal of various pollutants (e.g., chromium) from wastewater with adsorption capacity of 45.23 mg/g being reported (Pakade et al., 2017).

Methylene blue removal from aqueous media with adsorption capacity ranging from 134 to 144 mg/g has also been reported (Wongcharee et al., 2018). Macadamia nutshell-based activated carbon consist of microporous and mesoporous structures with large surface areas ranging from 700-1100 m^2/g (Melaphi et al., 2023). Furthermore, these activated carbon materials have high adsorption capacity due to the presence of many reactive sites on their surfaces (Rotorcarb-activated carbon, 2020). Therefore, they can be used as effective and affordable adsorbent for the treatment of oily wastewater. In a previous study, Melaphi et al. (2023) reported the synthesis of macadamia nut shells-based activated carbon for adsorptive removal of BTEX (benzene, toluene, ethylbenzene, and xylene) compounds from synthetic wastewater. The results showed removal efficiencies of 85.56%, 78.49%, 70.40% and 58.90% for xylene, ethylbenzene, toluene and benzene, respectively. This confirms that macadamia nutshells-based activated carbon is a promising adsorbent for BTEX removal from synthetic wastewater.

The beneficiation of macadamia nutshells will improve waste management of the nutshells by reducing their environmental load and enhancing the economic base for the farmers. Similarly, in this study, specific attention is paid to addressing the challenge posed by waste macadamia nutshells by using them to lessen environmental pollution posed by oily wastewater. Such an approach offers cheaper adsorption alternatives which, it is envisaged, will in future replace conventional techniques.

2.7. Diatomaceous earth

Diatomaceous earth is a naturally sedimentary rock that has a permeable structure, low coefficient of conductivity, and minimal density (Nefzi et al., 2018). Diatomaceous earth contains different impurities, including clay minerals, carbonate minerals, silica sand, iron oxides, and organic materials, and it consists of 80 to 90% amorphous hydrated silica ($SiO_2.nH_2O$) which accumulates in their cell walls (Akafu et al., 2019). Diatoms are tiny, single-celled, watery dead algae (Antonides, 2017).

2.7.1. Uses of diatomaceous earth

Diatomaceous earth has a variety of uses, such as water filtration, animal performance enhancement, mycotoxin binding, and insect management for stored grains (Ikusika et al., 2019). Animals can also use it as a nutritional supplement (Koster, 2013). In its natural state, diatomaceous earth has been used in bricks making and as a trinitroglycerin stabilizer in dynamites (Antonides, 2017). Diatomaceous earth has also been used as a filter aid in

wastewater treatment. Its chemical composition and physical structure make its commercial value greater for various applications such as beer filter aids, uptake of different water contaminants, textile dyes removal from wastewater, and heavy metal ions sorption (Shaobin and Peng, 2010). Bandura et al. (2017a) investigated the application of this mineral sorbents in the removal of petroleum substances. The diatomaceous earth was used as a silica adsorbent and the generated results demonstrated that diatomite has a high sorption capacity, is environmentally friendly, has recycling potential, and has low acquisition costs.

2.8. Acid leaching of diatomaceous earth

Acid is typically used to improve the surface properties of raw diatomaceous earth. Acid leaching of diatomaceous earth is targeted at the removal of contaminates such as iron oxides, silica sand, clay minerals, carbonate minerals, carbonates, and organic matter (Tesfaye et al., 2019). These contaminants frequently hinder photocatalytic processes based on hydroxyl ions. Carbonates which are naturally present in the pores of the diatomaceous earth make the radicals less reactive. Consequently, eliminating carbonates clears blocked pores and enhances the specific surface area of the diatomaceous earth.

Benkacem et al. (2016) have performed acid leaching of diatomaceous earth using nitric acid, and an increase in the surface area from 8 mg/g to 11.9 mg/g was recorded. In addition, the treatment of diatomite earth with 5M nitric acid reduced mineral impurities, such as Fe_2O_3 and alkali metal oxides (CaO, MgO), eliminated carbonates, and increased SiO_2 ratio from 88 to 98%.

Using 2.2M nitric acid, Abdellaoui et al. (2018) developed a procedure for removing impurities from raw diatomaceous earth to produce high-purity silica. The study achieved lower impurity levels of Ca, Mg and Fe and the final purified silica was 99.99 wt% (four nines) pure.

2.9. Response surface methodology

The term "response surface methodology" (RSM) is a collection of mathematical and statistical techniques that are useful for analysis and modelling when a response of interest is affected by a number of variables, and the ultimate goal is to improve this response (Montgomery, 2017). Due to its capability to consider the interaction between two or more components at once, RSM is a highly developed method that saves time and resources (Pilkington et al., 2014). According to Rushing et al. (2013), RSM is appropriate for quadratic surface fitting since it aids in optimizing the efficient measures with the least experiments amounts while also analysing how different parameters interact.

Rathilal and Tetteh (2019) employed a laboratory-dissolved air floatation for the remediation of oil refinery wastewater using poly ferric-sulphate. Optimization was accomplished by Box-Behnken design to assess the interactive effects of three main independent process parameters (coagulant dosage, flotation time, and pH) upon the elimination of the COD, soap oil and grease, total suspended solid, and turbidity.

To characterize the effectiveness of oil removal by polypyrrole-modified silica under the control of initial oil concentration, adsorbent dose, and contact duration, a central composite model was constructed by Izevbekhai et al. (2020) in design expert software to remove oil by synthesized polypyrrole-silica polymer composite using RSM.

2.10. Summary and knowledge gaps

Oily wastewater is wastewater containing different types and concentrations of oils such as lipids, hydrocarbons, and fuel fractions such as gasoline, diesel, and kerosene oils. Oil refineries are significant sources of pollution because they use significant amounts of oil and water, which results in copious amounts of wastewaters being generated. Water bodies are affected by oily water, and this impacts aquatic lives. Since humans are part of the ecosystem and food chain, these impacts can be transferred humans. Due to inadequate reporting, sensitivity, and lack of public availability of wastewater data, prior studies in South Africa have revealed loopholes in wastewater data and wastewater generation. Given the little data being reported in literature, it suffices to say that the risk posed to water bodies remains indefinite.

Several conventional treatment techniques for the treatment of oily wastewater are known, and these include coagulation, flotation, biological treatment, and membrane separation technology, and adsorption. Adsorption appears to be the most preferred technique due to its straightforward design, cheap start-up costs, simplicity of use, and sensitivity to lethal contaminants and higher removal efficiency. The adsorption technique can make use of abundant and green agricultural wastes to fabricate adsorbents. Although most of the materials reported in literature are effective, limited to lack of recyclability capability of these materials poses a challenge for their application as adsorbent for the removal of oil from oily wastewaters. That being the case, the removal efficiency and recyclability of the adsorbent are important factors when developing relatively cheap and reusable adsorbents that can be used in developing countries such as South Africa.

References

Abass, O. A., Ahmad T.J., Suleyman, A. M. & Mohamed, I. A. K. 2011. Removal of oil and grease as emerging pollutants of concern in wastewater stream. *Engineering Journal* 12, 161-169.

Abdellaoui, I., Islam, M. M., Sakurai, T., Hamzaoui, S. & Akimoto, K. 2018. Impurities removal process for high-purity silica production from diatomite. *Hydrometallurgy,* 179, 207-214.

Adetunji, A. I. & Olaniran, A. O. 2021. Treatment of industrial oily wastewater by advanced technologies: A review. *Applied Water Science,* 11, 98.

Ahmad, A. L., Bhatia, S., Ibrahim, N. & Sumathi, S. 2005. Adsorption of residual oil from palm oil mill effluent using rubber powder. *Brazilian Journal of Chemical Engineering,* 22, 371-379.

Ahmad, A. L., Sumathi, S & Hameed, B.H. 2006. Coagulation of residue oil and suspended solid in palm oil mill effluent by chitosan, alum and pac. *Chemical Engineering Journal,* 118, 99-105.

Ahmed, A. F., Ahmad, J., Basma, Y. & Ramzi, T. 2007. Oily wastewater treatment from oil refining. *Journal of Hazardous Material,* 141, 557-564.

Al-Shamrani, A. A., Jamesa, A. & Xiao, H. 2002. Separation of oil from water by dissolved air flotation. *Colloids and Surfaces A Physicochemical and Engineering Aspects,* 209.

Al Zarooni, M. & Elshorbagy, W. 2006. Characterization and assessment of al Ruwais refinery wastewater. *Journal of Hazard Material,* 136, 398-405.

Akafu, T., Chimdi, A & Gomoro, K. 2019. Removal of fluoride from drinking water by sorption using diatomite modified with aluminum hydroxide. *Journal of analytical methods in chemistry*, *2019*.

Amari, A., Noreen, A., Osman, H., Sammen, S. S., Al-Ansari, N. & Salman, H. M. 2023. Investigation of the viable role of oil sludge-derived activated carbon for oily wastewater remediation. *Frontiers in Environmental Science,* 11, 240.

Anifa, E. M., Ariani, I. K., Hayati, R. N. & Nugraha, S. A. 2022. Adsorption of oil and grease in wastewater using activated carbon-derived from sewage sludge. *IOP Conference Series: Earth and Environmental Science,* 1098.

Antal, M. J. & Gronli, M. 2003. The art, science and technology of charcoal production. *Industrial and Engineering Chemistry Research,* 42, 1619-1640.

Antonides, L. E. 2017. Diatomite.

Ao, W., Fu, J., Mao, X., Kang, Q., Ran, C., Liu, Y., Zhang, H., Gao, Z., Li, J. & Liu, G. 2018. Microwave assisted preparation of activated carbon from biomass: A review. *Renewable and Sustainable Energy Reviews,* 92, 958-979.

Arkhangelsky, E., Duek, A. & Gitis, V. 2012. Maximal pore size in UF membranes. *Journal of Membrane Science,* 394-395, 89-97.

Azzouz, A., Nousir, S., Bouazizi, N. & Roy, R. 2015. Metal-inorganic-organic matrices as efficient sorbents for hydrogen storage. *ChemSusChem* 8, 800-803.

Bakke, T., Klungsøyr, J. & Sanni, S. 2013. Environmental impacts of produced water and drilling waste discharges from the Norwegian offshore petroleum industry. *Marine Environmental Research,* 92, 154-169.

Bandura, L., Woszuk, A., Kolodynska, D. & Franus, W. 2017. Application of mineral sorbents for removal of petroleum substances: A review. *Minerals,* 7(3), 37.

Benkacem, T., Hamdi, B., Chamayou, A., Balard, H. & Rachel, C. 2016. Physicochemical characterization of a diatomaceous upon an acid treatment: A focus on surface properties by inverse gas chromatography. *Powder Technology,* 294, 498-507.

Bouazizi, N., Vieillard, J., Samir, B. & Le Derf, F. 2022. Advances in amine-surface functionalization of inorganic adsorbents for water treatment and antimicrobial activities: A review. *Polymers,* 14(3), 378.

Cai, L., Zhang, Y., Zhou, Y., Zhang, X., Ji, L., Song, W., Zhang, H. & Liu, J. 2019. Effective adsorption of diesel oil by crab-shell-derived biochar nanomaterials *Materials,* 12.

Che, J. 2019. *Penguins in South Africa rescued after 400 liters of oil spilled during refuelling* [Online].

Cloete, T. E., Gerber, A & Maritz, L. V. 2010. A first order inventory of water use and effluent production by SA industrial, mining and electricity generation sectors. *Pretoria: Water Research Commission*.

Crini, G. & Lichtfouse, E. 2018. Advantages and disadvantages of techniques used for wastewater treatment. *Environmental Chemistry Letters, Springer Verlag.,* 17, 145-155.

Dao, M. T., Tran, T. P. L., Vo, D. T., Nguyen, V. K & Hoang, L. T. T. T. 2021. Utilization of macadamia nutshell residue for the synthesis of magnetic activated carbon toward zinc (II) ion removal. *Advances in Materials Science and Engineering*, *2021*, 1-10.

Dickhout, J. M., Moreno, J., Biesheuvel, P. M., Boels, L., Lammertink, R. G. H. & De Vos, W. M. 2017. Produced water treatment by membranes: A review from colloidal perspectives. *Journal of Colloid and Interface Science,* 487, 523-534.

Diya'udeen, B. H., Daud, W. M. A. W. & Abdul, A. A. R. 2011. A review: Treatment technologies for petroleum refinery effluent. *Process Safety and Environmental Protection,* 89, 95-105.

Djilani, C., Zaghdhoudi, R., Djazi, F., Bouchekima, B., Lallam, A., Modarresi, A. & Rogalski, M. 2015. Adsorption of dyes on activated carbon prepared from apricot stones and commercial activated carbon. *Journal of the Taiwan Institution of Chemical Engineers,* 53, 112-121.

Dong, X., Chen, J., Ma, Y., Wang, J., Chan-Park, M. B., Liu, X., Wang, L., Huang, W. & Chen, P. 2012. Superhydrophobic and superoleophilic hybrid foam of graphene and carbon nanotube for selective removal of oils or organic solvents from the surface of water. *Chemical Communications,* 48, 10660-10662.

Duzi Disaster Fund 2019. Urgent clean-up after Kwa-Zulu-Natal River spill.

Elimelech, M., Gregory, J & Jia, X. 2013. *Particle deposition and aggregation: measurement, modelling and simulation*. Butterworth-Heinemann.

Friedler, E. 2004. Quality of individual domestic greywater streams and its implication for on-site treatment and reuse possibilities. *Environmental Technology,* 25, 997-1008.

Ghalib, L., Abdulkareem, A., Ali, B. S. & Mazari, S. A. 2020. Modeling the rate of corrosion of carbon steel using activated diethanolamine solutions for CO_2. *Chinese Journal of Chemical Engineering,* 28, 2099-2110.

Han, M., Zhang, J., Chu, W., Chen, J. & Zhou, G. 2019. Research progress and prospects of marine oily wastewater treatment: a review. *Water*, *11*(12), 2517.

Igwegbe, C. A., Umembamalu, C. J., Osuagwu, E. U., Oba, S. N. & Emembolu, L. N. 2020) Studies on adsorption characteristics of corn cobs activated carbon for the removal of oil and grease from oil refinery desalter effluent in a downflow fixed bed adsorption equipment. *European Journal of Sustainable Development Research*, *5*(1), 1-15.

Ikusika, O. O., Mpendulo, C. T., Zindove, T. J. & Okoh, A. L. 2019. Fossil shell flour in livestock production: A review. *Animals,* 9(3), 70.

Izanloo, H., Mesdaghinia, A., Nabizabeh, R., Naddafi, K., Nasseri, A. H. & Nazmara, S. 2007. The treatment of wastewater containing crude oil with aerated submerged fixed-film reactor. *Pakistan Journal of Biological Sciences,* 10, 2905-2909

Izevbekhai, O., Gitari, W., Tavengwa, N., Ayinde, W. B. & Mudzielwana, R. 2020. Response surface optimization of oil removal using synthesized polypyrrole-silica polymer composite. *Molecules,* 25(20), 4628.

Jain, A., Balasubramanian, R. & Srinivasan, M. P. 2016. Hydrothermal conversion of biomass waste to activated carbon with high porosity. *A review in Chemical Engineering Journal,* 283, 789-805.

Jamaly, S., Giwa, A & Hasan, S. W. 2015. Recent improvements in oily wastewater treatment: Progress, challenges, and future opportunities. *Journal of environmental sciences*, *37*, 15-30.

Jou, C. J. G. & Huang, G. C. 2003. A pilot study for oil refinery wastewater treatment using a fixed-film bioreactor. *Advances in Environmental Research,* 7, 463-469.

Khader, E. H., Mohammed, T. J. & Adnan, S. W. 2021. Reduction of oil and cod from produced water by activated carbon, zeolite, and mixed adsorbents in a fixed-bed column. *Desalination and Water Treatment,* 227, 216-227.

Koster, H. 2013. Diatomite in animal feeds.

Kriipsalu, M., Marques, M. & Nammari, D. R., & Hogland, W 2007. Bio-treatment of oily sludge: The contribution of amendment material to the content of target contaminants, and the biodegradation dynamics. *Journal of Hazard Matter,* 148, 616-622.

Kuyukina, M. S., &, K. A. V. & I.B., I. 2020. Advanced bioreactor treatments of hydrocarbon-containing wastewater. *Applied Sciences,* 10(3), 831.

Lan, W. U., Gang, G. E. & Jinbao, W. A. N. 2009. Biodegradation of oil wastewater by free and immobilized yarrowia lipolytica w29. *Journal of Environmental Sciences,* 21, 237-242.

Lee, K. E., Morad, N., Teng, T. T. & Poh, B. T. 2012. Development, characterization and the application of hybrid materials in coagulation/flocculation of wastewater. *A review in Chemical Engineering Journal,* 203, 370-386.

Lin, A. G., Liu, P. Y., Liu, G. & Zhang, G. Z. 2006. Progresses of membrane separation technique in oil-bearing water treatment in oil fields. *Industrial Water Treatment,* 26, 5-8.

Liu, Y., Zhou, S., Liu, R., Chen, M., Xu, J., Liao, M. & Yang, L. 2022. Study on amino-directed modification of oil sludge-derived carbon and its adsorption behavior of bisphenol A in water. *Separation and Purification Technology*, *298*, 121625.

Ma, Q., Li, G., Liu, X., Wang, Z., Song, Z. & Wang, H. 2018. Zeolitic imidazolate framework-8 film coated stainless steel meshes for highly efficient oil/water separation. *Chemical Communications,* 54, 5530-5533.

Melaphi, K., Sadare, O. O., Simate, G. S., WAgenaar, S. & Moothi, K. 2023. Adsorptive removal of BTEX compounds from wastewater using activated carbon-derived from macadamia nut shells. *Water SA,* 49, 36-45.

Montgomery, D. C. (2017). *Design and analysis of experiments*. John wiley & sons.

Nefzi, H., Abderrabba, M., Ayadi, S. & Labidi, J. 2018. Formation of palygorskite clay from treated diatomite and its application for the removal of heavy metals from aqueous solution. *Water, Air, and Soil Pollution,* 10(9), 1257.

Nekhavhambe, H. H. 2021. *Fabrication of macadamia nutshell powder-al/fe metal oxide modified diatomaceous earth composite beads for fluoride and pathogen removal from groundwater.* Masters Dissertation, University of Venda.

Nwadiogbu, J. O., Okoye, P. A. C. & Ajiwe, V. I. 2016. Removal of crude oil from aqueous medium by sorption on hydrophobic corncobs: Equilibrium and kinetic studies. *Journal of Taibah University for Science,* 10, 56-63.

Pakade, V. E., Ntuli, T. D. & Ofamaja, A. E. 2017. Biosorption of hexavalent chromium from aqueous solutions by macadamia nutshell powder. *Applied Water Science,* 7, 3015-3030.

Pan, Y. Q., Wang, W., Wang, T. H. & Yao, P. J. 2007. Fabrication of carbon membrane and microfiltration of oil-in-water emulsion: An investigation on fouling mechanisms. *Separation and Purification Technology,* 57, 388-393.

Pilkington, J. L., Preston, C. & Gomes, R. L. 2014. Comparison of response surface methodology (RSM) and artificialneural networks (ANN) towards efficient extraction of artemisinin from artemisia annua. *Industrial Crops and Products,* 58, 15-24.

Poinern, G. E. J., Senanayake, G., Shah, N., Thi-Le, X. N., Parkinson, G. M. & Fawcett, D. 2011. Adsorption of the aurocyanide, complex on granular activated carbons derived from macadamia nut shells—a preliminary study. *Minerals Engineering,* 24, 1694-1702.

Ramli, A. N. & Ghazi, R. M. 2020. Removal of oil and grease in wastewater using palm kernel shell activated carbon. *IOP Conference Series: Earth and Environmental Science,* 549(1), 012064.

Rashidi, N. A. & Yusup, S. 2016. An overview of activated carbons utilization for the post-combustion carbon dioxide capture. *Journal of Carbon Dioxide Utilization,* 13, 1-16.

Rathilal, S. & Tetteh, E. K. 2019. Response surface optimization of oil refinery wastewater treatment process. *Proceedings of 2nd International Conference on Research Advances in Engineering, Technology, Science and Management.*, 16-22.

Ratshomo, K. & Nembahe, R. 2018. Energy data collection, management and analysis. South Africa, Pretoria.

Rotorcarb-activated carbon. 2020. *Rotorcarb products* [Online]. Available: www.rotocarb.co.za [Accessed 3 August 2020].

Rushing, H., Karl, A. & Wisnowski, J. 2013. Response surface methodology and designs. In: Design and analysis of experiments vy douglas montgomery: A supplement for using JMP. *Quality and Reliability Engineering International*, 201-226.

Santo, C. E., Vilar, V. J. P., Bhatnagar, A., Kumar, E., Botelho, C. M. S. & Boaventura, R. A. R. 2013. Biological treatment by activated sludge of petroleum refinery wastewaters. *Desalination and Water Treatment,* 51, 6641-6654.

Shaobin, W. & Peng, Y. 2010. Natural zeolites as effective adsorbents in water and wastewater treatment. *Chemical Engineering Journal,* 156, 11-24.

Song, C. W., Wang, T. H., Pan, Y. Q. & Qiu, J. S. 2006. Preparation of coal-based microfiltration carbon membrane and application in oily wastewater treatment. *Separation and Purification Technology,* 51, 80-84.

Sulyman, M., Sienkiewicz, M., Haponiuk, J. & Zalewski, S. 2018. New approach for adsorptive removal of oil in wastewater using textile fibers as alternative adsorbent. *ACTA Scientific Agriculture (ISSN: 2581-365X),* 2.

Sun, X. F., Sun, R. C. & Sun, J. X. 2004. Acetylation of sugarcane bagasse using NBS as a catalyst under mild reaction conditions for the production of oil sorption—active materials. *Bioresource Technology,* 95, 343-350.

Tasker, T. L., Burgos, W. D., Piotrowski, P., Castillo-Meza, L., Blewett, T. A., Ganow, K. B., Stallworth, A., Delompré, P. L. M., Goss, G. G. & Fowler, L. B. 2018. Environmental and human health impacts of spreading oil and gas wastewater on roads. *Environmental Science and Technology,* 52, 7081-7091.

Teli, M. & Valia, S. 2013. Acetylation of banana fibre to improve oil adsorbency. *Carbohydrate Polymers,* 92, 328-333.

Tobiszewski, M., Tsakovski, S., Simeonov, V. & Namiesnik, J. 2012. Chlorinated solvents in a petrochemical wastewater treatment plant: An assessment of their removal using self-organising maps. *Chemosphere,* 87, 962-968.

Travis, M. J., Weisbrod, N. & Gross, A. 2008. Accumulation of oil and grease in soils irrigated with greywater and their potential role in soil water repellency. *Science of the Total Environment,* 394, 68-74.

Vlaev, L., Petkov, P., Dimitrov, A. & Genieva, S. 2011. Cleanup of water polluted with crude oil or diesel fuel using rice husks ash. *Journal of the Taiwan Institution of Chemical Engineers,* 42, 957-964.

Wang, F., Lei, S., Xue, M., Ou, J. & Li, W. 2014. In situ separation and collection of oil from water surface via a novel superoleophilic and superhydrophobic oil containment boom. *Langmuir,* 30, 1281-1289.

Wang, Q., Puerto, M. C., Warudkar, S., Buehler, J. & Biswal, S. L. 2018. Recyclable amine-functionalized magnetic nanoparticles for efficient demulsification of crude oil-in-water emulsions. *Environmental Science: Water Research and Technology,* 4.

Wang, X., Ma, X., Song, C., Locke, D. R., Siefert, S., Winansc, R. E., Mollmer, J., Lange, M., Moller, A. & Glaser, R. 2013. Molecular basket sorbents polyethylenimine-sba-15 for co_2 capture from flue gas: Characterization and sorption properties *Microporous and Mesoporous Material,* 169, 103-111.

Wongcharee, S., Aravinthan, V., Erdei, L. & Sanongraj, W. 2018. Mesoporous activated carbon prepared from macadamia nut shell waste by carbon dioxide activation: Comparative characterisation and study of methylene blue removal from aqueous solution. *Asia-Pacific Journal of Chemical Engineering,* 13(2), e2179.

Wu, P., Jiang, L. Y., He, Z. & Song, Y. 2017. Treatment of metallurgical industry wastewater for organic contaminant removal in China: Status, challenges, and perspectives. *Environmental Science: Water Research and Technology,* 3, 1015-1031.

Yakout, S. M. & Daifullah, A. A. M. 2013. Adsorption/desorption of BTEX on activated carbon prepared from rice husk. *Desalination and Water Treatment,* 52, 4485-4491.

Yang, Y., Jiang, X., Liu, H., Ai, G., Shen, L., Feng, X., Ye, F., Zhang, Z., Yuan, H. & Mi, Y. 2022. Diethylenetriamine modified biological waste for disposing oily wastewater *Environmental Research,* 212, 113395.

Ye, F., Jiang, X., Liu, H., Ai, G., Shen, L., Yang, Y., Feng, X., Yuan, H., Zhang, Z., Mi, Y. & Yan, X. 2022. Amine functional cellulose derived from wastepaper toward oily wastewater treatment and its demulsification mechanism. *Journal of Molecular Liquids,* 360, 119459.

Yessenbek, A., Satayev, M. & Azimov, A. 2023. Activated carbon production from plum pit shells for oily wastewater treatment. *Water Practice & Technology,* 18(3), 563-573.

You, Z., Zhang, L., Zhang, S., Sun, Y. & Shah, K. J. 2018. Treatment of oil-contaminated water by modified polysilicate aluminum ferric sulfate. *Processes,* 95(7), 95.

Yu, L., Han, M. & He, F. 2013. A review of treating oily wastewater. *Arabian Journal of Chemistry,* 7, S1913-S1922.

Zhang, G., Ji, S. & Xi, B. 2006. Feasibility study of treatment of amoxillin wastewater with a combination of extraction, Fenton oxidation and reverse osmosis. *Desalination,* 196(1-3), 32-42.

Zhao, P., Zhang, G., Yan, H. & Zhao, Y. 2021. The latest development on the amine functionalized solid adsorbents for post-combustion CO_2 capture: Analysis review. *Chinese Journal of Chemical Engineering,* 35, 17-43.

Zouboulis, A. I. & Avranas, A. 2000. Treatment of oil-in-water emulsions by coagulation and dissolved-air flotation. *Colloids and Surfaces A Physicochemical and Engineering Aspects,* 172, 153-161.

Chapter 3: Preparation and Characterization of Acid Leached Diatomaceous Earth for Application in Treatment of Oily Wastewater

Abstract

This chapter evaluated the potential application of acid-leached diatomaceous earth in oily wastewater treatment. Acid-leached diatomaceous earth was prepared by treating diatomaceous earth using 2.2 M HNO_3 to remove impurities. The leached diatomaceous earth was characterized using X-ray diffraction (XRD), X-ray fluorescence (XRF), scanning electron microscopy (SEM) and Brunauer Emmett Teller (BET) analytical techniques to determine the crystallinity, elemental content, morphology, and surface area, respectively. Response surface methodology (RSM) was employed to establish the optimum conditions on the treatment of oily wastewater using acid-leached diatomaceous earth. Elemental composition of the acid-leached DE showed an increase in silica content from 78.98% to 91.57% and a decrease in the composition of CaO, K_2O, MgO, and Fe_2O_3 which are associated with impurities such as carbonates and clay minerals. BET analysis showed an increase in pore volume and surface area from 60.88 to 68.71 Å and 15.02 to 22.40 m^2/g, respectively, following the acid leaching. The oil removal experiments revealed a maximum adsorption capacity of 124.16 mg/g and oil removal efficiency of 78.55% at an initial oil concentration of 3229.69 using 0.05 g adsorbent dosage and 119.20 mins contact time. The adsorption kinetics data are fitted better the pseudo-second order model (R^2=0.98) of reaction kinetics indicating that adsorption occurred through chemisorption. The adsorption isotherms were described better by the Freundlich isotherms model (R^2=0.87) indicating that adsorption occurred in a heterogeneous and multilayer surface. Acid-leached diatomaceous earth has the potential to remove contaminants from oily wastewater.

Keywords: Acid leaching; Adsorption; Diatomaceous earth; Response Surface Methodology; Synthetic Oily Wastewater.

3.1. Introduction

Diatomaceous earth (DE), which is also be referred to as diatomite, is known to be a siliceous sedimentary rock that contains between 80 and 90% amorphous hydrated silica ($SiO_2.nH_2O$), as well as a variety of impurities such clay minerals, carbonate minerals, silica sand, iron oxides, and organic matter (Akafu et al., 2019). The chemical and physical characteristics of DE make it versatile and has found application in beer filter aids, in the water purification industry, as a mycotoxin binder, as a dietary supplement for animals, as a performance enhancer in livestock, as a dynamite stabilizer for trinitroglycerin, in brick-making, and in pest control of stored grain (Shaobin & Peng, 2010, Koster, 2013, Antonides, 2017, Ikusika et al., 2019).

According to Benkacem et al. (2018), the hydroxyl groups on the surface of DE, which are the most significant reactive sites, are responsible for much of the material's reactivity. Apart from the hydroxyl groups, acidic sites such as iron oxide and aluminum oxide are significant sites on the surface of DE (Yuan et al., 2004). However, the utilization of DE is constrained by the presence of contaminants such as clay and calcium carbonate on its surface. Acid leaching is used to improve the surface characteristics and chemistry of the DE by removing these contaminants. Acid leaching removes impurities such as carbonate groups that may obstruct the natural pores of the DE (Benkacem et al., 2018). Acid-leached DE has been employed in a variety of processes, including electrochemistry, optoelectronics, photodegradation of organic contaminants, and the production of porous ceramics (San et al., 2009, Benkacem et al., 2016, Benkacem et al., 2018, Aggrey et al., 2021).

DE has been previously used for the adsorption of various contaminants, including heavy metals and methylene blue from wastewaters, and the results were promising and positive (Tsai et al., 2006, Aivalioti et al., 2010, Bandura et al., 2017). It has shown potential capabilities to adsorb petroleum contaminants, due to its high adsorption capacity (Tasker et al., 2018). Literature related to the application of acid-leached DE in oily wastewater treatment is scarce. However, impurities in the raw DE affect the uptake of toxicants from aqueous solutions, resulting in low adsorption capacity (Bello et al., 2014). Therefore, leaching DE will eliminate impurities and lower impurity material contents, leading to an enhanced adsorption capacity of DE. Thus, in this chapter, we hypothesize that acid-leached DE will have enhanced oil adsorption capacity. The specific objective set were: 1) to activate DE via acid-leaching, 2) to optimize the conditions for oil removal, and 3) to model the adsorption mechanism using adsorption kinetics and isotherm models.

3.2. Materials and methods

3.2.1. Materials

The DE used here was procured from Eco-Earth Company (Midrand, South Africa). Sodium hydroxide and hydrochloric acid were acquired from Rochelle Chemicals in Johannesburg, South Africa, and were of analytical grade. Deionized water (18.2 µm/cm) from the Merck Millipore water system was used to prepare working solutions. Sea salt was purchased from Shoprite Store in Thohoyandou. Kerosene, gasoline, and diesel were purchased at the Shell garage as petroleum fractions (Thohoyandou, Limpopo).

3.2.2. Preparation of acid-leached diatomaceous earth

The acid-leached DE was prepared following the procedure outlined by Abdellaoui et al. (2018). Briefly, 10 g of DE was added into a 250 mL beaker containing 120 mL of 2.2 M HNO_3. The mixture was stirred using a hotplate at 60 ºC and 300 rpm for a period of 3 hrs. During stirring, 40 mL of HNO_3 solution was added gradually to eliminate small amounts of impurity mineral and increase the leaching ratio of impurities and a final volume of 120 mL of HNO_3 was used. The obtained mixture was filtered through Macherey-Nagel 615 125 mm filter papers, and the residues were washed to near neutral pH using 1.5 L of deionized water and thereafter oven-dried at 50°C for 12 hours. The acid-leached DE was then ground into fine powder using mortar and pestle and then kept in a zip-locked sample bag.

3.2.3. Characterization

The S1 titan handheld X-ray fluorescence (XRF) spectrometer was used to determine the elemental compositions of raw DE and acid-leached DE (Bremen, Germany). Tristar II was used to determine the surface area and pore characteristics according to Brunauer Emmet Teller (BET) (Micromeritics, USA). The X-ray diffractometer (XRD) (Bruker, Germany) was used to assess the crystallinity and mineral phase composition of the DE. The morphological analysis of the material and electron mapping was performed using scanning electron microscopy coupled with energy dispersion X-ray spectroscopy (SEM-EDS) (FEI Nova NanoSEM 230 from Eindhoven, Netherlands).

3.2.4. Preparation of synthetic oily wastewater

Synthetic oily wastewater used in this study was prepared following the procedures used by Kehinde (2012) and Dickhout et al. (2019) with slight modification. Briefly, 0.02 g of each of the three petroleum fractions (kerosene, petrol, and diesel), 1.3 g of sea salt, and 0.23 g of sodium dodecyl sulphate were weighed and transferred into a 500 mL beaker of deionized

water. Each mixture adhered to the range of optimised parameters generated using the response surface methodology (RSM) shown in Table 3.1 and subsequently homogenized through sonication for 5 mins.

3.2.5. Oil removal experiments

Optimization of conditions for oil removal using acid-leached DE was carried out using the response surface methodology (RSM) experimental design software (version 11, Stat-Ease Inc., Minneapolis, USA). Table 3.1 summarizes the conditions and ranges considered for optimization. The experiments were performed as follows; various amounts of acid-leached DE were weighed and enclosed in a tea bag. Thereafter, tea bags containing the adsorbents were placed in 250 mL beakers containing 25 mL of synthetic oily effluent and left undisturbed for various periods as guided by the experimental design from RSM. At the end of the experiment, mixtures were filtered through an EZ-Pak ® membrane filter. The residual oil contents were estimated in the form of total organic carbon using Spectroquant UV spectrophotometer from Merck group (Germiston, South Africa). For quality assurance, a blank experiment was performed using an empty tea bag. The oil removal efficiencies and adsorption capacities were estimated using Equation 3.1 and 3.2, respectively.

$$\% \text{ Removal} = \left(\frac{(C_i - C_f)}{C_i}\right) 100 \qquad (3.1)$$

$$Qe = \left(\frac{(C_i - C_f)}{m}\right) V. \qquad (3.2)$$

Where Qe (mg/g) denotes the adsorbent's equilibrium adsorption capacity per milligram dry weight, V (L) symbolizes the solution volume, and m (g) denotes the adsorbent mass. Ci and Cf denote the oil concentrations (mg/L) before and after treatment, respectively.

Table 3.1: Range of optimized parameters as predicted by the RSM

Name	Low	High
Adsorbent dosage (g)	0.01	0.05
Contact time (min)	60	180
Initial oil concentration (mg/L)	500	10000

3.2.6. Adsorption kinetics

The adsorption kinetics were determined for a solution of synthetic oil wastewater containing 500 mg/L initial oil concentration of 0.1 g/25 mL of adsorbent dosage for various contact times ranging from 10 to 120 min. The obtained data was analyzed using non-linear equations of pseudo-first order and pseudo-second order models of reaction kinetics (Eq. 3.3-3.4), as well as Weber-Morris model of intraparticle diffusion (Eq. 5).

$$qt = qe\ (1 - e^{-k_1 t}) \tag{3.3}$$

$$qt = \frac{qe^2 k_2 t}{1 + k_2 q_e t} \tag{3.4}$$

$$qt = k_i t^{0.5} + ci \tag{3.5}$$

Where q_e and q_t symbolizes the adsorption capacities at equilibrium and time t, respectively; k_1 and k_2 are the rate constants for pseudo-first order and pseudo-second order, respectively. The constant of intra particle diffusion rate, K_i (mg/g min^{-1}), is determined by the slope of $t^{0.5}$ vs. q_t, while C_i is the constant of the boundary layer thickness (Mudzielwana et al., 2018).

3.2.7. Adsorption isotherms

The adsorption isotherms were determined using linear equations of Langmuir and Freundlich adsorption isotherms models (Eq. 3.6-3.7) and were used determine the adsorbate-adsorbent interaction. The isotherms were determined at concentration ranges of 50 to 200 mg/L.

$$\frac{C_e}{q_e} = \frac{1}{K_a q_m} + \frac{1}{q_m} C_e \tag{3.6}$$

$$Log q_e = Log K_F + \frac{1}{n} Log C_e \tag{3.7}$$

Where, C_e, K_a, q_e and q_m denote the adsorption capacity (mg/g), the equilibrium concentration (mg/L), the Langmuir constant associated to enthalpy of adsorption (L/mg) and theoretical maximum adsorption capacity (mg/g), respectively. The K_F values correspond to the Freundlich constant that is interrelated to adsorption capacity and adsorption intensity. The heterogeneity factor is 1/n, where n represents the process's intensity, the diversity of the adsorbent's reactive sites, and the relative energy distribution (Abdulkareem et al., 2021). When $0 < 1/n < 1$, the adsorption is favourable; when 1/n=1, the adsorption is irreversible; and when $1/n > 1$, the adsorption is unfavourable (Abbas, 2020).

3.2.8. Goodness-of-fit valuation

The goodness-of-fit calculations for the model was carried out to confirm the suitability of the kinetics, and isotherm models which were attained from the data derived from the experiments via the correlation coefficient (R^2) and root mean square error (RMSE) expressed by Eq. 3.8-3.9.

$$R^2 = 1 - \frac{\Sigma(q_{e,exp} - q_{e,calc})2}{\Sigma(q_{e,exp} - q_{e,mean})2} \tag{3.8}$$

$$RMSE = \sqrt{\frac{1}{n-1}\sum_{i=1}^{n}\left(q_{e,exp} - q_{e,calc}\right)^2}_{i} \tag{3.9}$$

where $q_{e,\,calc}$ refers to the adsorbate theoretical concentration on the adsorbent, which has been calculated using an isotherm model. $q_{e,\,exp}$ is the concentration of adsorbed solid-phase which is experimentally measured.

3.3. Results and discussion

3.3.1. Bulk chemical analysis

Table 3.2 depicts the elemental composition of the raw and acid-leached DE. The silica (SiO_2) content in the acid-leached DE reached 91.57% due to silica to the fact that silica is relatively resistant to acid attack (Benkacem et al., 2018). This shows that HNO_3 has the ability to remove metals such as alkali and alkaline earth from DE, and these include potassium (K), magnesium (Mg) and calcium (Ca). Also, CaO, MgO, Fe_2O_3, P_2O_5, S, and Cl decreased during the leaching process (Abdellaoui et al., 2018). The increase in Al_2O_3 may be due to the removal of alkali and alkaline earth from the DE as stated above. The decrease in elemental composition of alkali

earth metals after acid leaching indicates the successful removal of carbonate and clay mineral impurities, and this shows that the DE was successfully acid-leached. Furthermore, the removal of alkali earth metals from acid-leached DE contributes to the improved chemistry of the material.

Table 3.2: Elemental composition of raw diatomaceous earth and acid-leached diatomaceous earth.

Element Name	Raw diatomaceous earth (%)	Acid-leached DE (%)
SiO_2	73.98	91.57
CaO	6.64	0.11
MgO	0.97	0.53
Al_2O_3	0.88	1.15
Fe_2O_3	0.81	0.62
K_2O	0.37	0.40
S	0.19	0.02
P_2O_5	0.08	0.01
TiO_2	0.06	0.15
Cl	0.01	0.00

3.3.2. Morphological analysis

Figure 3.1 shows the raw DE micrograph image with rectangular pores organized in a regular form on each diatom (Figure 3.1a). The EDS spectra showed the presence of Si, O, and Ca in the DE, which confirms that DE is rich in silicate. Similar findings were reported by Izuagie et al. (2016). The presence of carbon could be attributed to carbon material used for coating during SEM analysis (Banerjee et al., 2017). Fig. 3.1c shows the micrograph of acid-leached DE, which appears to be more porous. The pores could be attributed to the removal of impurities. The absence of Ca in the EDS spectra of acid-leached DE confirms the removal of the impurities.

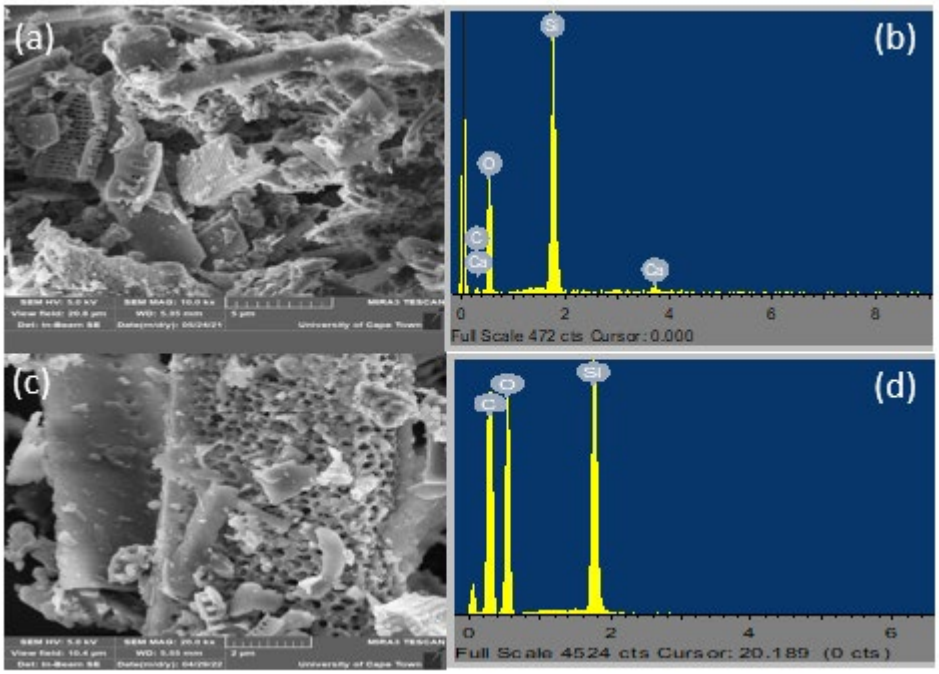

Figure 3.1: Micrographs and EDS-Spectrum of Raw DE (a-b) and Acid-leached DE (c-d).

3.3.3. X-ray diffraction analysis

Figure 3.2 depicts the diffractogram of the raw DE and acid-leached DE. The results show the presence of amorphous and quartz phases of SiO_2 in both raw and acid-leached DE.

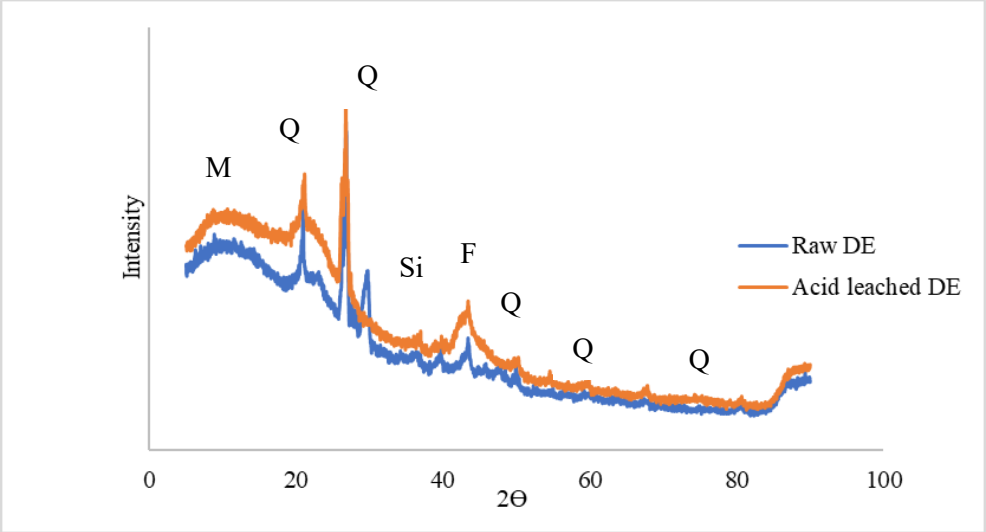

Figure 3.2: Diffractogram of raw and acid-leached DE (Q, M, F, and Si stand for Quartz, Mica, Feldspar, and Silica, respectively).

Amorphous phase was detected at 2θ range of 0-20º. Benkacem et al. (2018) also reported similar results and attributed these amorphous to mica mineral phases. There was no

significant change in the mineral phases of the DE after acid-leaching. However, the intensity of quartz peaks increased, indicating the abundance of SiO_2 minerals.

3.3.4. Surface area and pore characteristics

Table 3.3 depicts the BET surface area and pore characteristics of raw and acid leached DE. It is noted that there was an increase in pore, diameter, and surface area after acid-leaching was observed (Table 3.3). These correspond to the SEM results showing large pores in acid-treated DE (Figure 3.1c). In addition, the resulting pore diameter affirms the macroporosity of the acid-leached DE. The increased surface area and pore diameter could be essential for the enhancement of the adsorption capacity of the material.

Table 3.3: BET analysis results of raw DE and acid-leached DE.

	Raw DE	Acid leached DE
BET surface area (m^2/g)	15.02	22.40
Pore volume (cm^3/g)	0.02	0.03
Pore diameter (Å)	60.88	68.71
Average particle size (Å)	3 925.92	2 678.35

3.4. Oil removal experiments

Figure 3.3 shows (a) the adsorbent-treated solution, and (b) synthetic oily wastewater. The treated solution appears clear while the untreated solution appears cloudy, mainly because of the adsorbed oil molecules on the surface of the acid-leached adsorbent. The response surface plots obtained from the oil removal experiments are shown in Figures 3.4-3.6.

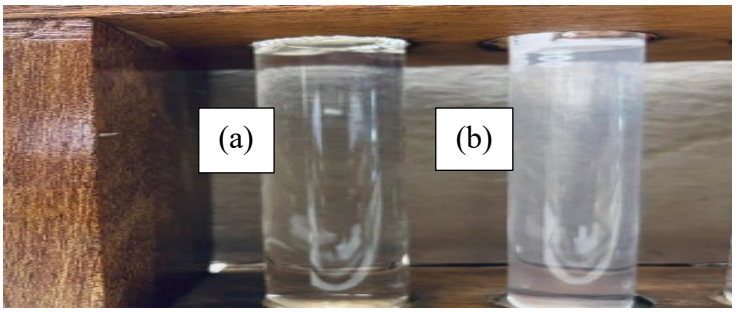

Figure 3.3: Adsorbent-treated solution (a) and Synthetic oily wastewater (b).

3.4.1. Response surface plots

The effect of adsorbent dosage and contact time on oil removal percentage is shown in Figure 3.4. It is noted that an increase in both contact time and adsorbent dosage increases the oil

removal percentage. This could be attributed to the fact that longer contact time gives enough time for molecules to attach to the binding sites and further diffuses onto the internal pores of the material. An increase in adsorbent dosage, on the other hand, leads to an increase in active sites for adsorption of the oil droplets (Singhal et al., 2014, Syuhada et al., 2017, Rahdar et al., 2019, Izevbekhai et al., 2020b). The highest percentage of oil removed was 78.01%. This was achieved by an adsorbent dosage of 0.03 g and a contact time of 120 mins.

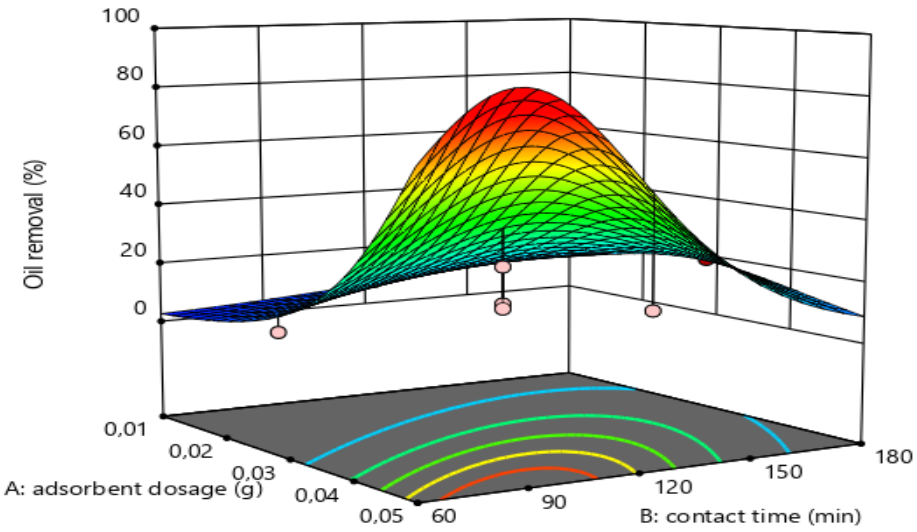

Figure 3.4: Variation of oil removal percentage against contact time and adsorbent dosage.

Figure 3.5 illustrates the effects of adsorbent dosage and initial oil concentration on oil removal percentage. It is observed that the percentage of oil removal increased with increasing adsorbent dosage and decreased with increasing initial concentration. Izevbekhai et al. (2020) also noted similar results. They attributed this to the fact that increasing initial concentration leads to more adsorbate molecules in the solution with limited adsorption sites, while increasing adsorbent dosage gives rise to more sorption sites. The maximum oil uptake of 78.01% was noted at an initial concentration of 5250 mg/L and an adsorbent dosage of 0.05 g.

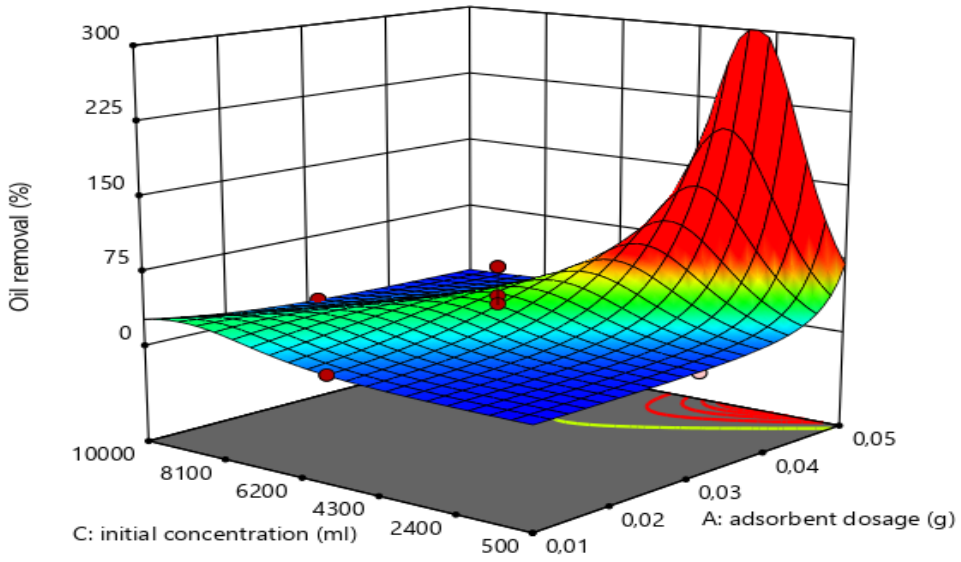

Figure 3.5: Variation of oil removal percentage against initial oil concentration and adsorbent dosage.

Figure 3.6 depicts the variation of oil removal percentage with initial oil concentration and contact time. The oil removal percentage increased with increasing contact time.

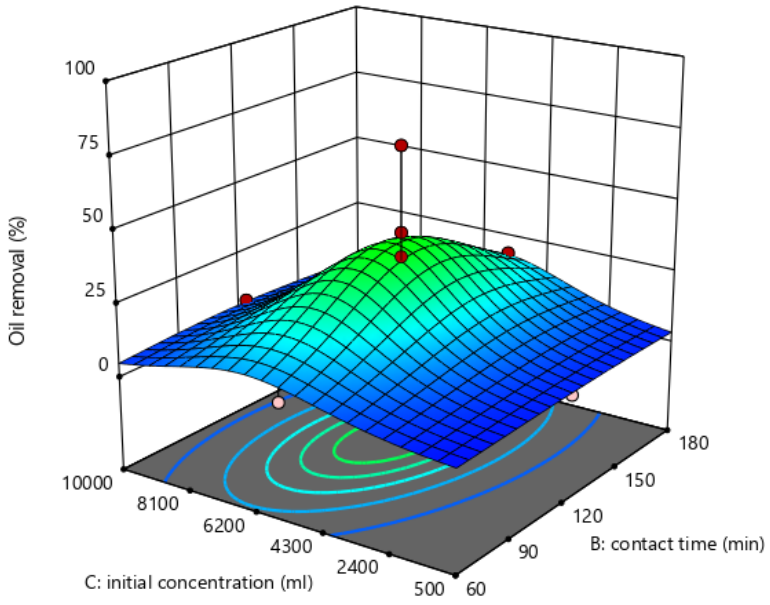

Figure 3.6: Variation of oil removal percentage against initial oil concentration and contact time.

This is described to increased interaction between oil and the adsorbent since the adsorbent spends a longer period in contact with the synthetic oily wastewater solution (Najaa Syuhada, 2017). The maximum oil removal percentage of 78.01% was achieved at the contact time and initial oil concentration of 120 mins and 5250 mg/L, respectively.

3.4.2. Response surface cube plot

The cube plot in Figure 3.7 presents the performance summary of the RSM model. The minimum and maximum percentages of oil removal accomplished are shown on the axis of the plot. The values displayed within the cube correspond to the predicted oil removal efficiency of 34.66%. Mid-range adsorbent dosage (0.03 g), initial oil concentration (5250 mg/L), and contact time (180 mins) resulted in maximum oil removal (78.01%), while higher ranges of adsorbent dosage (0.05 g), initial oil concentration (10000 mg/L), and contact time (180 mins) resulted in minimum oil removal (0.98%). (120 mins).

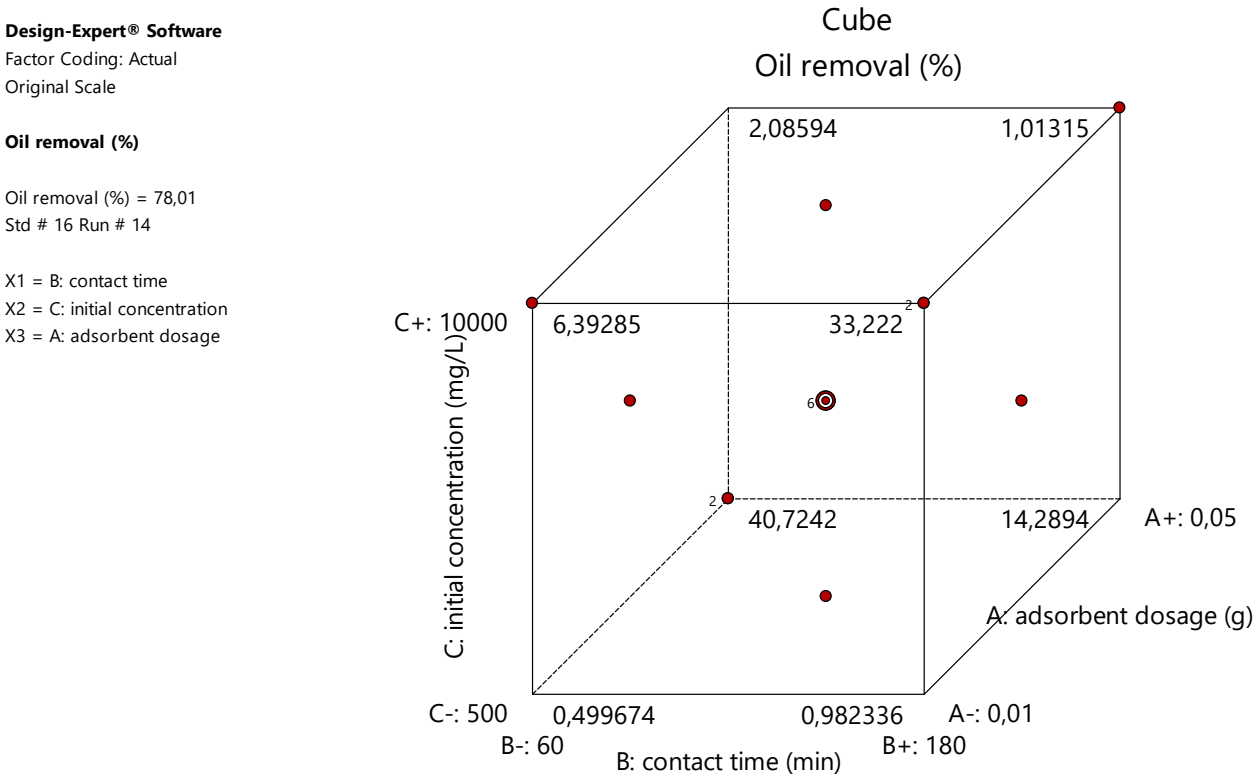

Figure 3.7: Summary of the RSM model.

3.4.3. Optimum conditions obtained from response surface methodology

Table 3.4 depicts the optimum conditions that yielded the maximum oil removal percentage and adsorption capacity. The model showed that the optimum conditions for the oil removal were an initial oil concentration of 3229.69 mg/L with an adsorbent dosage of 0.05 g and

contact time of 119.20 mins, which yielded a maximum percentage of 78.55% and an adsorption capacity of 124.16 mg/g with the desirability of 1.

Table 3.4: Optimum conditions for oil removal percentage and adsorption capacity.

Initial Oil Concentration (mg/L)	Adsorbent Dosage (g)	Contact Time (mins)	Oil removal percentage (%)	Adsorption Capacity (mg/g)	Desirability
3229.69	0.05	119.20	78.55	124.16	1

3.4.4. Predicted and actual value plot

The model-predicted values acquired from the model prediction were compared with the actual values plotted in Figure 3.8. Points with a green colour were equivalent to the predicted values, points with a red colour denoted points that were higher than the predicted values, while the blue-coloured points denote values lower than the predicted values.

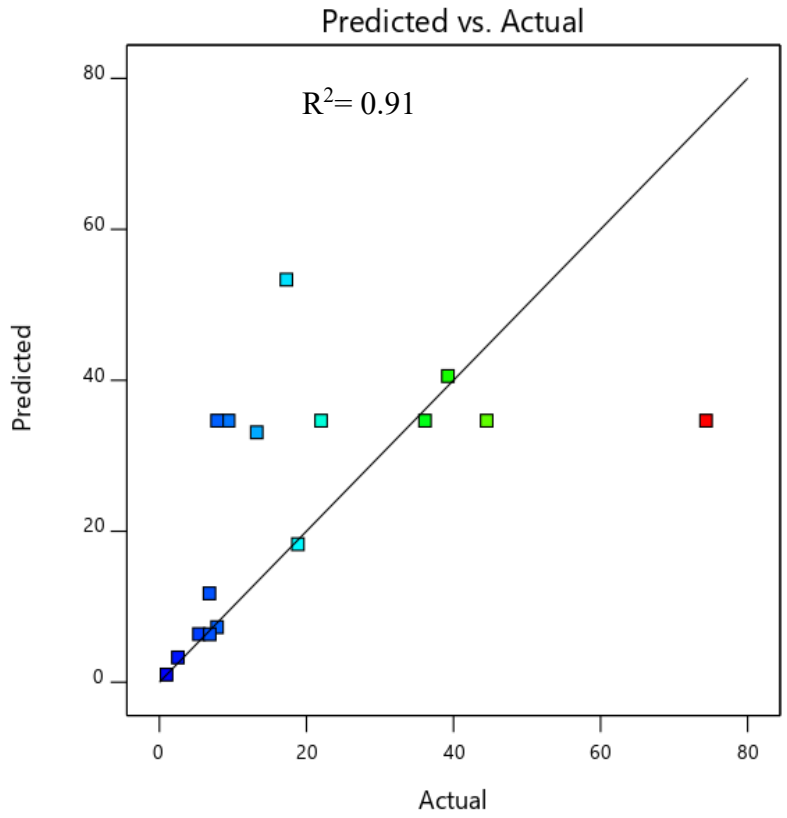

Figure 3.8: Comparison between predicted and actual values by Response Surface Methodology.

The coefficient of determination R^2 was found to be 0.91. This demonstrated that the predicted and actual values were in good agreement, and that the model of quadratic polynomials selected was enough to account for the correlation between the optimized variables and the response.

3.4.5. Analysis of variance

The significance of the model was tested using analysis of variance (ANOVA) and the results are shown in Table 3.5. The *p*-value and F-value were found to be 0.02 and 6.50, respectively, indicating a significant fit of the model. The model term, such as the quadratic function (C^2) of the initial oil concentration, is significant and influenced the percentage of oil removed. Initial oil concentration directly impacts the oil removal percentage; an increase in the initial oil concentration results in a decrease in the oil removal percentage. Additionally, a non-significant lack of fit was observed with an F-value of 2.04. Consequently, a non-significant lack of fit indicates that the model fits and is sufficient to signify the parameters-response relationship (Tetteh and Rathilal, 2019).

Table 3.5: ANOVA for Quadratic model and model terms.

Source	**F-value**	**p-value**	
Model	6.50	0.012	Significant
A-adsorbent dosage	2.73	0.15	
B-contact time	0.17	0.70	
C-initial concentration	1.27	0.30	
AB	0.46	0.52	
AC	4.26	0.08	
BC	0.08	0.79	
A^2	0.79	0.41	
B^2	0.96	0.37	
C^2	10.60	0.02	
Residual			
Lack of Fit	2.04	0.21	not significant

3.5. Adsorption Kinetics

Table 3.6 presents the values obtained from adsorption kinetics data modelling using pseudo first-order and second-order reaction kinetics models as well as Webber-Morris intraparticle diffusion model. Their respective plots are presented in Figures 3.9a and 3.9b. Based on the correlation coefficient values, the adsorption kinetics followed the pseudo second-order reaction kinetics (R2=0.98) rather than the pseudo first-order (R^2=0.84). This suggests that the dominant uptake mechanisms of oil molecules by the acid-leached DE is with the chemisorption process (Ho, 2006, Lim et al., 2020).

The intra-particle diffusion plot (Figure 3.9) showed two clearly defined regions, demonstrating that the adsorption of oil molecules by acid-treated DE involves more than one rate-limiting process (Zhu et al., 2019). Phase 1 of the plot is attributed to adsorption on the boundary layer of the adsorbent, where oil molecules were physically attached to the surface of the material. Phase 2 is associated with the diffusion of the molecules into the internal layer of particles through the macro-pores leading to chemisorption. Phase 1 had a larger intraparticle rate constant (Ki), which suggests that adsorption at the boundary layer occurred more quickly. The value of C was noted to be increasing (Table 3.6), suggesting an increase in the boundary layer of the adsorbent particles. A negative intercept (C) in phase 1 could be explained by a combination of effects of surface reaction control and film diffusion effects (Tan and Hameed, 2017).

Table 3.6: Constant parameters for pseudo first-order and pseudo second-order of reaction kinetics and intraparticle diffusion.

Parameters	Pseudo first-order	Pseudo-second order
K (min^{-1})	0.04	0.001
Q_e (mg/g)	34.73	42.97
R^2	0.84	0.98
X^2	0.48	0.46
RMSE	3.93	3.99
Intraparticle diffusion		
Parameters	Phase 1	Phase 2
K_i ($mg/g.min^{1/2}$)	21.11	1.95
R^2	1	0.99

C_I	-60.24	14.40

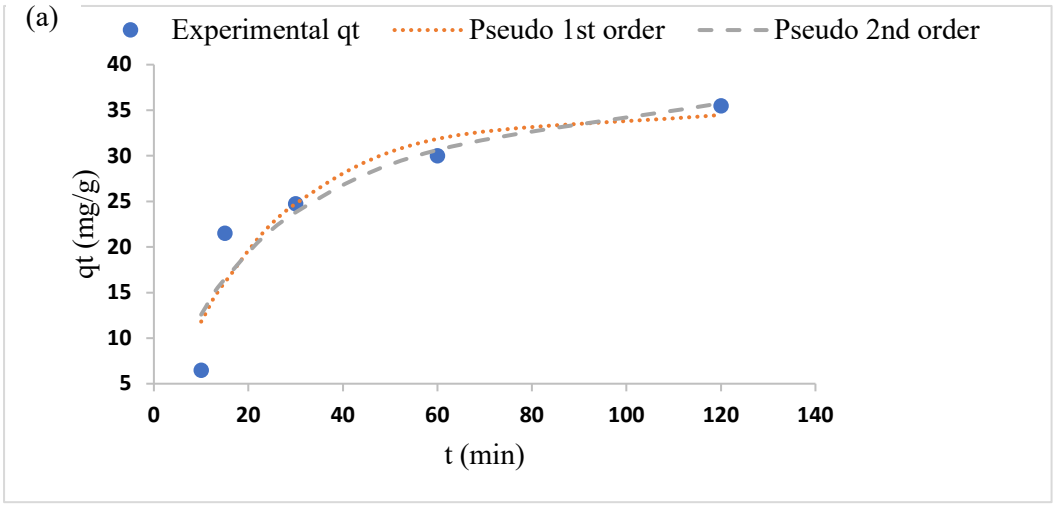

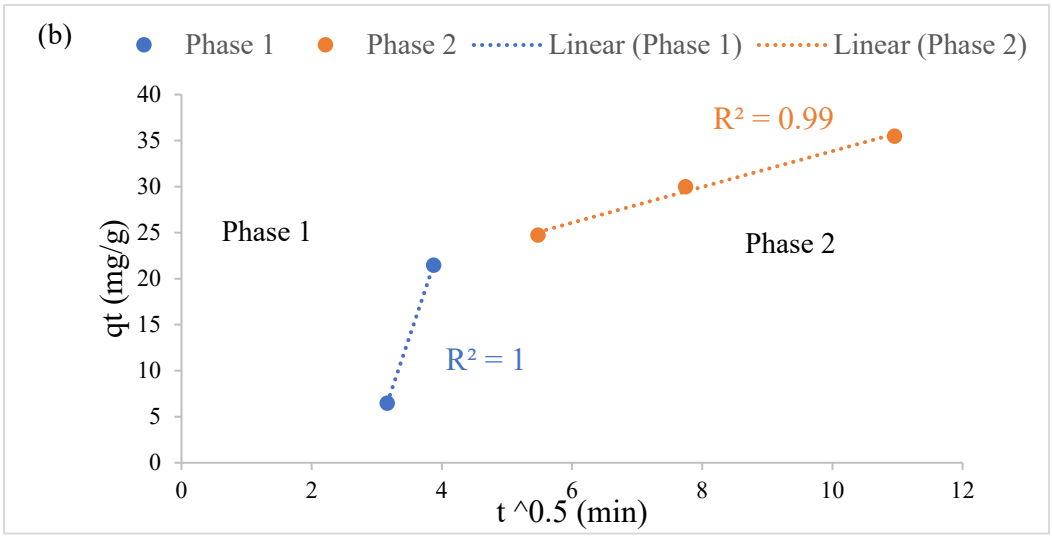

Figure 3.9: Kinetic models: (a) pseudo-first- and second order for oil adsorption onto the acid-leached DE, and (b) intraparticle diffusion plot for oil adsorption onto the acid-leached DE.

3.6. Adsorption Isotherms

The linear plots of adsorption isotherms are presented in Figure 3.10, while values for Langmuir and Freundlich isotherm model parameters are presented in Table 3.7. The findings demonstrated that the experimental data can be adequately fitted to Freundlich isotherms with high correlation coefficient of determination (R^2=0.87) compared to the Langmuir isotherms (R^2=0.13). This indicates that adsorption occurred on a heterogeneous and multilayer surface. Furthermore, the Freundlich intensity parameter (1/n) values that are less than 1 confirm the favourability of the sorption processes (Munzhelele et al., 2021).

Table 3.7: Adsorption isotherm parameters for oil adsorption onto the acid-leached diatomaceous earth

Freundlich Parameters	Values	Langmuir Parameters	Values
K_F (mg/g)	0.25	Q_m (mg/g)	0.46
1/n	0.83	*Ka* (L/mg)	-217.39
R^2	0.87	R^2	0.13

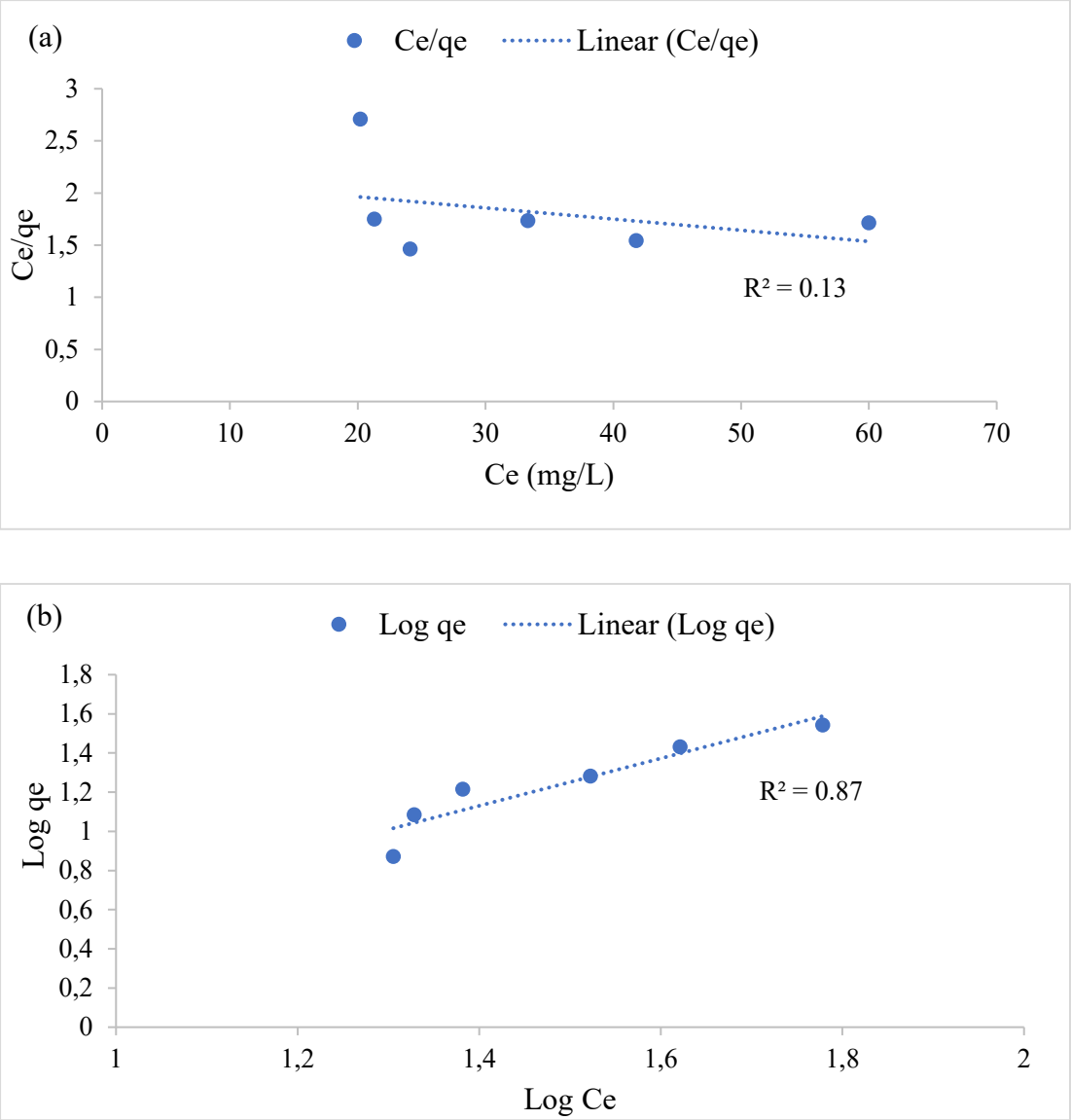

Figure 3.10: Linear plot (a) Langmuir and (b) Freundlich for oil adsorption onto the acid leached diatomaceous earth.

3.7. Summary

This chapter has successfully demonstrated the preparation and characterization of acid-leached DE as a highly effective and sustainable solution for treating oily wastewater. The raw DE was successfully activated through the leaching of impurities using HNO_3. It was noted that SiO_2 content increased from 78% to 91%, with other exchangeable fractions decreasing, confirming the removal of impurities. The oil adsorption of this acid-leached DE adsorbent in synthetic oily wastewater was then optimized using response surface methodology. When applied in the adsorption of oil from synthetic oily wastewater, the leached DE showed maximum oil removal efficiency of 78.55% with adsorption capacity of 124.16 mg/g at optimum conditions 3229.69 mg/L, 0.05 g adsorbent dosage and 119.20 mins contact time. It was found that the quadratic model chosen was fit and sufficient to signify the parameters-response relationship between the optimized parameters. The adsorption kinetics data showed better fitting to pseudo-second order of reaction while the isotherm data was described by Freundlich adsorption isotherm model. The obtained results imply that the acid-leached DE is a promising adsorbent for use in remediation of oily wastewater.

References

Abbas, M. 2020. Removal of brilliant green (BG) by activated carbon-derived from medlar nucleus (ACMN) – kinetic, isotherms and thermodynamic aspects of adsorption. *Adsorption Science and Technology,* 38, 464-482.

Abdellaoui, I., Islam, M. M., Sakurai, T., Hamzaoui, S. & Akimoto, K. 2018. Impurities removal process for high-purity silica production from diatomite. *Hydrometallurgy,* 179, 207-214.

Abdulkareem, A., Popelka, A., Sobol˘ciak, P., Tanvir, A., Ouederni, M., AlMaadeed, M. A., Kasak, P., Adham, S. & Krupa, I. 2021. The separation of emulsified water/oil mixtures through adsorption on plasma-treated polyethylene powder. *Materials Science and Engineering,* 14(5), 1086.

Akafu, T., Chimdi, A & Gomoro, K. 2019. Removal of fluoride from drinking water by sorption using diatomite modified with aluminum hydroxide. *Journal of analytical methods in chemistry*, *2019*.

Banerjee, S., Dubey, S., Gautam, R. K., Chattopadhyaya, M.C and & Sharma, Y. C. 2017. Adsorption characteristics of alumina nanoparticles for the removal of hazardous dye, orange g from aqueous solutions, *Arabian Journal of Chemistry,*12(8), 5339-5354.

Bello, O. S., Adegoke, K. A. & Oyewole, R. O. 2014. Insights into the adsorption of heavy metals from wastewater using diatomaceous earth. *Separation Science and Technology,* 49, 1787-1806.

Benkacem, T., Hamdi, B., Chamayou, A., Balard, H. & Calvet, R. 2018. Physicochemical characterization of a diatomaceous upon an acid treatment: a focus on surface properties by inverse gas chromatography. *Powder Technology*, *294*, 498-507.

Dickhout, J. M., Virga, E., Lammertink, R. G. H. & De Vos, W. M. 2019. Surfactant specific ionic strength effects on membrane fouling during produced water treatment. *Journal of Colloid and Interface Science,* 556, 12-23.

Ho, Y. 2006. Review of second-order models for adsorption systems. *Journal of Hazardous Materials,* 136, 681-689.

Izevbekhai, O., Gitari, W., Tavengwa, N., Ayinde, W. B. & Mudzielwana, R. 2020. Response surface optimization of oil removal using synthesized polypyrrole-silica polymer composite. *Molecules,* 25(20), 4628.

Izuagie, A. A., Gitari, W. M. & Gumbo, J. R. 2016. Defluoridation of groundwater using diatomaceous earth: Optimization of adsorption conditions, kinetics and leached metals risk assessment. *Desalination and Water Treatment,* 57, 16745-16757.

Kehinde, T. J. 2012. *Treatment of oilfield produced water with dissolved air flotation.* Master of Applied Science, Dalhousie University.

Lata, S. & Samadder, S. R. 2016. Removal of arsenic from water using nano adsorbents and challenges. *Journal of Environmental Management,* 166, 387-406.

Lim, A., Chew, J. J., Ngu, L. H., Ismadji, S., Khaerudini, D. S. & Sunarso, J. 2020. Synthesis, characterization, adsorption isotherm, and kinetic study of oil palm trunk-derived activated carbon for tannin removal from aqueous solution. *American Chemical Society OMEGA,* 5, 28673-28683.

Mudzielwana, R., Gitari, M. W., Akinyemi, S. A. & Msagati, T. A. 2018. Performance of Mn^{2+}-modified bentonite clay for the removal of fluoride from aqueous solution *South African Journal of Chemistry,* 71, 15-23.

Munzhelele, E. P., Ayinde, W. B., Mudzielwana, R. & Gitari, W. M. 2021. Synthesis of Fe doped poly p-phenylenediamine composite: Co-adsorption application on toxic metal ions (F^- and As^{3+}) and microbial disinfection in aqueous solution. *Toxics,* 9(4),74.

Najaa Syuhada, M. T., Rozidaini, M.G. & Norhisyam, I. 2017. Response surface methodology optimization of oil removal using banana peel as biosorbent. *Malaysian Journal of Analytical Sciences,* 21, 1101-1110.

Rahdar, S., Taghavi, M., Khaksefidi, R. & Ahmadi, S. 2019. Adsorption of arsenic (V) from aqueous solution using modified saxaul ash: Isotherm and thermodynamic study. *Applied Water Science,* 9, 87-95.

Singhal, S., Agarwal, S., Bahukhandi, K., Sharma, R. & Singhal, N. 2014. Bio-adsorbent: A cost-effective method for effluent treatment. *International Journal of Environmental Sciences and Research* 3, 151-156.

Syuhada, N., Mohd Ghazi, R. & Ismail, N. 2017. Response surface methodology optimization of oil removal using banana peel as biosorbent. *Malaysian Journal of Analytical Science.,* 21, 1101-1110.

Tan, K. L. & Hameed, B. H. 2017. Insight into the adsorption kinetics models for the removal of contaminants from aqueous solutions. *Journal of the Taiwan Institute of Chemical Engineers,* 74, 25-48.

Tasker, T. L., Burgos, W. D., Piotrowski, P., Castillo-Meza, L., Blewett, T. A., Ganow, K. B., Stallworth, A., Delompré, P. L. M., Goss, G. G. & Fowler, L. B. 2018. Environmental and human health impacts of spreading oil and gas wastewater on roads. *Environmental Science and Technology,* 52, 7081-7091.

Tetteh, E. K. & Rathilal, S. Response surface optimization of oil refinery treatment process. *In:* Insight, T., ed. 2nd International Conference on Research Advances in Engineering, Technology, Science and Management 2019 Dubai-United Arab Emirates. Tech Insight.

UN Water 2017. Statistics.

Yuan, P., Wu, D. Q., He, H. P. & Lin, Z. Y. 2004. The hydroxyl species and acid sites on diatomite surface: A combined IR and Raman study. *Applied Surface Science,* 227, 30-39.

Zhu, X., Wang, X., Liu, Y. & Li, Y. 2019. Efficient adsorption of oil in water by hydrophobic nonwoven fabrics coated with cross-linked polydivinylbenzene fibers. *Journal of Chemical Technology and Biotechnology,* 94, 128-135.

Chapter 4: Preparation and characterization of amine-functionalized macadamia nutshell-derived activated carbon for the treatment of oily Wastewater

Abstract

In this chapter, H_3PO_4 activated carbon was synthesized from macadamia nutshells (MNS) and further modified with amine groups using 98 wt% hydroxylamine hydrochloride. The synthesized material was then applied in the remediation of oily wastewater. Response surface methodology (RSM) was used to optimize the experimental conditions for preparation of activated carbon from MNS and oil removal using the amine-functionalized activated carbon. The optimum conditions for preparation of activated carbon were 30 min activation time, 410 ºC and 1:1 (H_3PO_4: MNS) activation ratio. Oily wastewater treatment experiments using functionalized activated carbon showed a maximum percentage removal of 82.93% with adsorption capacity of 167.96 mg/g at optimum conditions of 10 000 mg/L initial oil concentration, 0.1 g/25 mL adsorbent dosage and contact time of 60 mins. The adsorption kinetics data fitted the pseudo-second order model (R^2=0.92) indicating that adsorption occurred via chemisorption. The adsorption isotherm data fitted Freundlich adsorption isotherms model (R^2=1) indicating that adsorption took place in heterogeneous and multilayer surface. Results attained from this study demonstrated that the functionalized activated carbon has potential to remove oil from synthetic oily wastewater.

Keywords: Activated Carbon, Functionalization, Chemical Activation H_3PO_4 impregnation, Macadamia Nutshells, Oily Wastewater and Response Surface Methodology.

4.1. Introduction

Oily wastewater is considered hazardous to the environment because it consists of a wide variety of toxic organic and inorganic substances in a suspension (Jamaly et al., 2015). It important to reduce the toxicity of contaminants in the wastewaters prior to their discharge into the environment (Huang et al., 2018).

Accordingly, several processes have been developed and tested for treatment of oily wastewater. These include, adsorption (Jamaly et al., 2015), membrane filtration (Dickhout et al., 2017), electrochemical advanced oxidation (Moreira et al., 2017), reverse osmosis (Makisha, 2020), coagulation-flocculation (Zhao et al., 2020) and ion exchange (Comstock & Boyer, 2014). However, some of these processes have technical and economical constraints (Sohaimi et al., 2017). Adsorption process is often considered for treatment of oily wastewater due to its environmental friendliness, effectiveness in the removal of contaminants, and cost effectiveness. The cost effectiveness arises from the fact that most adsorbents are derived from green agricultural wastes and naturally-available clay materials (Kalash & Albayati, 2021).

Activated carbon (AC) is an example of a low-cost adsorbent that is typically prepared via carbonization of agricultural wastes such as wood chips (Yan et al., 2021), rice straws (Zhao et al., 2019) and MNS (Gummas & Okpeke, 2015). AC is an amorphous material with a highly developed porous structure and is primarily composed of carbon atoms organized. It often contains macropores bigger than 50 nanometers, mesopores between 2 and 50 nanometers, and micropores less than 2 nanometers of radius (Djilani et al., 2015). Du et al. (2017) prepared macadamia nutshell derived activated carbon via KOH activation under microwave radiation for efficient adsorption of reactive blue. Results obtained showed that the material has 876.77 m^3/g surface area and 0.53 cm^3/g total pore volume. Moreover, SEM micrograph showed that the material has a highly porous structure. MNS have proven to be suitable for utilization as a precursor of activated carbon.

The absence of active functional groups in activated carbon-based adsorbents limit their applicability in the adsorption of contaminants from wastewater (Liu et al., 2022). To enhance its adsorption efficiency, the surface of the activated carbon can be modified with amine groups (Lekene et al., 2021). Amine groups are widely considered as effective functional groups in adsorption of various contaminants (Yang et al., 2022). This was evident in a study by Liu et al. (2022) which modified oil sludge-derived carbon using polyethyleneimine (PEL) for the

adsorption of bisphenol-A in water. Their result showed 393.2 mg/g and 95% of the adsorption capacity and removal efficiency, respectively after a contact time of 1 hour.

This chapter aims to prepare amine-functionalized activated carbon and thereafter evaluate its efficiency in the treatment of oily wastewater. The specific objectives are to: 1) optimize conditions for synthesis of activated carbon from MNS, 2) functionalize activated carbon with an amine functional group, 3) characterize the prepared activated carbon and amine-functionalized activated carbon, and lastly, 3) evaluate the effectiveness of the prepared amine-functionalized activated carbon in the treatment of oily wastewater.

4.2. Material and methods

4.2.1. Materials

MNS were obtained from Royal Macadamia Farm in Levubu, South Africa. The analytical grade orthophosphoric acid used for activation was purchased from Rochelle Chemicals (Johannesburg, South Africa) and the working solutions were prepared using deionized water from Millipore water (18.2 MΩ/cm). Sea salt was purchased from Shoprite at the Thohoyandou Venda Plaza. Petroleum fractions (kerosene, petrol, and diesel) were purchased from Shell garage in Thohoyandou, Limpopo, South Africa.

4.2.2. Preparation of macadamia nutshells

MNS were repeatedly washed using deionized water to remove impurities. Thereafter, the washed nutshells were air-dried for 2 days before they were milled into <75 µm particles using a Retsch ball milling machine. The obtained fine powder was stored in zip-lock plastic bags awaiting further use.

4.2.3. Preparation of activated carbon

Activated carbon was synthesized by following, with slight modification, a procedure developed by Benadjemia et al. (2011). Figure 4.1 shows the flow chart for the synthesis of activated carbon. RSM was used to determine the optimum conditions for synthesis of activated carbon. The parameters varied are depicted in Table 4.1. A total of 13 runs were completed under the various conditions outlined in Table 4.2. To determine the optimum conditions, the percentage carbon yield was quantified using Eq. 4.1. Furthermore, oil removal experiments were performed with all 13 samples of activated carbon using 1 g/25 mL adsorbent dosage, a contact time of 180 mins and an initial concentration of 500 mg/L. Equation 4.2 was used to compute oil removal percentage.

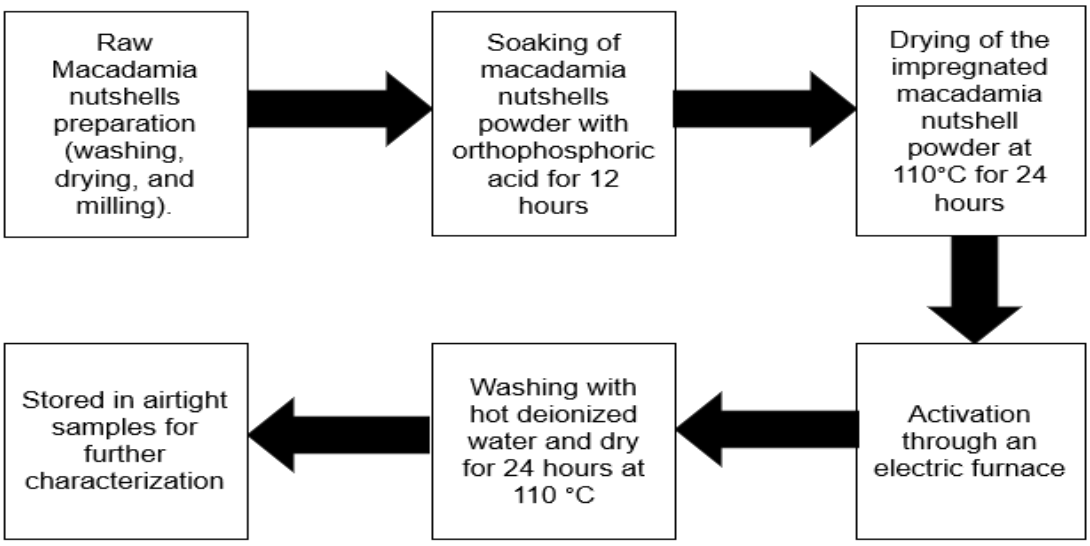

Figure 4.1: The flow chart to produce activated carbon.

Table 4.1: Range of optimized parameters as predicted by the RSM

Name	Low	High
Temperature (°C)	410	600
Impregnation ratio -	1:1	3:2
Activation time (min)	30	90

Table 4.2: Experimental runs for preparation of activated carbon from MNS predicted by the RSM.

Run	Temperature (°C)	Impregnation ratio	Activation time (min)
1	505	1:1	60
2	410	1:2	90
3	600	3:2	90
4	505	1:1	60
5	505	1:1	60
6	410	1:2	90
7	505	1:1	60
8	600	1:2	30
9	410	3:2	30
10	600	3:2	90
11	600	1:2	30
12	505	1:1	60
13	410	3:2	30

The carbon yield % was calculated using Eq.4.1.

$$\text{Yield } \% = \left(\frac{m_f}{m_i}\right) 100 \quad . \qquad (4.1)$$

Where, m_f and m_i denote the weights of the activated carbon (g) and weight of the dried raw material before activation (g), respectively.

4.2.4. Amine-functionalization of activated carbon

Sample obtained from Run 11 (Table 4.2) prepared (under 600 °C, 1:2 impregnation ratio, and 30 mins activation time) was considered for modification using amine functional groups. The functionalization was performed following the method used by Bezerra et al. (2011). Briefly, 2 g of activated carbon was soaked in 50 mL of hydroxylamine hydrochloride (98 wt% concentration) for 3 hours at 120 °C under continuous stirring at 250 rpm. The amine-functionalized activated carbon was then separated from the amine solution by evaporation to dryness at 300 °C using a rotary vapor. The equation of the functionalization process of the activated carbon is given in Eq. 4.2.

$$AC + NH_3\mathrm{OH.Cl} \rightarrow \mathrm{AC} - NH_2 + \mathrm{OH} + \mathrm{HCl} \quad (4.2)$$

4.2.5. Characterization of prepared adsorbents

The S1 titan handheld x-ray fluorescence (XRF) (Bremen, Germany) and Thermo Flash 2000 series CHNS/O organic Elemental analyzer (Cert Ref Std Sulfamethazine) were used to determine the elemental compositions of raw MNS and activated carbons. Fourier Transform Infrared Spectroscopy (FTIR) was used to determine the functional groups (Bruker, Germany). Tristar ll. was used to determine the surface area and pore characteristics according to Brunauer Emmet Teller (BET) (Micromeritics, USA). The X-ray diffractometer (XRD) was used to assess the crystallinity and mineral phase composition (Bruker, Germany). The morphological analysis of the materials and electron mapping was performed using scanning electron microscopy coupled with energy dispersion x-ray spectroscopy (SEM-EDS) (FEI Nova NanoSEM 230 from Eindhoven, Netherlands).

4.2.6. Preparation of synthetic oily wastewater

Synthetic oily wastewater used in this study was prepared following the procedures used by kehinde (2012) and Dickhout et al. (2019) with slight modification. Briefly, 0.02 g of each of the three petroleum fractions (kerosene, petrol, and diesel), 1.3 g of sea salt, and 0.23 g of sodium dodecyl sulphate were weighed and transferred into the 500 mL beaker containing deionized water corresponding to each concentration generated using RSM shown in Table 4.3 and subsequently homogenized through sonication for 5 mins.

4.2.7. Oil removal experiments

Optimization of conditions for oil removal using amine-functionalized activated carbon was carried out through RSM experimental design software (version 11, Stat-Ease Inc., Minneapolis, USA). Table 4.3 summarizes the conditions considered for optimization. The

experiments were performed as follow; various amounts of amine-functionalized activated carbon were weighed and enclosed in a tea bag. Thereafter, tea bags containing the adsorbents were placed into 250 mL beakers containing 25 mL of synthetic oily effluent and left undisturbed for various times as guided by the experimental design from RSM. At the end of experiment, mixtures were filtered through an EZ-Pak ® membrane filter. The residual oil contents were estimated in the form of total organic carbon using Spectroquant UV spectrophotometer from Merck group (Germiston, South Africa). For quality assurance, blank experiment was performed using empty tea bag. The oil removal efficiencies and adsorption capacities were estimated using Equation 4.3 and 4.4, respectively.

$$\% \text{ Removal} = \left(\frac{(C_i - C_f)}{C_i}\right) 100 \quad (4.3)$$

$$Qe = \left(\frac{(C_i - C_f)}{m}\right) V. \quad (4.4)$$

Where Q_e (mg/g) denotes the adsorbent's equilibrium adsorption capacity per milligram dry weight, V (L) symbolizes the solution volume, and m (g) denotes the adsorbent mass. C_i and C_f denote the oil concentrations (mg/L) before and after treatment, respectively. Table 4.3 shows the optimized parameters for oil removal.

Table 4.3: Range of optimized parameters as predicted by the RSM.

Name	Low	High
Adsorbent dosage (g)	0.1	0.3
Initial oil concentration (mg/L)	500	10000
Contact time (mins)	60	300

4.2.8. Adsorption kinetics

The adsorption kinetics was determined for a solution of synthetic oil wastewater containing 500 mg/L initial oil concentration of with 0.1 g/25 mL of adsorbent dosage for various contact times ranging from 10 to 120 min. The obtained data was analyzed using non-linear equations

of pseudo-first order and pseudo-second order models of reaction kinetics (Eq. 4.5-4.6), as well as Weber-Morris model of intraparticle diffusion (Eq. 4.7).

$$qt = qe\ (1 - e^{-k_1 t}) \quad (4.5)$$

$$qt = \frac{qe^2 k_2 t}{1 + k_2 q_e t} \quad (4.6)$$

$$qt = k_i t^{0.5} + ci \quad (4.7)$$

Where q_e and q_t symbolizes the adsorption capacities at equilibrium and time t, respectively; k_1 and k_2 are the rate constants for pseudo-first order and pseudo-second order, respectively. The constant of intra particle diffusion rate, K_i (mg/g min-1), is determined by the slope of $t^{0.5}$ vs. q_t, while C_i the constant of the boundary layer thickness (Mudzielwana et al., 2018).

4.2.9. Adsorption Isotherms

The adsorption isotherms were determined using linear equations of Langmuir and Freundlich adsorption isotherms models (Eq. 4.8-4.9) to determine the adsorbate-adsorbent interaction (Langmuir, 1918, Freundlich, 1906). The isotherms were determined at concentration ranges of 50 to 200 mg/L.

$$\frac{C_e}{q_e} = \frac{1}{K_a q_m} + \frac{1}{q_m} C_e \quad (4.8)$$

$$Log q_e = Log K_F + \frac{1}{n} Log C_e \quad (4.9)$$

Where; C_e, K_a, q_e and q_m and denote the adsorption capacity (mg/g), the equilibrium concentration (mg/L), the Langmuir constant associated to enthalpy of adsorption (L/mg) and theoretical maximum adsorption capacity (mg/g), respectively. The K_F values correspond to the Freundlich constant that is interrelated to adsorption capacity and adsorption intensity. The heterogeneity factor is 1/n, where n represents the process's intensity, the diversity of the adsorbent's reactive sites, and the relative energy distribution (Abdulkareem et al., 2021). When $0 < 1/n < 1$, the adsorption is favourable; when $1/n=1$, the adsorption is irreversible; and when $1/n > 1$, the adsorption is unfavourable (Priyadarshini et al., 2018).

4.2.10. Goodness-of-fit valuation

The goodness-of-fit calculations for the model was carried out to confirm the suitability of the kinetics, and isotherm models which were attained from the data from the experiments via the correlation coefficient (R^2) and root mean square error (RMSE) expressed by (Eq. 4.10-4.11).

$$R^2 = 1 - \frac{\Sigma(q_{e,exp} - q_{e,calc})2}{\Sigma(q_{e,exp} - q_{e,mean})2} \quad (4.10)$$

$$RMSE = \sqrt{\frac{1}{n-1}\sum_{i=1}^{n}\left(q_{e,exp} - q_{e,calc}\right)^2}_{i} \quad (4.11)$$

where $q_{e,\text{ calc}}$ refers to the adsorbate theoretical concentration on the adsorbent, which has been calculated an isotherm model. $q_{e,\text{ exp}}$ means is the concentration of adsorbed solid-phase which is experimentally measured.

4.3. Results and discussion

4.3.1. Optimization of conditions for synthesis of activated carbon using response surface methodology

4.3.1.1 Effect of activation time and impregnation ratio

The effect of activation time and impregnation ratio on the percentage carbon yield is shown in Figure 4.1. It is apparent from Figure 4.1 that activation time has an inversely proportional relationship with the percentage carbon yield, thus, as the activation time increases, the percentage carbon yield declines and vice versa. The lowest percentage carbon yield of 15 was observed at the highest activation time of 90 min and impregnation ratio of 1.5; a comparable trend was reported by Nuru-Shuhada et al. (2016). This might be due to the volatilization of carbon atoms on the surface becoming predominant as the impregnated macadamia nutshell stay for the longest time under heat environment which leads to an increase in weight loss and carbon burn-off (Amzi et al., 2015). Furthermore, the highest carbon yield of 52% was observed at 30 min interval and impregnation ratio of 1.5. As shown in Table 4.4, the ANOVA results suggest that the impregnation ratio did not have a significant impact on the percentage carbon yield.

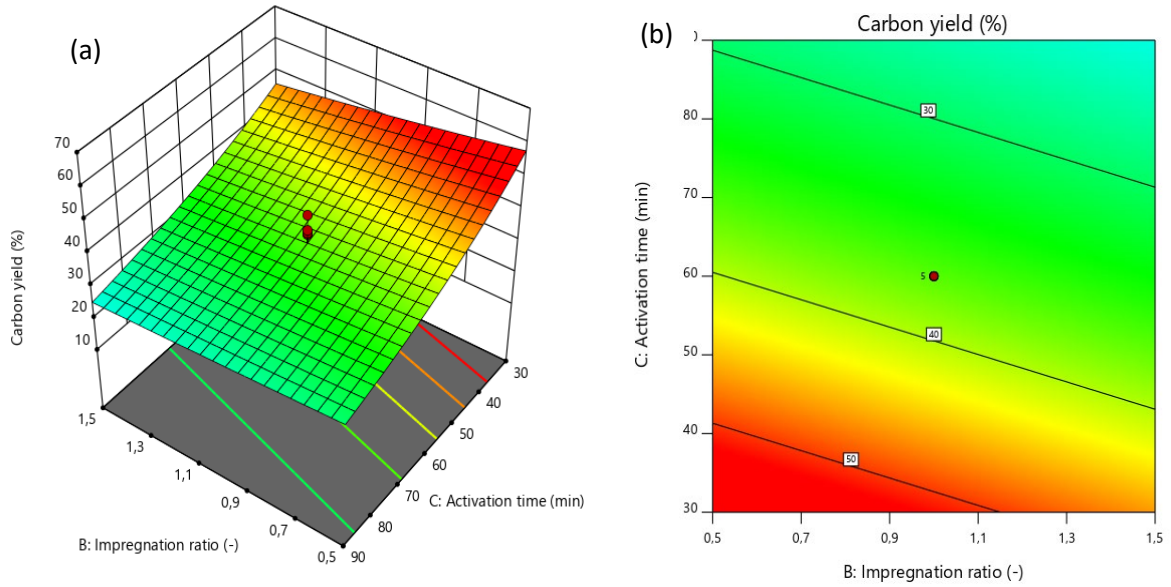

Figure 4.1: Response Surface (a) and Contour (b) plots for variation of percentage carbon yield against activation time and impregnation ratio.

4.3.1.2. Effect of activation time and temperature

The effect of activation time and activation temperature on the percentage carbon yield is shown in Figure 4.2. The lowest carbon yield of 15% was observed at the 90 min time interval and an activation temperature of 600 °C while the highest carbon yield of 52% was observed after the 30 min activation time interval and activation temperature of 410 °C. According to Ghani et al. (2017) and Amzi et al. (2015), during the activation process, the volatile matter immediately diffuses out of the particles' surfaces. In addition, at high activation temperature and longer activation time, the volatilization of carbon atoms on the surface becomes predominant leading to an increase in weight loss and carbon burn-off. (Amzi et al., 2015).

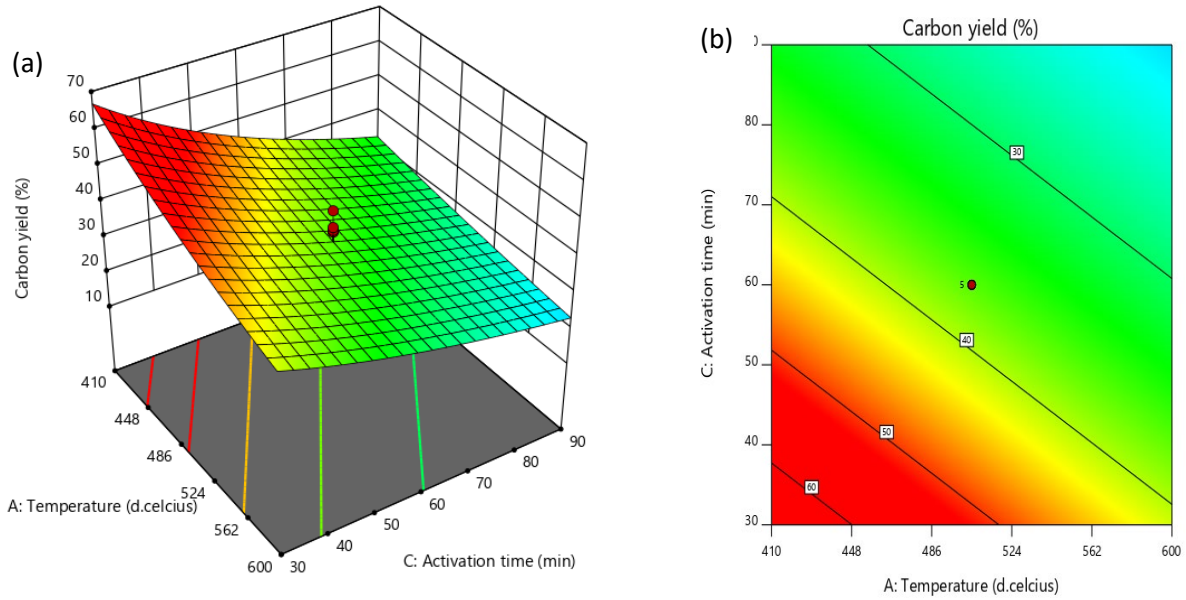

Figure 4.2: Response Surface (a) and Contour (b) plots for variation of percentage carbon yield against activation time and temperature.

4.3.1.3. Effect of temperature and impregnation ratio

The effect of impregnation ratio and activation temperature on the carbon yield percentage is shown in Figure 4.3. It is clear from Figure 4.3 that, at high temperature, there is low carbon yield, and this is ascribed to the dehydration and elimination reaction of the impregnated macadamia nutshell powder (Ahmad et al., 2017). The H_3PO_4 impregnation of the macadamia nutshell powder and high activation temperature result in the breakage of the C–O–C and C–C bonds and carbon burn-off, and this leads to less percentage carbon yield. However, impregnation ratio did not have a significant impact on the percentage carbon yield as shown in the ANOVA results (Table 4.4), where it was found to be insignificant.

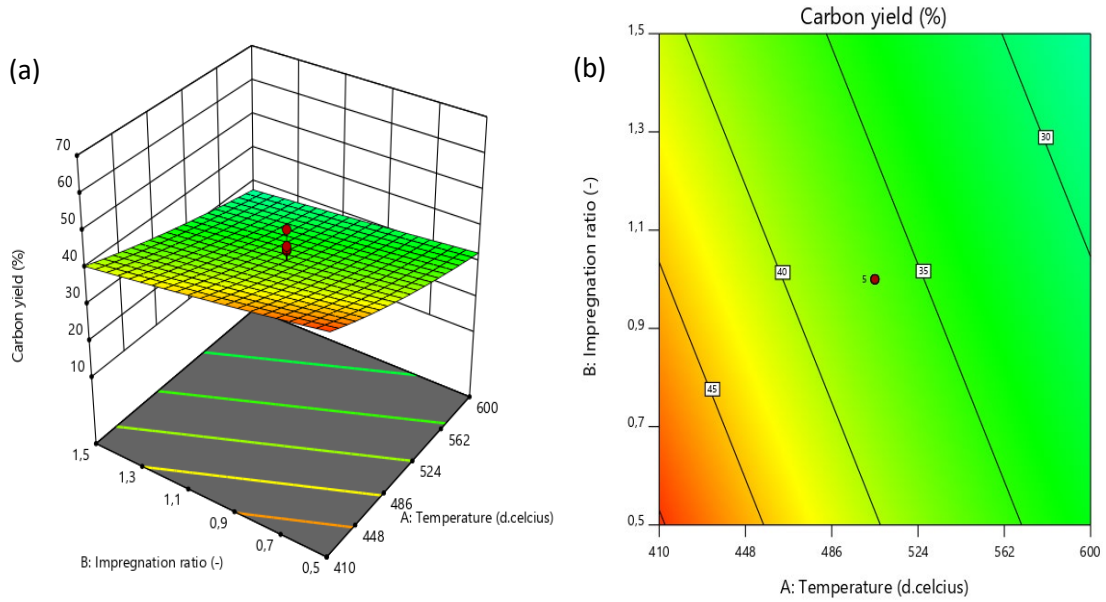

Figure 4.3: Response Surface (a) and Contour (b) plots for variation of percentage carbon yield against activation temperature and impregnation ratio.

4.3.1.4. Response surface cube plot

Figure 4.4 illustrates the performance summary of the RSM model. The minimum and maximum percentages carbon yield accomplished are shown on the axes of the plot (Kumar & Gupta, 2019). The values shown inside the cube represent the optimum predicted (34.66%) carbon yield efficiency of the RSM. The lowest percentage carbon yield (15%) was achieved at higher ranges of activation temperature (600 °C), activation time (90 min) and impregnation ratio (1.5) while the highest percentage carbon yield (52%) was achieved at low range of activation temperature (410 °C), activation time (30 min) and high impregnation ratio (1.5).

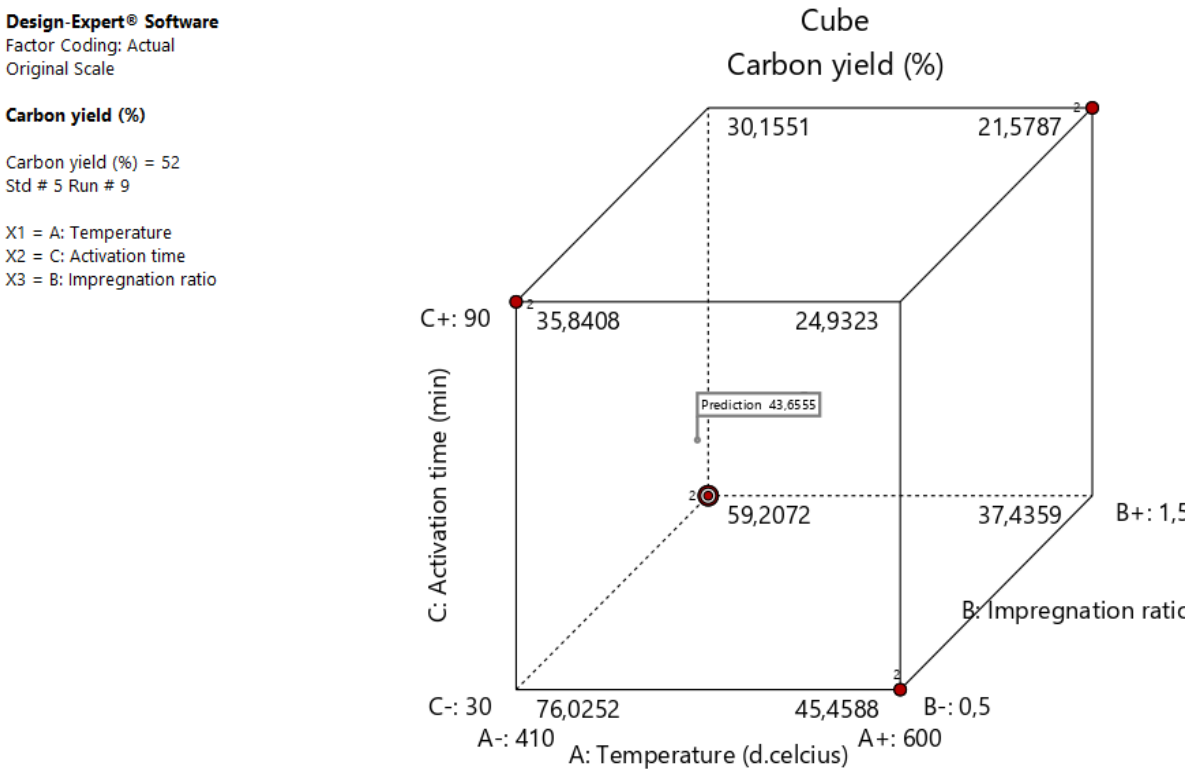

Figure 4.4: The summary of RSM model.

4.3.1.5. Predicted and actual value plot

The actual results obtained from trials are presented in Figure 4.5 together with model estimates for the percentage carbon output from activated carbon. The red, green, and blue colours on the graphs denotes points that exceeded, were equivalent to, and were below to the predicted values, respectively. The coefficient of determination R^2 was found to be 0.70. This indicates that the predicted and actual values agreed rather well, and that the model selected was good enough to account for the correlation between the optimized variables and the response.

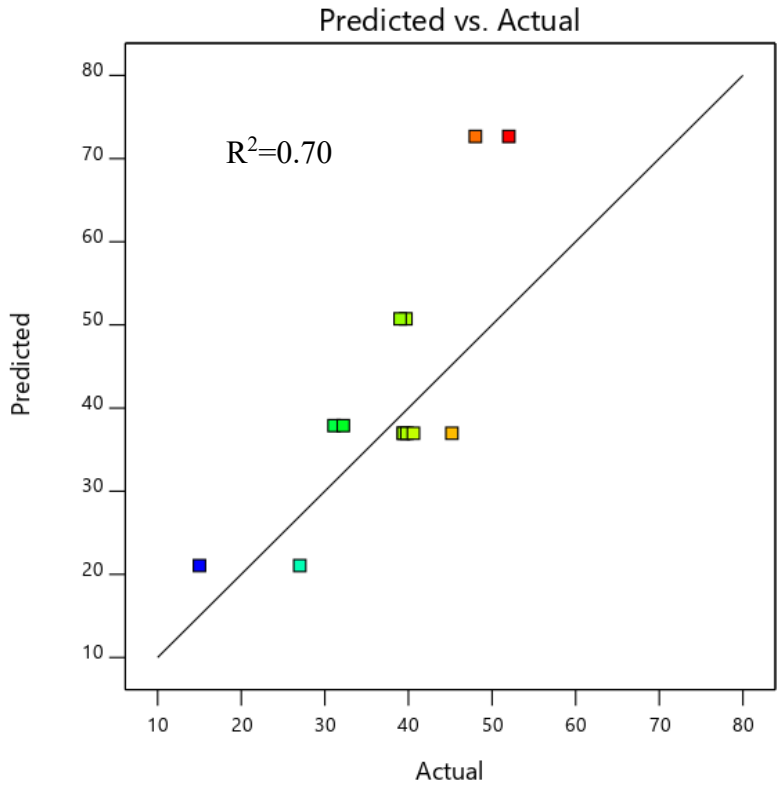

Figure 4.5: Predicted and Actual values Plot

4.3.1.6. ANOVA quadratic model

Table 4.4 presents the results of ANOVA quadratic model and the model terms. The statistical significance of the impact of activated carbon composition on carbon production was assessed using the ANOVA test. The ANOVA test was conducted to determine the importance and fitness of the model and the model terms. Model terms are regarded as being significant when their P-values are lower than 0.05. Similar to activation time and temperature, significant model variables also had an impact on the percentage carbon yield as their P-values are lower than 0.05. The lack of fit is insignificant, based on the lack of fit F-value of 4.11. The model fits and is sufficient to reflect the relationship between the parameters and response when there is a non-significant lack of fit (Tetteh and Rathilal, 2019).

Table 4.4: ANOVA for response surface Two-Factorial Interaction model

Source	**F-value**	**p-value**	
Model	6.83	0.01	Significant
A-Temperature	5.63	0.04	
B-Impregnation ratio	1.15	0.31	
C-Activation time	13.71	0.00	
Residual			
Lack of Fit	4.11	0.08	not significant

4.4. Oil Removal test for product activated carbon samples

Table 4.5 presents the oil removal percentage values of the product activated carbon samples. These experiments were conducted to enable the selection of generated activated carbon possessing higher oil removal capacity and samples for characterization by SEM-EDS, BET, XRD, and CHNS techniques. Runs 2, 3, 5, 7 and 11 were sent for characterizations based on the oil removal percentage results. Runs 7 and 11 were selected because run 7 showed the least oil removal percentage while 11 showed the highest oil removal percentage as shown in Table 4.5.

Table 4.5: Oil removal test using the produced activated carbon samples.

Run	Adsorbent dosage (g)	Contact time (min)	Initial oil concentration (mg/L)	Final oil concentration (mg/L)	Oil removal (%)
1	0.1	180	184	132	28.26
2	0.1	180	184	126	31.52
3	0.1	180	184	115	37.5
4	0.1	180	184	139	24.57
5	0.1	180	184	101	45.11
6	0.1	180	184	149	19.02
7	0.1	180	184	177	3.80
8	0.1	180	184	101	45.11
9	0.1	180	184	153	16.85
10	0.1	180	184	135	26.63
11	0.1	180	184	98	46.74
12	0.1	180	184	116	36.96
13	0.1	180	184	129	29.89

4.5. Characterization of raw macadamia nutshells and activated carbon

4.5.1 Elemental analysis

Table 4.6 presents the elemental analyses of the MNS and selected activated carbon samples. Raw MNS is composed mainly of C (49.56 %) and (6.20 %) with small amounts of MgO (1.02 %). Activated samples showed increase in % C except for run 3 which showed a decrease in the carbon content to 4.01%. Run 3 showed the lowest carbon content compared to other samples. This may be due to carbon burn-off during activation time. After activation, the content of P_2O_5 increased in all of the activated carbon samples. This is attributed to the

successful incorporation of the orthophosphoric acid during the activation of the orthophosphoric-impregnated macadamia nutshell powders.

Table 4.6: Elemental composition of raw macadamia nutshells and activated carbon samples

Elements	Raw MNS (%)	Run 2 (%)	Run 3 (%)	Run 5 (%)	Run 7 (%)	Run 11 (%)
MgO	1.02	0.8	0.61	0.51	0.85	0.71
P_2O_5	0.02	14.15	13.46	19.08	18.84	20.03
C	49.56	51.34	14.01	58.80	55.01	55.90
H	6,20	3.33	2.72	3.17	3.32	3.74
N	0,17	0.24	BDL	BDL	BDL	BDL
S	BDL	0,17	BDL	BDL	BDL	BDL

BDL= Below Detection Level

4.5.2. SEM-EDS analysis of the raw macadamia nutshells and product activated carbon samples

Figure 4.6a-i shows the SEM micrograph of the raw macadamia nutshells and selected samples of activated carbon together with their EDS spectra. The MNS (Fig 4.6a) showed a flaky fold-like surface structure with some crystals on top which represent the surface of plant based organic materials (Pakade et al., 2017b). Figure 4.6g shows EDS of the raw MNS which confirms that carbon and oxygen are the main elements with no trace of heavy metals being detected. Similar observations were made by Pakade et al. (2017b). Micrograph of the activated carbons (Figure 4.6b-f) showed a change in the surface of the activated carbons where there was development of pores except for run 3 in Figure 4.6c which displayed a flat surface with large particle material on the surface of the adsorbent instead of pore development. Energy dispersion X-ray spectroscopic analysis of the produced activated carbons (Figure 4.6h-I) displayed the presence of phosphorus element which confirms successful incorporation of the orthophosphoric acid during impregnation and activation.

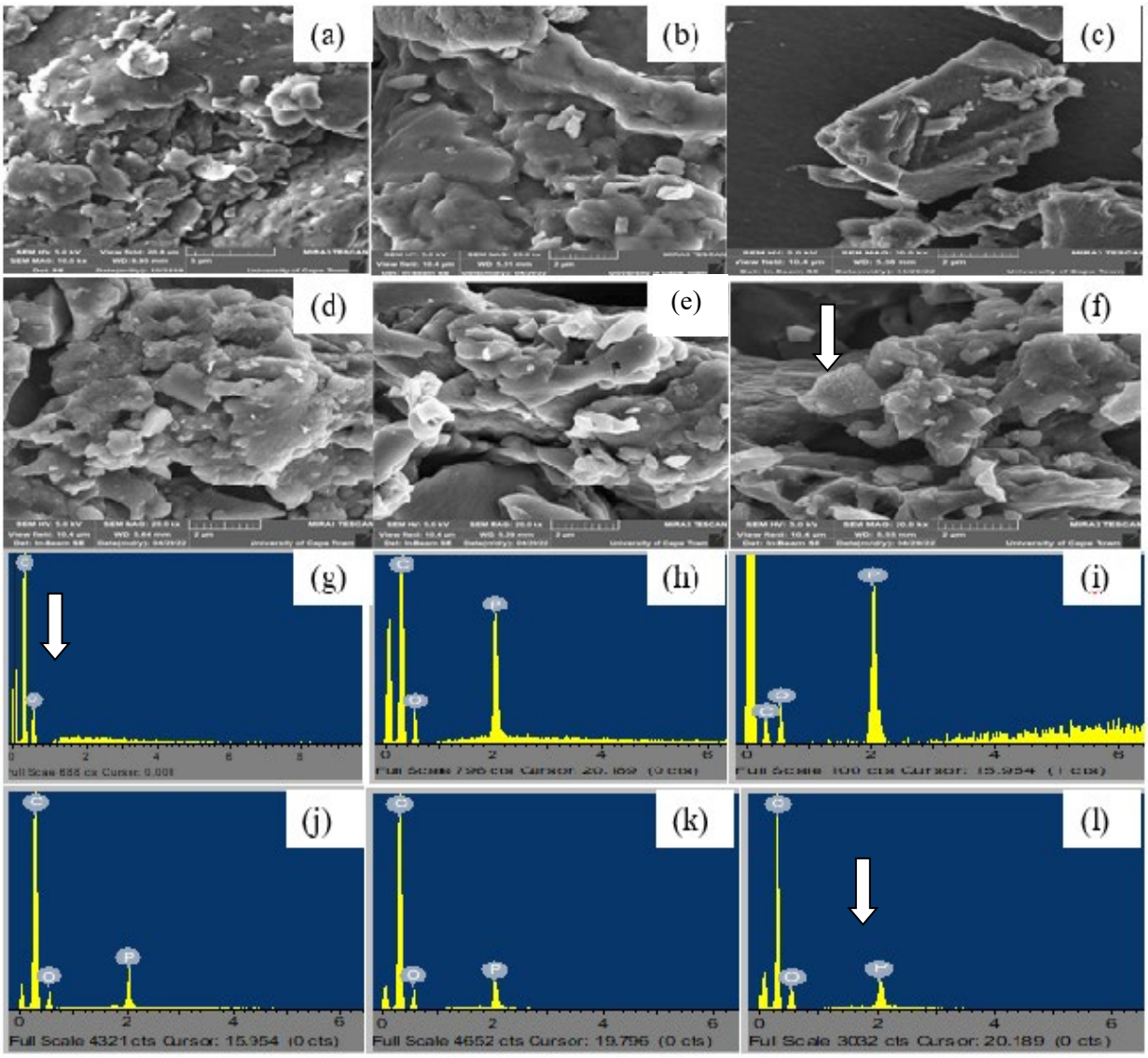

Figure 4.6: SEM-EDS for raw MNS and produced activated carbon.

4.5.3. XRD results for raw macadamia nutshells and product activated carbons samples

Figure 4.7 shows the XRD pattern of the raw MNS and activated carbon. The XRD pattern of the raw MNS (Figure 4.7a) shows a major diffraction peak at 2Θ degree (22.17 and 34.35 °), which is attributed to the natural crystalline cellulose ($C_6H_{12}O_6$) structure. Instead of the sharp peaks, the XRD pattern of the activated carbons shows broad diffraction peaks indicating amorphous carbon (Figure 4.7b).

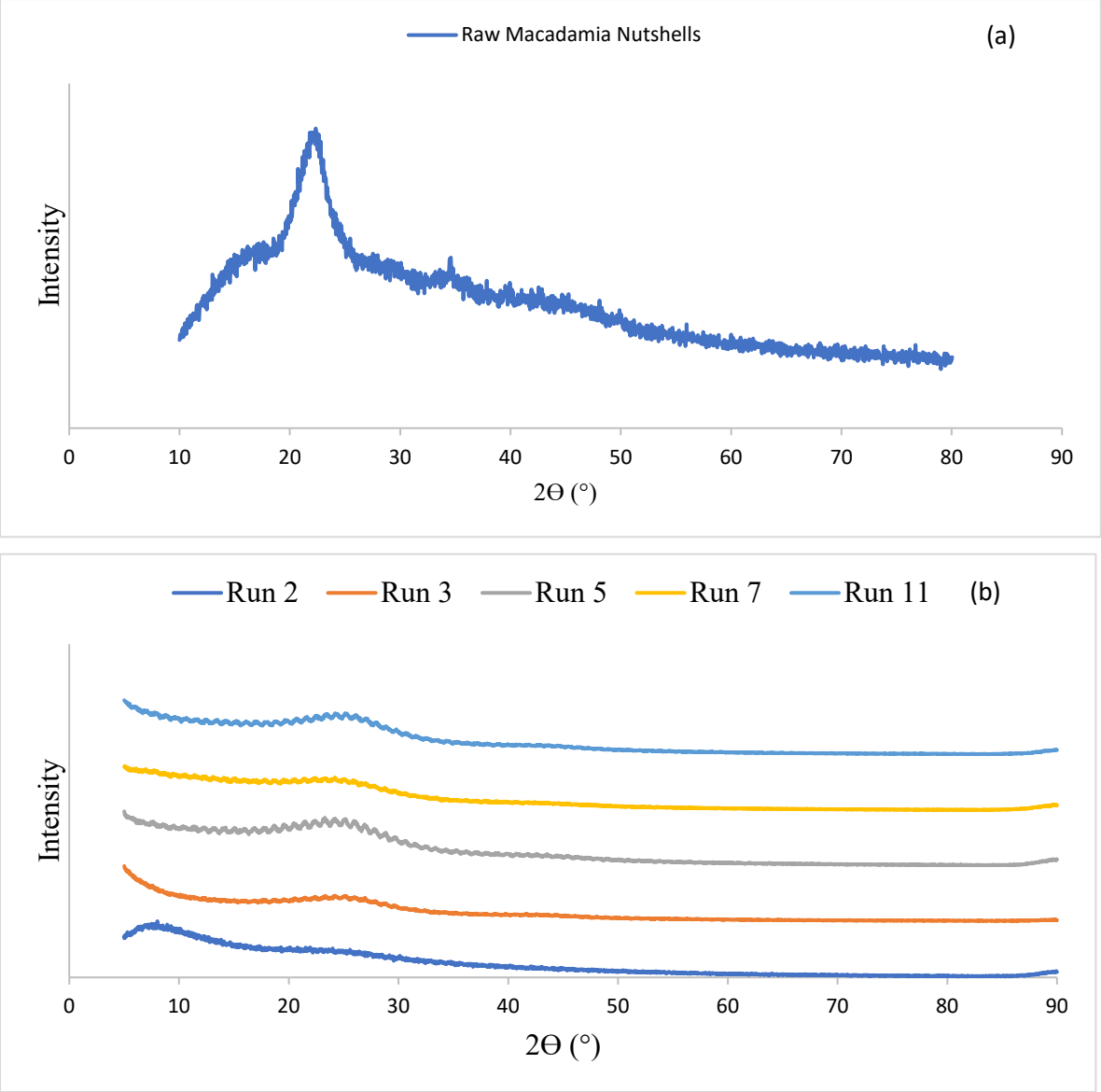

Figure 4.7: XRD diffractogram of raw macadamia nutshell (a) and selected activated carbon (b).

4.5.4. BET analysis of surface area and pore characteristics

Table 4.7 shows the BET surface area and pore characteristics of raw MNS and selected activated carbons. The results showed an increase in surface area, pore diameter and pore volume in the activated carbon samples when compared with the raw MNS. The activated carbon sample for run 3 sample (prepared at an optimum temperature of 600 °C, impregnation ratio of 3:2, and activation time of 90 minutes) has the lowest surface area (13.5 m^2/g) and highest average pore size (4 428.28 Å) when compared with other activated carbon samples. Amongst all activated carbon samples, the run 11 samples displayed the highest surface area (1 517.65 m^2/g) and pore volume (0.83 cm^2/g). This could be attributed to operational conditions of low temperature and low activation time. Consequently, run 11 yielded the

highest percentage of oil removal and this is corroborated by the high carbon percentage yield, thus affirming the importance of high surface area in adsorption. An increase in the surface area leads to an enhanced sorption capacity. Additionally, the resulting pore diameter of the activated carbon affirms mesoporosity emanating arising from the microporosity of the raw MNS.

Table 4.7: BET surface area and pore characteristics of raw macadamia nutshell and activated carbons.

BET Analysis	Raw MNS	Run 2	Run 3	Run 5	Run 7	Run 11
Surface area (m^2/g)	1.69	1 172.37	13.55	1 254.69	1 205.93	1 517.65
Average particle size (Å)	-	51.18	4 428.28	47.82	49.75	39.53
Pore diameter (Å)	15.4	21.05	30.66	21.90	19.70	21.76
Pore Volume (cm^2/g)	0.01	0.62	0.01	0.69	0.59	0.83

4.5.5. Fourier transform infrared spectroscopic analysis of the raw macadamia nutshells and product activated carbon samples

Figures 4.8a and b show Fourier Transform Infrared (FTIR) spectra of the raw MNS and selected activated carbon samples. The band appearing at 3385 cm^{-1} in the FTIR spectrum of the raw MNS is indicative of the stretching vibration of the hydroxyl (O-H) group arising from the moisture contained in the MNS. The band at 1454 cm^{-1} is associated with stretching and vibration of the C-C bond, while the band at 1248 cm^{-1} indicates the C-OH bond which is linked to vibration of phenols, ketones, ethers and esters occurring on the surface of the MNS. Nekhavhambe et al. (2022) have reported similar observations on the FTIR spectrum of the raw MNS. In accordance with results reported by Gao et al. (2016), the band at 1025 cm^{-1} is associated with the C-O stretching vibration. All the FTIR spectra of the activated carbon (Fig 4.8b) show the same trend where absorbance peaks associated with the C-O and C=O of the

carbonyl groups functionality are observed in the range of 1000 cm^{-1} to 2000 cm^{-1}. The carbonyl functional groups occur on the surface of the activated carbons and are a good indicator of the activated carbon (Dao et al., 2020). The strong band at 1582 cm^{-1} is ascribed to the stretching vibrations of C=C, which indicates an increase in the carbon content in the activated carbons. The vibration mode is observed at 1169-1173 cm^{-1} and is ascribed to hydrogen bonded to the P=O groups of phosphates or aromatic P–O–C bonds. These observations, which have also been reported by Myglovets et al. (2014), indicate successful incorporation of the orthophosphoric acid onto the surface of the MNS.

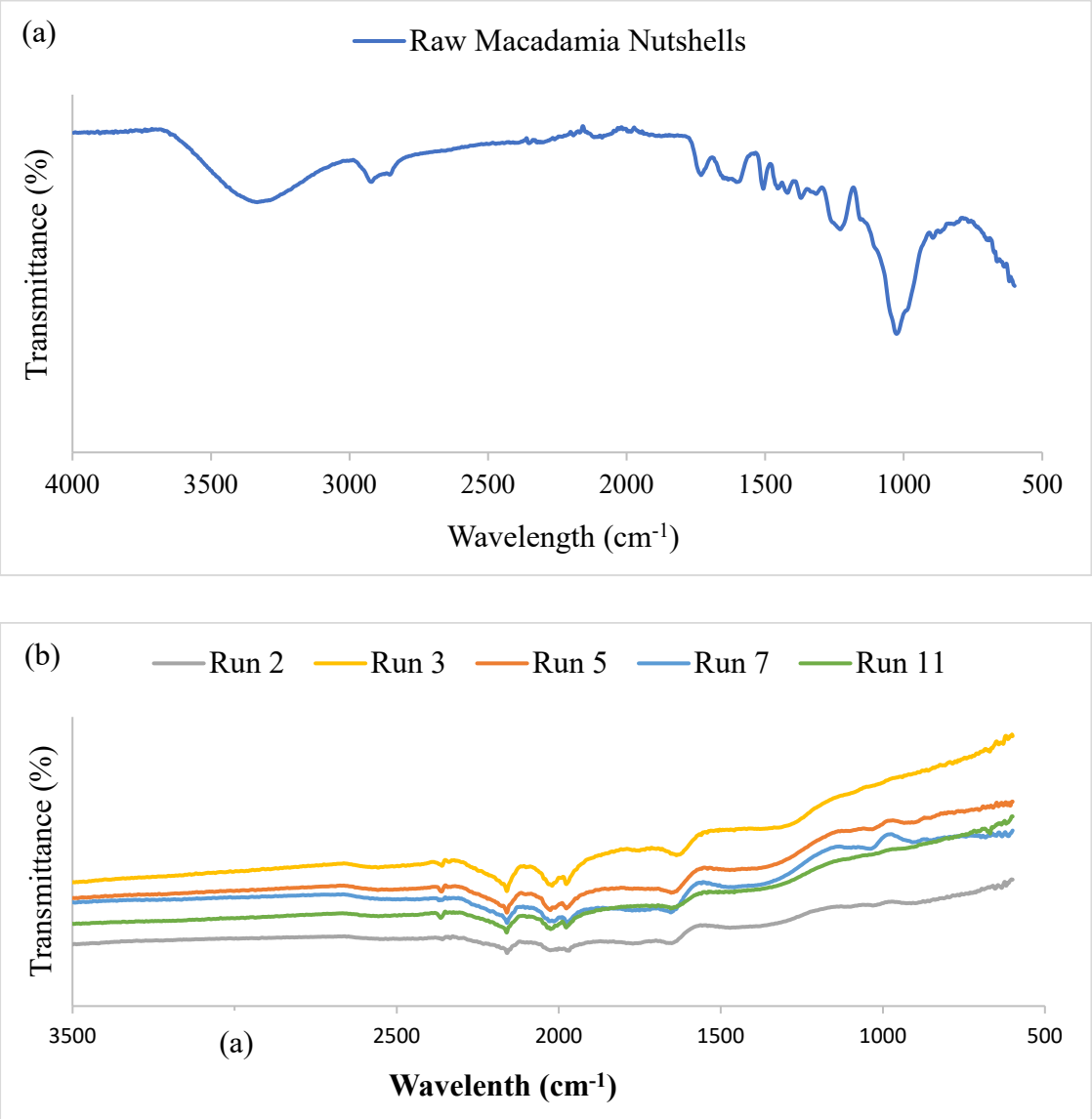

Figure 4.8: FT-IR spectrometer results of (a) raw MNS, and (b) selected samples of activated carbons.

4.6. Results and discussions: modification of activated carbon with amine groups and performance in oily wastewater treatment.

4.6.1. Morphological comparison of the activated carbon and amine-functionalized activated carbon

Figure 4.9 shows SEM micrographs of (a) activated carbon and (b)amine-functionalized activated carbon. The micrographs of the activated carbons (Figure 4.9a) showed a rough and irregular surface composed of pores. After functionalization, the surface appears to have a foam-like surface (Fig4.9b), which is attributable to the expansion of the particles during the intercalation of amine functional groups.

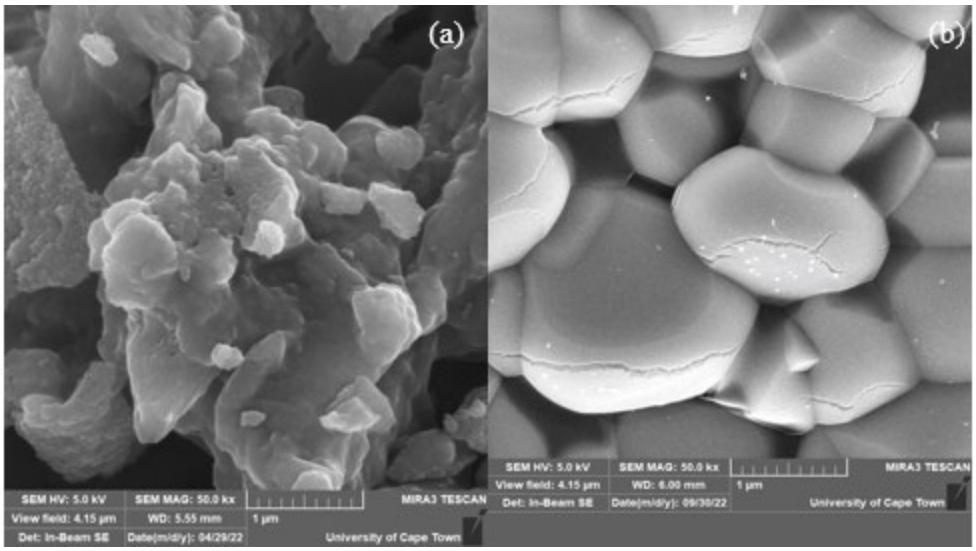

Figure 4.9: SEM micrographs of (a) activated carbon, and (b) functionalized activated carbon.

4.6.2. Fourier Transform Infrared Spectroscopic analyses

Figure 4.10a shows the FTIR spectrum of the activated carbon while Figure 4.10b shows the spectrum of the amine-functionalized activated carbon. FTIR spectrums (Fig 4.10a) shows the functional carbonyl groups C-O and C=O that occur on the surface of the activated carbons in wavelength range 1000 cm^{-1} to 2000 cm^{-1}; this is a good indication of formation of the activated carbon. A similar trend was reported by Dao et al. (2020). The strong band at 1582 cm^{-1} is attributed to the stretching vibrations of C=C, and this indicates an increase in the carbon content in the activated carbons, The vibration mode is observed at 1169-1173 cm^{-1}, and is ascribed to the hydrogen bonded P=O groups of phosphates or aromatic P–O–C bonds. Similar observations were reported by Myglovets et al. (2014), and this indicates successful incorporation of the orthophosphoric acid onto the surface of the MNS.

A change in the spectra of the amine-functionalized activated carbon was observed (Figure 4.10b). The amine-functionalized activated carbon can easily be identified by N-H functional groups (Avila et al. (2014). The N-H group corresponding to the bending of primary amines was observed at 1500-1750 cm^{-1}. These observation are comparable with results obtained by Faisal et al. (2021). The band at 1450 cm^{-1} is associated with C-N stretching, indicating the presence of amine moieties in the functionalized activated carbon. Rezaei and Jones (2013) have reported that this bond indicates the presence of amines. The new alkynes and aromatic C-H stretching bonds of the functionalized activated carbon were observed at about 2780 to 3200 cm^{-1}.

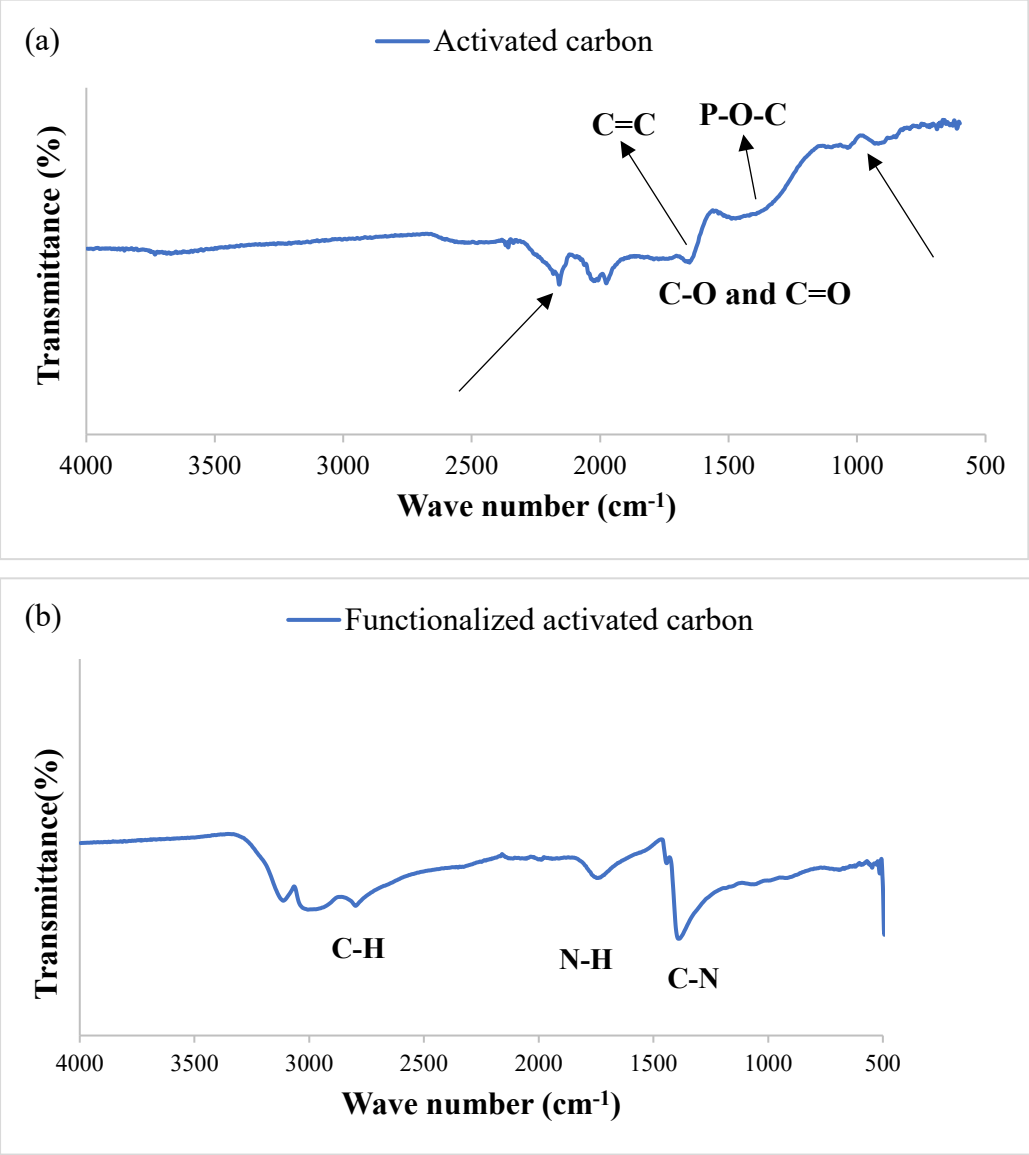

Figure 4.10: FT-IR spectra of activated carbon (a) and amine-functionalized activated carbon (b).

4.6.3. Analysis of the surface area and pore characteristics

Table 4.8 presents the BET surface area and pore characteristics of activated carbon and functionalized activated carbon. The results showed a reduction of the surface area, pore volume and diameter following amine functionalization from 1 517.65 to 0.43 m^2/g, 39.53 to 0 cm^3/g and 21.76 to 3.66 Å, respectively. However, an increase in the average particle size from 0.83 to 1 387 716.04 Å was noted. This is attributed to the expansion of the particles following the introduction of the amine functional groups onto the surface of the activated carbon. A similar trend was reported by Das and Meikap (2021), and this is evident in Figure 4.9b, which shows the larger particles in the amine-functionalized carbon. Additionally, a reduction in the pore diameter following amination of the activated carbon affirms the mesoporosity and microporosity, respectively.

Table 4.8: Surface area and pore characteristics of activated carbon and amine-functionalized activated carbon.

	Activated carbon	Functionalized activated carbon
BET surface area (m^2/g)	1 517.65	0.43
Pore volume (cm^3/g)	39.53	0
Pore diameter (Å)	21.76	3.66
Average particle size (Å)	0.83	1 387 716.04

4.7. Surface and cube plots of the response surface methodology models.

4.7.1. Response surface plots

Figure 4.11 displays the RSM plots for the effect of initial oil concentration and adsorbent dosage (A), initial oil concentration and contact time (B), and contact time and adsorbent dosage (C) on the oil removal percentage.

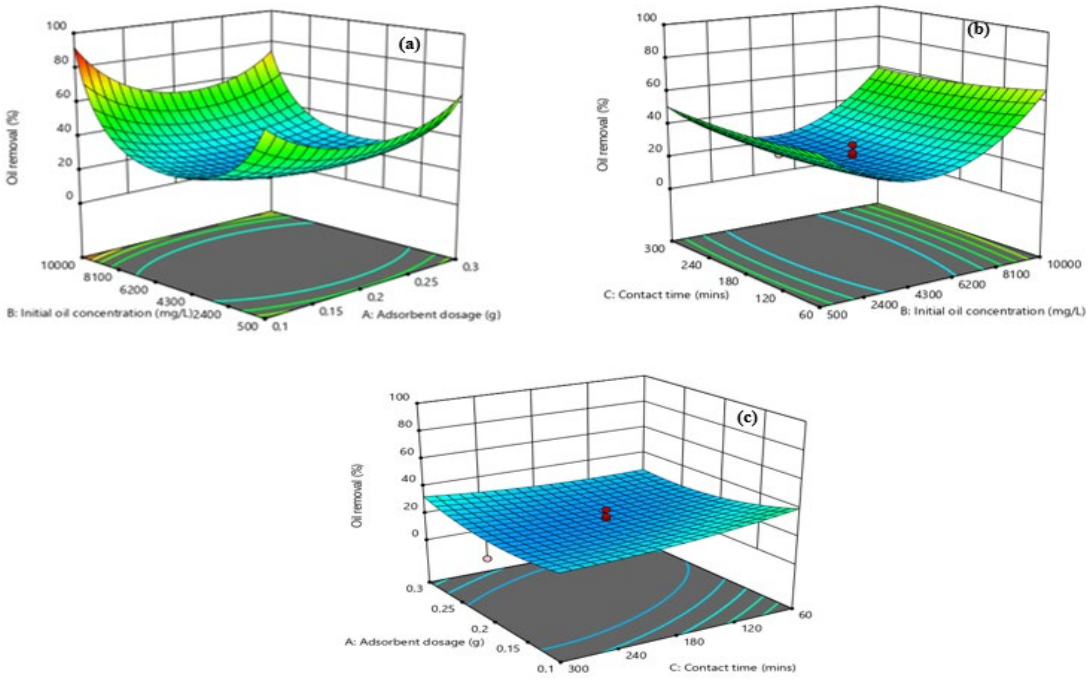

Figure 4.11: Variation of oil removal percentage against initial oil concentration and (a) adsorbent dosage, (b) initial oil concentration and contact time, and contact time and (c) adsorbent dosage

Figure 4.11a illustrates the plot for the effect of initial oil concentration and adsorbent dosage. It is seen that oil removal percentage increased with a declining initial oil concentration from 8 100 to 2 400 mg/L and this might be due to the limited active pores against the oil concentration gradient. Furthermore, oil removal percentage improved with adsorbent, and this was due to the adsorbent binding sites' introduction. The maximum oil removal percentage (88.98%) was achieved at adsorbent dosage of 0.1 g/25mL, highest initial oil concentration of 10 000 mg/L.

Figure 4.11b shows the plot of the effect of initial oil concentration against contact time. It can be seen that oil removal percentage initially increases with both initial oil concentration and contact time and thereafter reaches equilibrium before decreasing again due to limited binding sites available on the adsorbent surface for oil to be adsorbed (Kadir et al., 2014). Similarly, the oil removal percentage initially increased with the contact time due is an improving chance of positive interaction between the oil molecules and the adsorbent staying longer as the time

increases (Najaa Syuhada, 2017). The maximum oil removal percentage (65%) was achieved at the contact time of 60 mins and initial oil concentration of 10 000 mg/L.

Figure 4.11c shows the plot concerning the effect of Contact time against adsorbent dosage. It can be observed that both the contact time and adsorbent dosage had a slight influence on the oil removal percentage. The oil removal percentage increased slightly with a decline in the dosage of the adsorbent when the contact time was increased. However, as the contact time was increased, most of the active sites on the functionalized activated carbon became saturated and equilibrium was reached leading to a slower adsorption rate. The maximum oil removal percentage (40%) was achieved at a contact time of 60 mins and adsorbent dosage of 0.1 g.

4.7.2. Response surface cube plot

Figure 4.12 shows the results of the established response surface models via the cube plot. The minimum and maximum percentages of oil removal accomplished are shown on the axes of the plot. The values shown within the cube denote the predicted oil removal efficacy for the procedure adopted in this study. Minimum oil removal (11%) was achieved at the mid-range adsorbent dosage of 0.2 g, initial oil concentration of 5250 mg/L, and highest contact time of 300 mins while maximum oil removal (88.98%) was achieved at lowest range of adsorbent dosage (0.1 g), highest initial oil concentration (10 000 mg/L) and lowest contact time (60 mins).

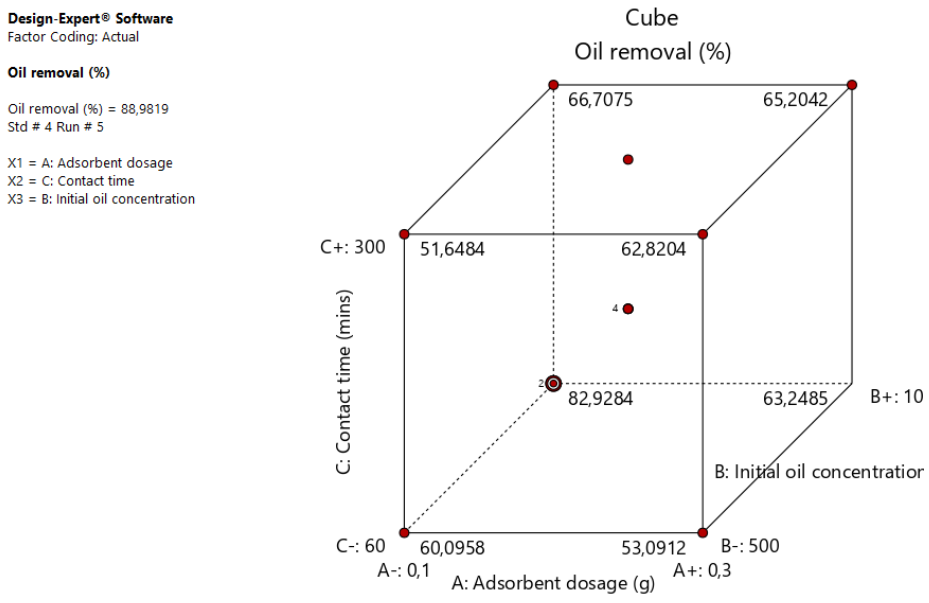

Figure 4.12: An illustration of the RSM model.

4.8. Optimum Conditions

Table 4.9 depicts the optimum conditions that yielded maximum oil removal percentage and adsorption capacity. The model shows that the optimum conditions for the oil removal were at the initial oil concentration of 10 000 mg/L, adsorbent dosage of 0.1 g, and contact time of 60 mins. These conditions yielded maximum percentage of 82.93% and adsorption capacity of 167.96 mg/g with desirability of 0.97.

Table 4.9: Optimum conditions for oil removal percentage and adsorption capacity.

Adsorbent dosage (g)	**Initial oil concentration (mg/L)**	**Contact time (mins)**	**Oil removal (%)**	**Adsorption Capacity (mg/g)**	**Desirability**
0.1	10 000	60	82.93	167.96	0.97

4.9. Predicted and actual value plot

The model prediction for the percentage of oil removal from synthetic oily wastewater was analysed and compared with the actual values attained from the experimental data plotted in Figure 4.13. While the red colour on the graphs denotes points that are greater than the predicted values, the green-coloured points denote points that are equivalent to the predicted values. Lastly, the points with a blue colour denote points that are lower than the predicted values. The coefficient of determination was found to be R^2 of 0.92. This suggests that the anticipated and actual values correspond very well, demonstrating the suitability of the selected quadratic polynomial model to explain the correspondence amongst the significant variables and the response.

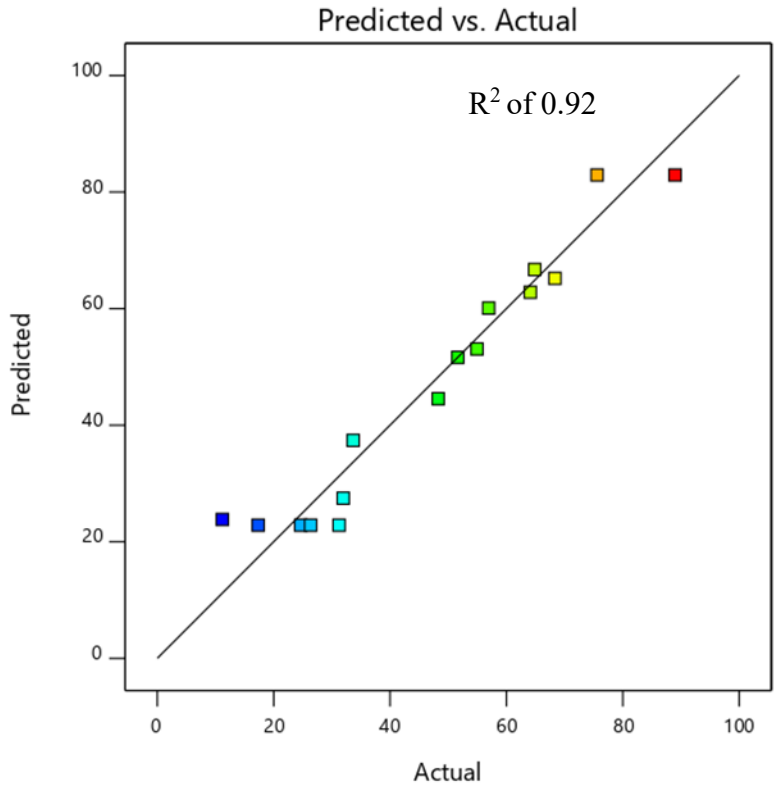

Figure 4.13: Comparison between predicted and actual values by RSM.

4.10. Analysis of variance

Table 4.10 shows a summary of results of the ANOVA test, which was used to test the significance of the model. The *p*-value and F-value were found to be 0.00 and 10.74, respectively, indicating a significant fit of the model. The model terms, such as the quadratic function (B^2) of the initial concentration and contact time (C^2), are significant and they influenced the percentage of oil removed. The lack of fit F-value of 0.18 suggested that the lack of fit was insignificant. A non-significant lack of fit confirmed that the model fits and is sufficient to justify the existence of relationship between the operational parameters and the response (Tetteh and Rathilal, 2019).

Table 4.10: ANOVA for Quadratic model and model terms.

Source	**F-value**	**p-value**	
Model	10.74	0.00	Significant
A-Adsorbent dosage	0.59	0.47	
B-Initial oil concentration	2.96	0.14	
C-Contact time	0.20	0.67	
AB	0.64	0.45	
AC	1.32	0.29	
BC	0.28	0.61	
A^2	6.11	0.05	
B^2	36.09	0.00	
C^2	0.41	0.54	
Residual			
Lack of Fit	2.68	0.18	not significant

4.11. Adsorption kinetics

The constant parameters for the pseudo first- and second-order kinetic models by non-linear regression are shown in Table 4.11, while the kinetic plots are presented in Figure 4.14. The data showed good fitting that is suited to pseudo second-order as indicated by a higher correlation coefficient (R^2=0.92) relative to the pseudo first-order (0.63). This suggests that the dominant uptake mechanisms of oil by the amine-functionalized activated carbon is the chemisorption.

Table 4.11: Constant parameters for pseudo first-order and pseudo second-order of reaction kinetics.

Parameters	Pseudo first-order	Pseudo second-order
K (min^{-1})	0.33	0.11
Q_e (mg/g)	86.50	85.57
R^2	0.63	0.92

X^2	0.95	0.94
RMSE	2.28	2.47

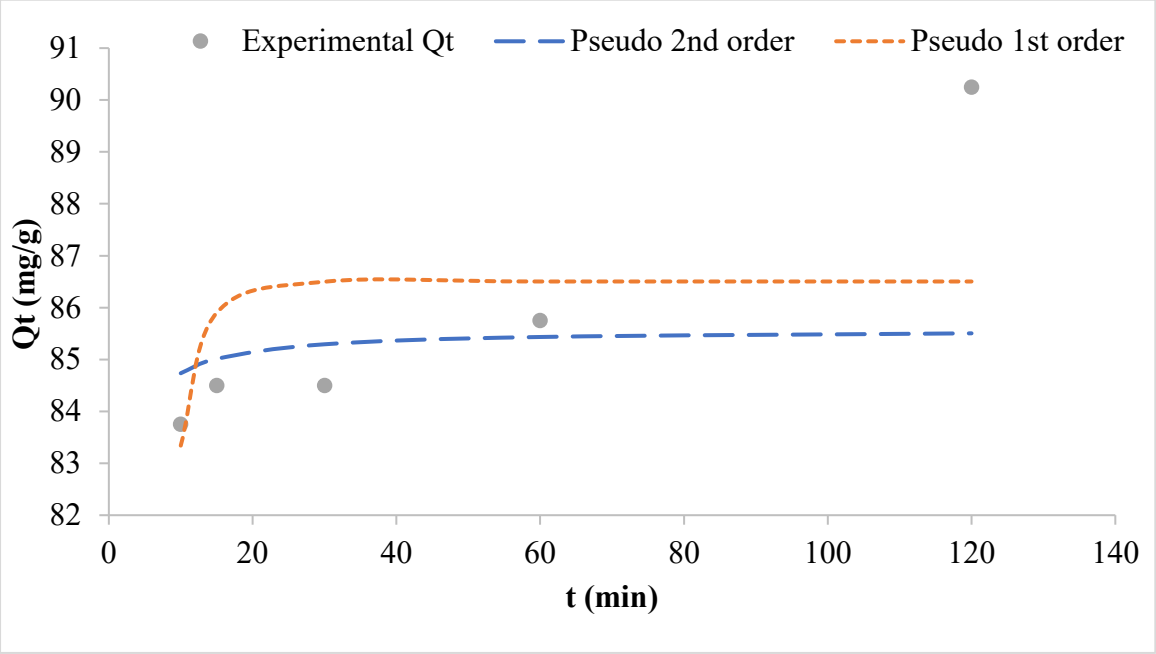

Figure 4.14: Plot for pseudo first-order and second-order models of reaction kinetics for oil adsorption onto the amine-functionalized activated carbon

The intraparticle diffusion plot in Figure 4.15 shows that the adsorption of the oil by the amine-functionalized activated carbon follows a three-phase process. The first phase relates to the adsorption on the adsorbent's boundary layer, whereby the oil molecules are attracted by the adsorbent's surface. The second phase involves intra-particle diffusion in which oil molecules diffuse inside the adsorbent's pores. The third and final phase involves equilibrium adsorption, which entails the chemical interaction of the oil with the atoms within the particles. The intraparticle rate constant (Ki) (Table 4.12) is larger in the third phase, indicating that equilibrium adsorption occurred much quicker than boundary layer and intraparticle diffusion adsorption. The value of C, the constant associated with the thickness of the boundary layer, was found to increase when the adsorption proceeds from phase 1 to phase two (Table 4.12), and this indicates an increase in the thickness of the border layer.

Table 4.12: Constant parameters for intra-particle diffusion model.

Parameters	Phase 1	Phase 2	Phase 3

Ki (mg/g.min$^{1/2}$)	1.06	0.34	1.40
R^2	1	0.83	1
C_I	80.41	82.99	74.89

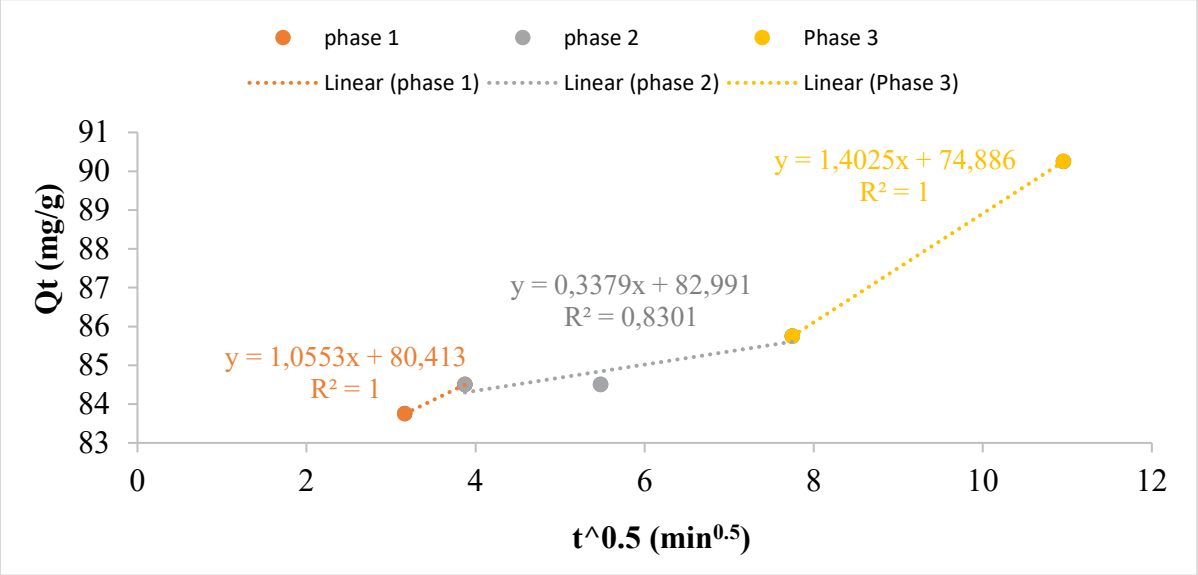

Figure 4.15: Intra-particle diffusion plot for oil adsorption onto amine-functionalized activated carbon.

4.12. Adsorption isotherms

The linear plots of adsorption isotherms are presented in Figure 4.16, while the constant parameters are presented in Table 4.13. As shown in Figure 4.16, the results show that the experimental data fits well with the Freundlich isotherms since as evidenced by a high correlation coefficient (R^2=0.96) Freundlich compared to the Langmuir isotherms. This finding indicates heterogeneity and multilayer adsorption. Furthermore, the Freundlich intensity parameter (1/n) values is less than 1 and therefore validates the favourability of the sorption processes (Munzhelele et al., 2021).

Table 4.13: Adsorption isotherm parameters for oil adsorption onto the functionalized activated carbon.

Freundlich Parameters	Values	Langmuir Parameters	Values
K_F (mg/g)	0.05	Q_m (mg/g)	2.17

1/n	0.6	K_a (L/mg)	14.29
R^2	0.96	R^2	0.72

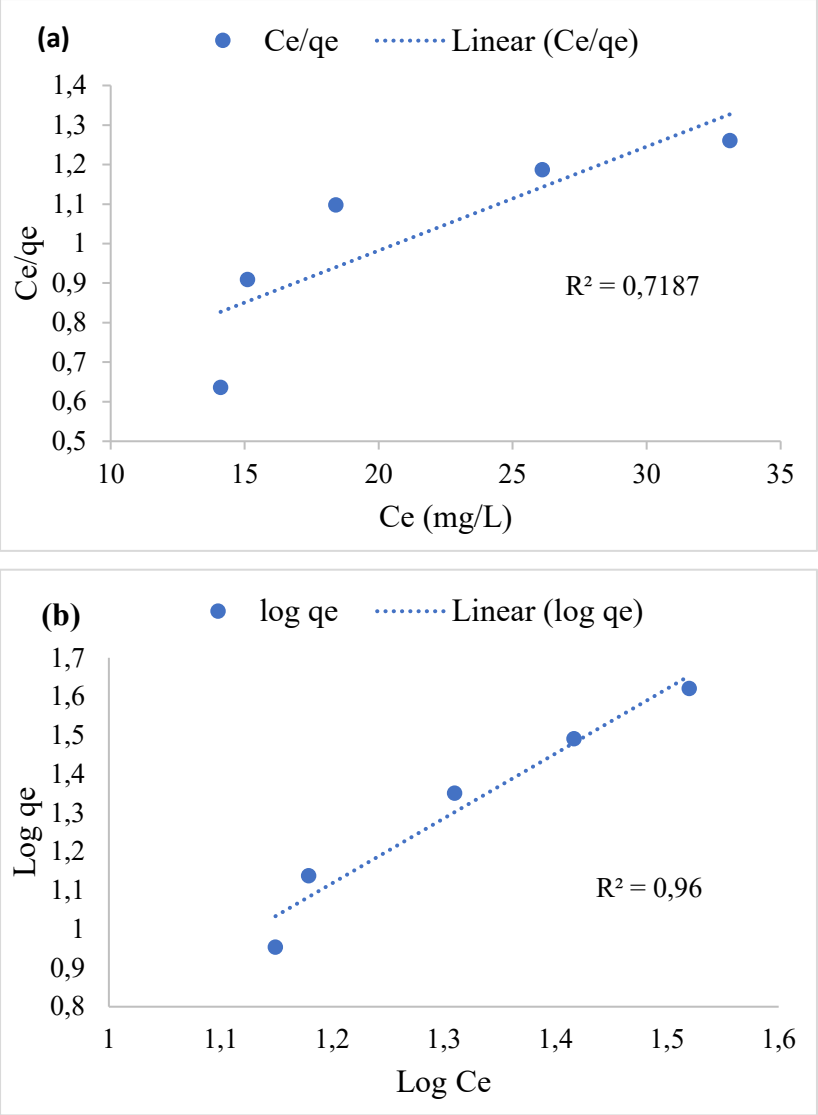

Figure 4.16: Linear plot of (a) Langmuir and (b) Freundlich for oil adsorption onto the amine-functionalized activated carbon.

4.13. Summary

Activated carbon was successfully synthesized from macadamia nutshells and further functionalized with the amine functional groups. Activated carbon was successfully functionalized and the FTIR results demonstrated the expansion of the particle sizes and incorporation of amine functional groups on the surface of the adsorbent. The surface area and pore diameter of amine-functionalized activated carbon decreased as result of the incorporation

of amine groups and expansion of the particles. The prepared amine-functionalized activated carbon showed a maximum adsorption capacity of 167.96 mg/g with a removal efficiency of 82.93% at initial oil concentration of 10 000 mg/L, adsorbent dosage of 0.1 g/ 25 mL and contact time of 60 mins. The response surface methodology model used for optimization was successful and this was confirmed by the results of the ANOVA model fitness. The adsorption kinetics data for oil adsorption showed better fit with pseudo second order reaction, indicating that adsorption occurred via chemisorption. The intra-particle model revealed that adsorption of the oil molecules by amine-functionalized activated carbon involve a three-phase adsorption process, namely boundary layer adsorption, diffusion into the pores of the adsorbent and equilibrium adsorption which takes place in the internal part of the adsorbent particles. The modelling of the adsorption isotherms revealed that data fitted the Freundlich adsorption model better, and this indicates heterogeneity and multilayer adsorption. The results attained from this study showed that the amine-functionalized activated carbon has the potential to be used as an adsorbent for the removal of oil from oil-contaminated wastewaters.

References

Abdulkareem, A., Popelka, A., Sobol˙ciak, P., Tanvir, A., Ouederni, M., AlMaadeed, M. A., Kasak, P., Adham, S & Krupa, I. 2021. The separation of emulsified water/oil mixtures through adsorption on plasma-treated polyethylene powder. *Materials Science and Engineering,* 14(5), 1086.

Ahmad, M. A., Afandi, A. S & Bello, O. S. 2017. Optimization of process variables by response surface methodology for malachite green dye removal using lime peel activated carbon. *Applied Water Science,* 7, 717-727.

Amzi, N. B., Bashir, M. J. K., Sethupathi, S., Wei, I. J & Aun, N. C. 2015. Stabilized landfill leachate treatment by sugarcane bagasse derived activated carbon for removal of colloid, COD and NH3-N-optimization of preparation conditions by RSM. *Journal of Environmental Chemical Engineering,* 3, 1287-1294.

Avila, M., Burks, T., Akhtar, F., Gothelid, M., Lansaker, T., Muhammed, M & Uheida, A. 2014. Surface functionalized nanofibers for the removal of chromium(vi) from aqueous solutions. *Chemical Engineering Journal,* 245, 201-209.

Benadjemia, M., Milliere, L., Reinert, L., Benderdouche, N & Duclaux, L. 2011. Preparation, characterization and methylene blue adsorption of phosphoric acid activated carbons from globe artichoke leaves. *Fuel Processing Technology,* 92, 1203-1212.

Bezerra, D. P., Oliveira, R. S., Vieira, R. S & Azevedo, D. C. S. 2011. Adsorption of co_2 on nitrogen-enriched activated carbon and zeolite 13x. *Adsorption Science and Technology,* 17, 235-246.

Comstock, S. E. H & Boyer, T. H. 2014. Combined magnetic ion exchange and cation exchange for removal of doc and hardness. *Chem Eng J,* 241, 366-375.

Dao, M. T., Tram Nguyen, T. T., Du Nguyen, X., Duong La, D., Duc Nguyen, D., Chang, S. W., Chung, W. J & Nguyen, V. K. 2020. Toxic metal adsorption from aqueous solution by activated biochars produced from macadamia nutshell waste. *Sustainability,* 12.

Das, D & Meikap, B. C. 2021. Role of amine-impregnated activated carbon in carbon dioxide capture. *Indian Chemical Engineer,* 63, 435-447.

Dickhout, J. M., Moreno, J., Biesheuvel, P. M., Boels, L., Lammertink, R. G. H & De Vos, W. M. 2017. Produced water treatment by membranes: A review from colloidal perspectives. *J. Colloid Interface Sci.,* 487, 523-534.

Dickhout, J. M., Virga, E., Lammertink, R. G. H & De Vos, W. M. 2019. Surfactant specific ionic strength effects on membrane fouling during produced water treatment. *Journal of Colloid and Interface Science,* 556, 12-23.

Faisal, M., Pamungkas, A. Z. & Krisnandi, Y. K. 2021. Study of amine functionalized mesoporous carbon as co_2 storage materials. *Processes,* 9(3), 456.

Freundlich, H. M. 1906. Over the adsorption in solution. *Journal of Physical Chemistry,* 57, 385-470.

Gao, P., Zhou, Y., Meng, F., Zhang, Y., Liu, Z., Zhang, W & Xue, G. 2016. Preparation and characterisation of hydrochar from waste eucalyptus bark by hydrothermal carbonization. *energy fuels,* 97, 238-245.

Ghani, Z. A., Yusoff, M. S., Zaman, N. Q., Zamri, M. F. M. A & Andas, J. 2017. Optimization of preparation conditions for activated carbon from banana pseudo-stem using response surface methodology on removal of color and cod from landfill leachate. *Waste Management,* 67, 177-187.

Gummas, R. H & Okpeke, I. 2015. Production of activated carbon and characterization from snail shell waste (helix pomatia). *Advances in Chemical Engineering and Science,* 5, 51-61.

Huang, S., Ras, R. H. S & Tian, X. 2018. Antifouling membranes for oily wastewater treatment: Interplay between wetting and membrane fouling. *Current Opinion in Colloid and Interface Science,* 36, 90-109.

Jamaly, S., Giwa, A & Hasan, S. W. 2015. Recent improvements in oily wastewater treatment: Progress, challenges, and future opportunities. *Journal of environmental sciences*, *37*, 15-30.

Kadir, S., Matali, S., Mohamad, N. F. & Rani, N. H. 2014. Preparation of activated carbon from oil palm empty fruit bunch (EFB) by stem activation using response surface methodology. *international journal of Materials Science and Applications,* 3, 159-163.

Kalash, K. R. a. & Albayati, T. M. 2021. Remediation of oil refinery wastewater implementing functionalized mesoporous materials mcm-41 in batch and continuous adsorption process. *Desalination and Water Treatment,* 220, 130-141.

kehinde, T. J. 2012. *Treatment of oilfield produced water with dissolved air flotation.* Master of Applied Science, Dalhousie University.

Kumar, M & Gupta, S. K. 2019. Response surface methodological (RSM) approach for optimizing the removal of trihalomethanes (THMS) and its precursors by surfactant modified magnetic nano adsorbents (SMNP) - an endeavor to diminish probable cancer risk. *Scientific Reports,* 9.

Langmuir, I. 1918. The adsorption of gases on the plane surfaces of the glass, mica and platinum. *Journal of the American Chemical Society,* 40, 1361-1403.

Lekene, R. B. N., Kouotou, D., Ankoro, N. O., Sone Kouoh, A. P.-M., Ndi, J. M & Ketcha, J. M. 2021. Development and tailoring of amino-functionalized activated carbon based cucumerupsi manni naudin seed shells for the removal of nitrate ions from aqueous solution. *Journal of Saudi Chemical Society,* 25(10), 101316.

Liu, Y., Zhou, S., Liu, R., Chen, M., Xu, J., Liao, M & Yang, L. 2022. Study on amino-directed modification of oil sludge-derived carbon and its adsorption behavior of bisphenol A in water. *Separation and Purification Technology*, *298*, 121625.

Makisha, N. 2020. Research of oily wastewater treatment by means of membrane methods. *IOP Conference Series: Earth and Environmental Science,* 459(4), 042015.

Moreira, F. C., Boaventura, R. A. R., Brillas, E & Vilar, V. J. P. 2017. Electrochemical advanced oxidation processes: A review on their application to synthetic and real wastewaters. *Applied Catalysis B: Environmental,* 202, 217-261.

Mudzielwana, R., Gitari, M. W., Akinyemi, S. A & Msagati, T. A. 2018. Performance of Mn 2+-modified bentonite clay for the removal of fluoride from aqueous solution *South African Journal of Chemistry,* 71, 15-23.

Munzhelele, E. P., Ayinde, W. B., Mudzielwana, R & Gitari, W. M. 2021. Synthesis of fe doped poly p-phenylenediamine composite: Co-adsorption application on toxic metal ions (f− and as3+) and microbial disinfection in aqueous solution. *Toxics,* 9(4), 74.

Myglovets, M., Poddubnaya, O. I., Sevastyanova, O., Lindstrom M.E., Gawdzik, B., Sobiesiak, M., Tsyba, M. M., Sapsay, V. I., Klymchuk, D. O & Puziy, A. M. 2014. Preparation of carbon adsorbents from lignosulfonate by phosphoric acid activation for the adsorption of metal ions. *Carbon,* 80, 771-783.

Najaa Syuhada, M. T., Rozidaini, M.G & Norhisyam, I. 2017. Response surface methodology optimization of oil removal using banana peel as biosorbent. *Malaysian Journal of Analytical Sciences,* 21, 1101-1110.

Nekhavhambe, H. H., Mudzielwana, R., Gitari, M. W., Ayinde, W. B & Izevbekhai, O. U. 2022. Fluoride bio-sorption efficiency and antimicrobial potency of macadamia nut shells. *Materials Science and Engineering,* 15.

Nuru-Shuhada, M.-D., Zaidi, A. G., Suhaimi, A.-T & Chia-Chay, T. 2016. Optimization of activated carbon preparation from spent mushroom farming waste (SMFW) via box-behnken design of response surface methodology. *Malaysian Journal of Analytical Sciences,* 20, 461-468.

Pakade, V. M., Ntuli, T. D & Ofomaja, A. E. 2017. Biosorption of hexavalent chromium from aqueous solutions by macadamia nutshell powder. *Applied Water Science,* 7, 3015-3030.

Priyadarshini, B., Rath, P. P., Behera, S. S., Panda, S. R., Sahoo, T. R. & Parhi, P. K. 2018. Kinetics, thermodynamics and isotherm studies on adsorption of eriochrome black-t from aqueous solution using rutile TiO_2. *IOP Conference Series: Materials Science and Engineering,* 310, 012051.

Rezaei, F & Jones, C. W. 2013. Stability of supported amine adsorbents to so_2 and NO_x in post combustion of co_2 capture. *Industrial and Engineering Chemical Research,* 52, 12192-12201.

Sohaimi, K. S. A., Ngadi, N., Mat, H., Inuwa, I. M & Wong, S. 2017. Synthesis, characterization and application of textile sludge biochars for oil removal. *Journal of Environmental Chemical Engineering,* 5, 122-135.

Tetteh, E. K & Rathilal, S. Response surface optimization of oil refinery treatment process. *In:* Insight, T., ed. 2nd International conference on research advances in engineering, technology, science and management 2019 Dubai-United Arab Emirates. Tech Insight.

Yan, Q., Li, J & Cai, Z. 2021. Preparation and characterization of chars and activated carbon from wood wastes. *Carbon Letter,* 31, 941-956.

Yang, Y., Jiang, X., Liu, H., Ai, G., Shen, L., Feng, X., Ye, F., Zhang, Z., Yuan, H & Mi, Y. 2022. Diethylenetriamine modified biological waste for disposing oily wastewater *Environmental Research,* 212, 113395.

Zhao, C., Zhou, J., Yan, Y & Yang, W. 2020. Application of coagulation/flocculation in oily wastewater treatment: A review. *Science of the Total Environment, 765, 142795*.

Zhao, Y., Fan, R & Feng, L. 2019. Preparation and application of straw activated carbon *IOP Conference Series: Earth and Environmental Science,* 330(4), 042035.

Chapter 5: Preparation and Characterization of Acid Leached Diatomaceous Earth and Amine-Functionalized Activated Carbon Composite Adsorbent for Application in Treatment of Oily Wastewater

Abstract

The previous chapters focused on the synthesis of acid-leached diatomaceous earth (DE) and amine-functionalized activated carbon (AC) adsorbents for the treatment of oily wastewater. The adsorbents were synthesized, characterized with a wide range of established analytical techniques, and evaluated for the treatment of synthetic oily wastewater. Acid-leached DE was successfully leached and therefore showed an increase on the SiO_2 content from 78% to 91%. Furthermore, it showed maximum oil removal efficiency of 78.55% with adsorption capacity of 124.16 mg/g at optimum conditions of 3229.69 mg/L initial oil concentration, 0.05 g adsorbent dosage and 119.20 mins contact time. The prepared amine-functionalized AC showed a maximum adsorption capacity of 167.96 mg/g with a removal efficiency of 82.93% at initial oil concentration of 10 000 mg/L, adsorbent dosage of 0.1 g/ 25 mL and contact time of 60 mins. In this chapter, the preparation of acid-leached DE/amine-functionalized AC composite adsorbent for the remediation of oily wastewater is reported. To prepare the composite adsorbent, the two adsorbents were mixed at three different ratios, 1:1, 1:2, and 2:1 (acid-leached DE: amine-functionalized AC) and homogenized through pestle and mortar grounding. Thereafter, the composite adsorbent was characterized and applied in oil removal experiments. The prepared composite adsorbent showed a maximum oil removal percentage of 90.02% with maximum adsorption capacity of 416.67 mg/g at initial oil concentration of 5250 mg/L, adsorbent dosage of 0.3 g, and contact time of 60 mins. The adsorption kinetics data showed a better fit to the pseudo-second order model (R^2=0.98), showing that adsorption took place via chemisorption. Freundlich adsorption isotherm model descried the adsorption better showing that adsorption occurred on a heterogeneous and multilayer surface. Regeneration studies showed that the composite adsorbent can be reused in oil removal from oily wastewater for up to five adsorption cycles. Results obtained in this chapter show that the prepared composite has the potential for use in oily wastewater treatment.

Keywords: Acid-leached Diatomaceous Earth; Activated Carbon; Adsorption; Amine Functionalization; Response Surface Methodology.

5.1. Introduction

Water is a vital resource that is crucial for the survival of the earth's ecosystem (Mohammed & Tanweer, 2018). However, freshwater bodies in South Africa have been declining in quality due to the increased pollution caused by increased energy demands, mining, industrialization, oil exploration, and agricultural activities. These activities result in the release of large amounts of pollutants such as oils, solvents, fungicides, antibiotics, and herbicides into the environment. Thus, the discharge of the polluted water results in contamination of receiving water bodies which pose serious risks to humans, animals and plants (Firdous et al., 2018, Huang et al., 2018, Humbatova & Hajiyev, 2019).

Oily wastewater is wastewater that contains various types of oils including hydrocarbons, lipids, and petroleum fractions such as kerosene, gasoline, and diesel oil (Jamaly et al., 2015). To safeguard freshwater sources, several techniques have been developed to remove oil pollutants from wastewater prior to their discharge into water bodies. These techniques include membrane filtration (Dickhout et al., 2017), electrochemical advanced oxidation (Moreira et al., 2017), reverse osmosis (Makisha, 2020), coagulation-flocculation (Zhao et al., 2020), evaporation (Han et al., 2019), ion exchange (Comstock & Boyer, 2014), and adsorption (Sohaimi et al., 2017). Owing to its fast and high removal efficiency, simple to operate characteristics, and cost-effectiveness, adsorption ranks amongst the most effective techniques for the remediation of oily wastewater (Li et al., 2022).

In recent years, research has been geared towards developing effective and dependable adsorbents with high adsorption capacity, simple separation process, chemical resistance, low cost, and eco-friendly with wide application in various industries (Ismail et al., 2022). Various carbon-based adsorbents have been applied in previous studies and these include multiwalled nanotubes (Li et al., 2018), and sponges (Zhao et al., 2011) together with silica based-adsorbent such as acetylated silica derived from DE (Izevbekhai et al., 2020), and raw and calcined DE (Bandura et al., 2017). These adsorbents showed high removal efficiencies and adsorption capacities of 12.62 g/g, 70 g/g, 1039 mg/g, and 0.05-0.8 mg/g, respectively.

In chapter 3, raw DE was successfully leached using HNO_3, and in chapter 4 AC from raw macadamia nutshells (MNS) was functionalized with hydroxylamine hydrochloride and both were investigated for ability to remove oil from synthetic oily wastewater. Amine-functionalized AC showed superior adsorption capacity compared to the acid-leached DE. Specifically, whereas the acid-leached DE showed an adsorption capacity of 124.16 mg/g,

the amine-functionalized AC showed an adsorption capacity of 167.96 mg/g. Therefore, this chapter aims to prepare a composite adsorbent consisting of acid-leached DE and amine-functionalized AC and evaluate its adsorption capacity towards oil removal from oily wastewaters. It is hypothesized that blending acid-leached DE and amine-functionalized AC could yield an improved adsorbent emanating from the physiochemical properties (e.g., high porosity, high surface area, and excellent heat resistance) and high adsorption capacity of the respective individual materials. The specific objectives of this study are to: 1) characterize and determine the physicochemical and mineralogical composition to the composite adsorbent using FTIR, BET, and SEM, 2) optimize operational parameters for the removal of oil removal from oily wastewater and determine the adsorption mechanism involved, and 3) investigate the recyclability of the composite adsorbent.

5.2. Materials and methods

5.2.1. Materials

DE was procured from Eco–Earth (Midrand, South Africa). MNS were obtained from the Royal Macadamia Farm in Levubu, South Africa. All chemical reagents including sodium hydroxide, orthophosphoric acid, hydrochloric acid, hydroxylamine hydrochloride and ethanol were of analytical grade and were purchased from Rochelle Chemicals Supplies (Johannesburg, South Africa). Working solutions of various chemical concentrations were prepared using deionized water (18.2MΩ/cm) from Merck Millipore water system. Sea salt was purchased from a local retailer chain store (Shoprite in Thohoyandou Venda Plaza, South Africa). Petroleum fractions (kerosene, petrol, and diesel) were purchased from Shell garage (Thohoyandou, Limpopo).

5.2.2. Preparation of acid-leached diatomaceous earth and amine-functionalized activated carbon composite

To prepare the composite adsorbent, acid-leached DE was prepared following the procedure set out in chapter 3, and amine-functionalized AC was prepared as per procedure set out in chapter 4. The two adsorbents were mixed by varying three different ratios (1:1, 1:2, and 2:1) of acid-leached DE: amine-functionalized AC and thereafter homogenized through grounding using pestle and mortar. After homogenizing, the composite adsorbent was stored in ziplocked bags, and characterization and oil removal experiments were conducted.

5.2.3. Adsorbent characterization

Fourier Transform Infrared Spectroscopy (FTIR) was used to determine the functional groups (Bruker, Germany) present in the adsorbents. Brunauer-Emmet-Teller (BET) surface area measurements and pore characteristics were performed using the Micromeritics Tristar II Surface Area and Porosity Analyser (USA). The morphological analysis of the materials and electron mapping was performed using scanning electron microscopy (SEM) (FEI Nova NanoSEM 230 from Eindhoven, Netherlands). The composition of carbon, hydrogen, nitrogen, and sulphur were determined using the Thermo Flash 2000 series CHNS/O organic Elemental analyzer (Cert Ref Std sulfamethazine).

5.2.4. Preparation of synthetic oily wastewater

Synthetic oily wastewater used in this study was prepared by adopting with slight modification the procedures used by kehinde (2012) and Dickhout et al. (2019). Briefly, 0.02 g of each of the three petroleum fractions (kerosene, petrol, and diesel), 1.3 g of sea salt, and 0.23 g of sodium dodecyl sulphate were weighed and transferred into a 500 mL beaker containing deionized water corresponding to each concentration generated using response surface methodology (RSM) shown in Table 5.1. Thereafter, the resultant mixture was homogenized through sonication for 5 mins.

5.2.5. Oil removal experiments

Optimization of conditions for oil removal using acid-leached DE/amine-functionalized AC composite was carried out using the response surface methodology (RSM) experimental design software (version 11, Stat-Ease Inc., Minneapolis, USA). Table 5.1 summarizes the conditions considered for optimization. The experiments were performed as follow: various amounts of acid-leached DE/amine-functionalized AC composite was weighed and enclosed in a tea bag. Thereafter, the tea bags containing the adsorbents were placed in 250 mL beakers containing 25 mL of the synthetic oily effluent before being left undisturbed for various periods as guided by the experimental design from RSM. At the end of experiment, mixtures were filtered through an EZ-Pak ® membrane filter. The residual oil contents were estimated in the form of total organic carbon using Spectroquant UV spectrophotometer from Merck group (Germiston, South Africa). For quality assurance, blank experiment was performed using empty tea bag. The oil removal efficiencies and adsorption capacities were estimated using Equation 5.1 and 5.2, respectively.

$$\% \text{ Removal} = \left(\frac{(C_i - C_f)}{C_i}\right) 100 \quad (5.1)$$

$$Qe = \left(\frac{(C_i - C_f)}{m}\right) V. \quad (5.2)$$

where C_i denotes the initial oil concentration and C_f denotes the oil concentrations (mg/L) following adsorbent treatment. V (L) symbolizes the volume of the solution, m (g) the mass of the adsorbent, and Qe (mg/g) an equilibrium adsorption capacity per milligram dry weight of the adsorbent.

Table 5.1: Range of optimized parameters

Name	Low	High
Adsorbent dosage (g)	0.1	0.3
Initial oil concentration (mg/L)	500	10000
Contact time (mins)	60	300

5.2.6. Adsorption Kinetics

The effect of contact time and oil sorption kinetics was evaluated by varying the contact time from 10 to 120 mins, and using the initial oil concentration of 500 mg/L and adsorbent dosage of 0.1 g/25 mL for each contact time. The linear equation of pseudo-first order (Eq. 5.3) and pseudo-second order (Eq. 5.4) reaction models (Ebelegi et al., 2020), and intraparticle diffusion model of Weber-Morris (5.5) (Weber and Morris, 1963) were used to provide insight into the adsorption kinetics and the rate limiting steps and to fit the experimental data.

$$\text{Log}(qe - qt) = Logqe - \frac{K_1}{2.303} t \quad (5.3)$$

$$\frac{t}{Qt} = \frac{1}{K_2 qe^2} + \frac{1}{q_e} t \quad (5.4)$$

$$qt = k_i t^{0.5} + ci \quad (5.5)$$

where q_e and q_t symbolizes the adsorption capacities at equilibrium and time t, respectively; k_1 and k_2 are the rate constants for pseudo-first order and pseudo-second order, respectively. The constant of intra particle diffusion rate, K_i (mg/g min-1), is determined by the slope of $t^{0.5}$ vs. q_t, while C_i the constant of the boundary layer thickness (Mudzielwana et al., 2018, Abbas, 2020).

5.2.7 Adsorption Isotherms

The adsorption isotherms were determined using linear equations of Langmuir and Freundlich adsorption isotherms models (Eq. 5.6-5.7) and were used to determine the adsorbate-adsorbent interaction. The isotherms were determined at concentration ranges of 50 to 200 mg/L.

$$\frac{C_e}{q_e} = \frac{1}{K_a q_m} + \frac{1}{q_m} C_e \quad (5.6)$$

$$Log q_e = Log K_F + \frac{1}{n} Log C_e \quad (5.7)$$

where C_e, K_a, q_e and q_m and denote the adsorption capacity (mg/g), the equilibrium concentration (mg/L), the Langmuir constant associated to enthalpy of adsorption (L/mg) and theoretical maximum adsorption capacity (mg/g), respectively. The K_F values correspond to the Freundlich constant that is interrelated to adsorption capacity and adsorption intensity. The heterogeneity factor is 1/n, where n represents the intensity of the process, the diversity of the reactive sites of the adsorbent, and the relative energy distribution (Abdulkareem et al., 2021). When $0 < 1/n < 1$, the adsorption is favourable; when $1/n=1$, the adsorption is irreversible; and when $1/n > 1$, the adsorption is unfavourable (Abbas, 2020).

5.2.8. Regeneration studies

The reusability of the adsorbent was investigated over 5 cycles using 25 mL of high purity ethanol as a regeneration solution. The spent adsorbent was vigorously stirred (300 rpm) 3 times in an ethanol solution (99 wt% concentration) for 10 mins to remove the adsorbed oil and after filtered, washed with 1.5 L of distilled water and further dried at 60 °C for 10 hours. The oil removal parameters used were 5250 mg/L of initial oil concentration, 60 mins of contact and 1 g/25 mL adsorbent dosage.

5.3. Results and discussions

5.3.1. Optimization of acid-leached diatomaceous earth/amine-functionalized activated carbon

Figure 5.1 shows the oil removal percentage using the three various ratios of the composite adsorbent. The three varied ratios, 1:1, 1:2, and 2:1 of the composite showed percentage removal of 84%, 64, and 77%, respectively. The ratio 1:1 was chosen for characterization and oil removal studies using the composite adsorbent based on its highest oil removal percentage.

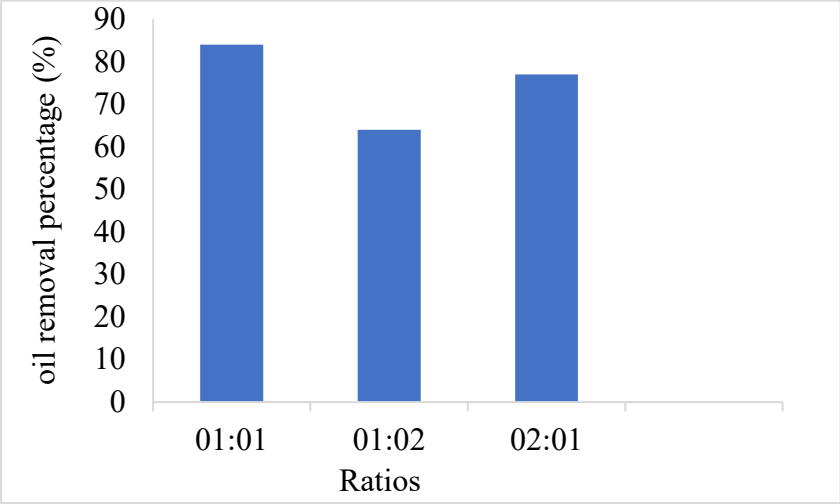

Figure 5.1: The oil removal percentage using the three varied ratios of the composite adsorbent.

5.3.2. Morphological analysis

Figure 5.2a-c shows micrographs of the (a) acid-leached DE amine-functionalized, (b), AC, and (c) the synthesized composite adsorbent. According to Figure 5.2a, the acid-leached diatomaceous earth has visible pores arranged in a regular pattern. The amine-functionalized AC (Figure 5.2b) has a foam-like structure which shows an expansion of the particles size of the material after introduction of the amine groups. Figure 5.2(c) shows the presence of pores on a rough surface with some particles of varying sizes on the surface of the composite material owing to the addition of some functional groups which allows ease of the transfer of the oil molecules into the inner surface of the composite material.

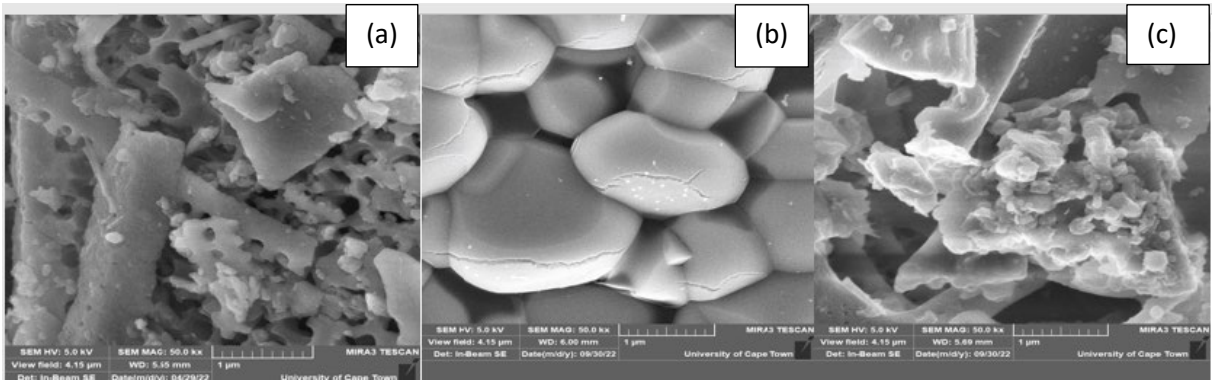

Figure 5.2: Micrographs of the acid-leached DE (a), amine-functionalized AC (b), and the synthesized composite adsorbent (c).

5.3.3. Fourier Transform Infrared Spectroscopy analyses

Figure 5.3 shows the FTIR spectrum of amine-functionalized AC, acid-leached DE, and the prepared adsorbent composite. The region between 1000-1500 cm^{-1} corresponds to C-N single bonding for amine-functionalized AC. A similar bond was identified by Yang et al. (2007) in a ultra-fine carbon nitride nanocrystal material. The adsorption peak at 795 cm^{-1} and 1100 cm^{-1}, which are ascribed to the Si-O-Si stretching vibration and Si-O bond were observed on the acid-leached DE. The absorbance bands appearing at 2900-3000 cm^{-1} exhibit C-H stretching vibration, and the 2500 cm^{-1} band is attributed to the stretching vibration of O-H from physically absorbed moisture on the composite surface. The N-H and C=O groups were observed on the surface of the composite at about 1390 cm^{-1}, which result from the amine-functionalization of the AC (Rashid et al., 2019). The adsorption peaks at 795 cm^{-1} and 1100 cm^{-1} are ascribed to the Si-O-Si stretching vibration and Si-O bond; these indicate that the amine-functionalized AC has been successfully blended with the acid-leached DE and has resulted in the formation of the composite.

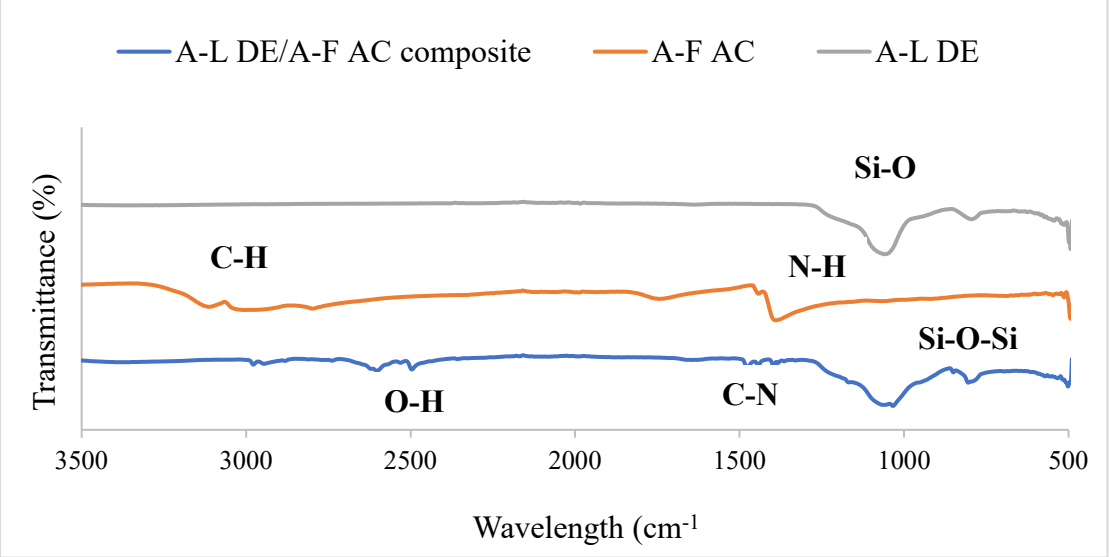

Figure 5.3: FTIR Spectrum of the acid-leached DE, amine-functionalized AC and the composite adsorbent.

5.3.4. Surface area and pore characteristics analysis

Table 5.2 shows the surface area and pore characteristics of acid-leached DE, amine-functionalized AC and the composite adsorbent. The results showed the surface area of 22.40, 0.43, and 2.06 m^2/g for the acid-leached DE, amine-functionalized AC, and the composite, respectively. The high surface area of the acid-leached DE can be related to the pores that are well developed on the surface of the acid-leached DE; this aspect was also observed in the SEM micrographs (Figure 5.1). The low surface area of the amine-functionalized AC is ascribed to the swelling of the particles on the surface of the amine-functionalized AC as shown in the SEM results (Figure 5.1). However, there was an enhancement in the surface area of the composite material of the amine functionalized AC; this is attributed to the high surface area of the acid leached DE and its well-developed porous surface. High surface areas of the acid leached DE and the composite might be associated with less than average particle sizes as seen in the results presented in Table 5.2. Additionally, a decrease in the average particle size has aided in increasing pore volume which leads to an increase in the pore diameter and subsequently allows multiple adsorptions of oil droplets on the surface of the adsorbent. The resulting pore diameters affirmed the mesoporosity, microporosity, and mesoporosity of the acid-leached DE, amine-functionalized AC, and composite, respectively.

Table 5.2: BET surface area and pore characteristics of acid-leached DE, amine-functionalized AC, and the composite.

	Acid-leached DE	**Amine-functionalized AC**	**Composite**
BET Surface area (m^2/g)	22.40	0.43	2.06
Pore Volume (cm^3/g)	0.03	0	0.03
Pore diameter (Å)	68.71	3.66	57.60
Average particle size (Å)	2 678.35	1 387 716.04	29 083.79

5.4. Optimization of oil removal

5.4.1. Response surface plots

Figure 5.4 shows the variation of oil removal percentage using the composite adsorbent against (a) contact time and adsorbent dosage, (b) initial oil concentration and adsorbent dosage, and (c) initial oil concentration and contact time.

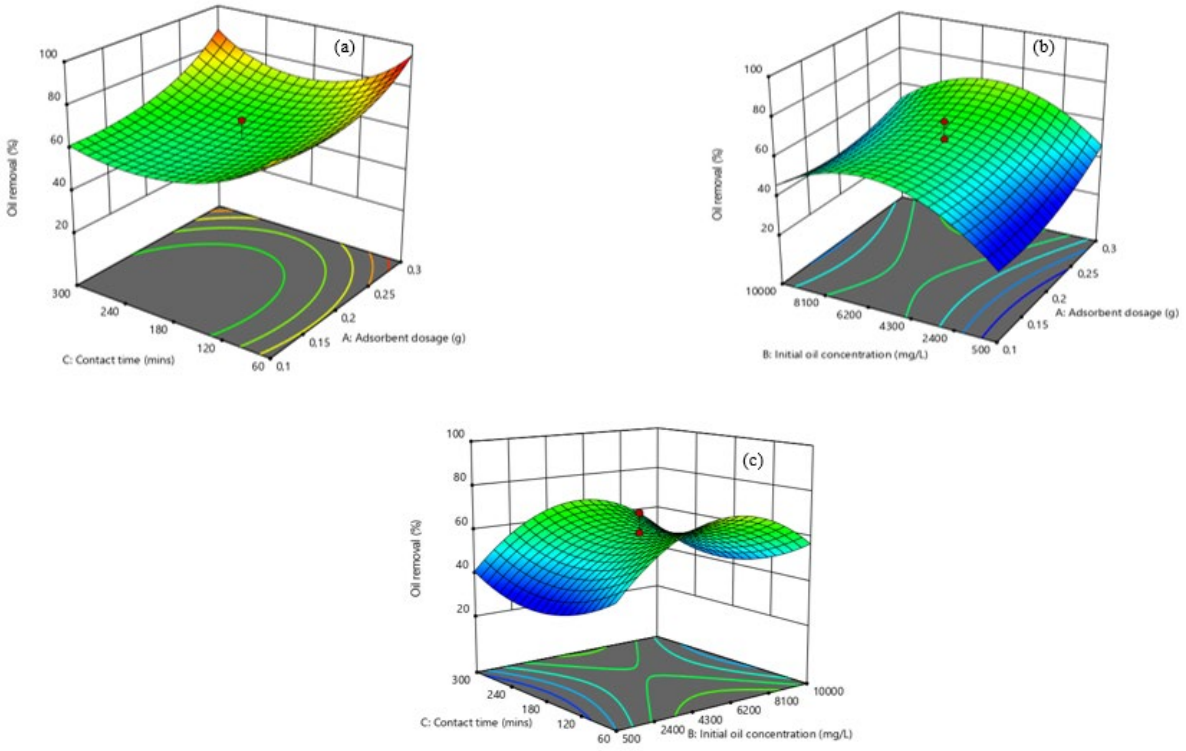

Figure 5.4: Variation of oil removal percentage against (a) contact time and adsorbent dosage, (b) initial oil concentration and adsorbent dosage, (c)initial oil concentration and contact time

Figure 5.4a shows the plot for the effect of contact time and adsorbent dosage on oil removal percentage. Oil removal percentage improved with an increasing adsorbent dosage resulting from more available binding sites accessible for the oil particles to be adsorbed on the surface of the composite (Syuhada et al., 2017, Abdel-Ghani & El-Chaghaby, 2014). At higher contact time (300 mins) and adsorbent dosage (0.3 g), the oil removal percentage was high due to more active sites being available for the oil molecules to be adsorbed on the surface of the composite adsorbent and adequate time for the oil molecules to bind on the adsorbent sites. A maximum oil removal percentage of 88% was achieved at 300 mins contact time and 0.3 g adsorbent dosage.

Figure 5.4b depicts the effect of initial oil concentration and adsorbent dosage on oil removal percentage. It is observed that the oil removal percentage increased with a decrease in initial oil concentration from 10 000 to 6 200 mg/L, and this attributed to limited active pores against the oil concentration gradient. At the highest initial oil concentration, more oil molecules were left un-adsorbed in the solution as a result of saturated binding sites (Abdel-Ghani and El-

Chaghaby, 2014). Oil removal percentage increased with adsorbent dosage and this was ascribed to the introduction of new adsorbent binding sites. At high initial oil concentration and adsorbent dosage, the oil removal percentage decreased. A maximum percentage of removal of 70% was achieved at 6200 mg/L initial oil concentration and 0.3 g adsorbent dosage.

Figure 5.4c shows the effect of initial oil concentration and contact time on oil removal percentage. It can be seen that the oil removal percentage increases with both initial oil concentration and contact time; this however decreases after it had reached equilibrium owing to inadequate binding sites on the adsorbent surface for the oil adsorbate molecules to be adsorbed (Kadir et al., 2014). The increasing contact time led to increased oil removal percentage is due to an increased chance of positive interaction between oil adsorbate molecules and the adsorbent since the adsorbent stays in contact with the synthetic oily wastewater solution for a longer period (Najaa Syuhada et al., 2017). After a longer contact time, the breakage of the oil molecules is enhanced thus reducing the emulsification of the synthetic oily wastewater, and this leads to a greater surface area at the interface for adsorption to occur and encourages the adsorption of oil by the adsorbent (Ahmad et al., 2005b, Syuhada et al., 2017). A maximum oil removal percentage of 70% was achieved at 6200 mg/L initial oil concentration and 60 and 300 mins contact time.

5.4.2. Analysis of variance

Table 5.3 summarizes the results of the ANOVA test. A *p*-value below 0.05 indicates that the model and its terms are significant. The quadratic model used to characterize the oil removal percentage by the composite was significant with a *p*-value of 0.04 and a F-value of 4.66. Adsorbent dosage (A) was found to have a significant effect on the oil removal percentage with a *p*-value of 0.03. The oil removal percentage improved with increasing adsorbent dosage. All the quadratic function of the model terms, adsorbent dosage (A^2), initial oil concentration (B^2), and contact time (C^2) were found to be significant with *p*-values of 0.03, 0.00, and 0.01, respectively. The lack of fit F-value of 1.54 suggests and insignificant lack of fit and that the model is adequate to represent the relationship between the parameters and the response.

Table 5.3: ANOVA for Quadratic model and model terms.

Source	F-value	p-value	
Model	4.66	0.04	Significant
A-Adsorbent dosage	8.29	0.03	
B-Initial oil concentration	4.10	0.09	
C-Contact time	0.96	0.37	
AB	1.18	0.32	
AC	0.06	0.82	
BC	0.02	0.91	
A^2	8.43	0.03	
B^2	23.26	0.00	
C^2	11.44	0.01	
Residual			
Lack of Fit	1.54	0.36	not significant

5.4.3. Predicted and actual value plot

The model prediction for the oil removal percentage from the synthetic oily wastewater by the composite was analysed and compared with actual values attained from experimental data plotted in Figure 5.5. The points with a red colour denote values are higher than the predicted values, the points with a green colour denote values equivalent to the predicted values, whereas points with a blue colour were less than the predicted values. The coefficient of determination R^2 was found to be 0.87. The quadratic model was suitable to elucidate the link between the response and significant parameters since the anticipated and actual values were corresponding (Ani et al., 2019).

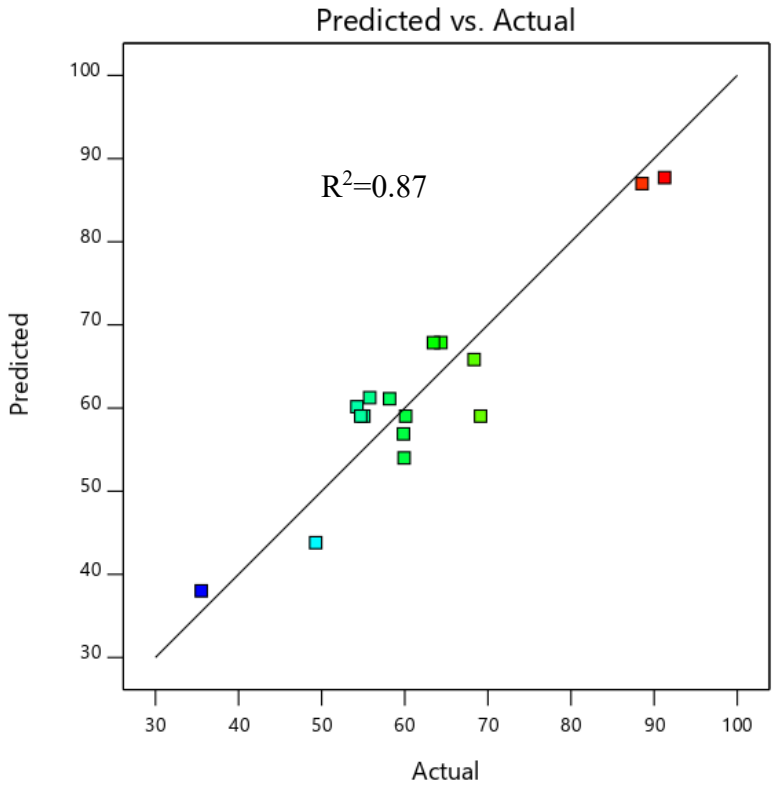

Figure 5.5: Comparison between predicted and actual values by Response Surface Methodology.

5.5. Optimum conditions

Table 5.4 depicts the optimum conditions for oil removal percentage and adsorption capacity. The model presented the optimum conditions for the oil removal which were an initial oil concentration of 5250 mg/L with an adsorbent dosage of 0.3 g, and a contact time of 300 mins leading to an adsorption capacity of 416.67 mg/g. The desirability of the model was found to be 0.99.

Table 5.4: Optimum conditions for oil removal percentage and adsorption capacity.

Initial Oil Concentration (mg/L)	Adsorbent Dosage (g)	Contact Time (mins)	Oil removal percentage (%)	Adsorption Capacity (mg/g)	Desirability
5250	0.3	60	90.02	416.67	0.99

5.6. Adsorption kinetics

Tables 5.5 and 5.6 present the data obtained from adsorption kinetics data modelling using pseudo first-order and second-order of reaction kinetics model as well as Webber-Morris

intraparticle diffusion model with their respective plots being presented in Figures 5.6a and b. The kinetic plots indicate a good fit followed by the pseudo second-order which is validated by a significantly higher correlation co-efficient (R^2=1) compared to pseudo first-order (R^2=0.84). This suggests that the dominant uptake mechanisms of oil molecules by the synthesized composite is via the chemisorption process (Ho, 2006, Lim et al., 2020).

Table 5.5: Constant parameters for pseudo first-order and pseudo second-order of reaction kinetics.

Parameters	Pseudo first-order	Pseudo second-order
K (min^{-1})	0.05	0.01
Q_e (mg/g)	0.05	100
R^2	0.84	1

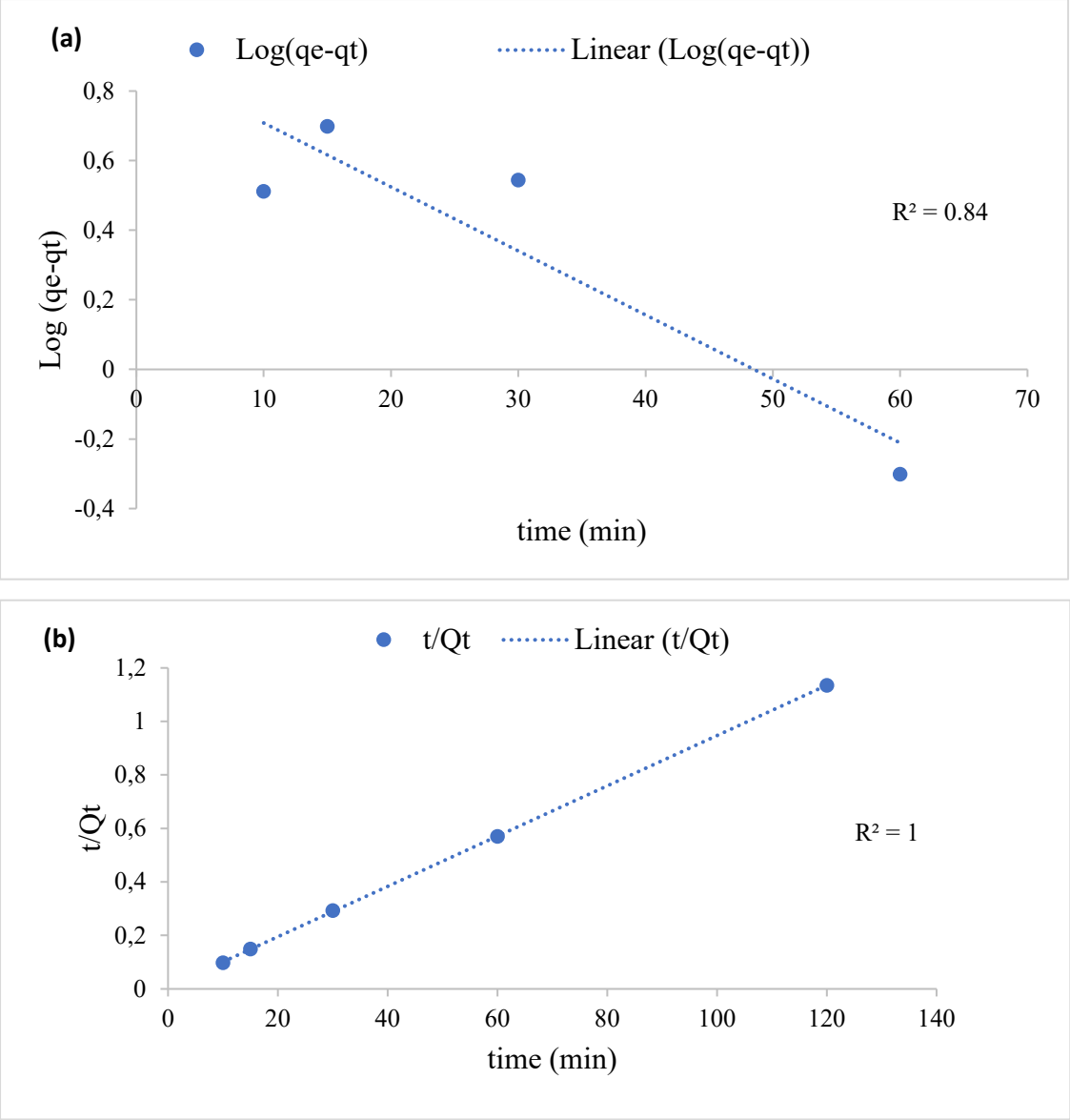

Figure 5.6: Linear plots for (a) Pseudo first-order, (b) Pseudo second-order for oil adsorption onto the prepared Composite.

Figure 5.7 shows the intraparticle diffusion plot for the adsorption of oil molecules onto the composite. Oil adsorption is regarded to be taking place in three phases. Oil molecules are first drawn to the surface of the composite adsorbent during the initial phase of adsorption on the boundary layer of the composite adsorbent. In the second phase, oil molecules diffuse within the pores of the composite adsorbent, a process known as intra-particle diffusion. During equilibrium, oil molecules adhere to the interior surface of the adsorbent, thus causing the third phase. Table 5.6 shows intra-particle rate constants for phases 1, 2, and 3 (K_1, K_2, and K_3). The adsorption process on the intra-particle diffusion was highly faster in comparison to the border layer and equilibrium adsorption, and this could be attributed to an existence of large pores.

An improvement in the boundary layer of the adsorbent particles was noticed. This improvement is evidenced by the fact that the value of C, a constant related to the thickness of the boundary layer, improved.

Table 5.6: Constant parameters for intra-particle diffusion model.

Parameters	Phase 1	Phase 2	Phase 3
$K_{1,2,3}$ (mg/g.min$^{1/2}$)	-2.46	1.17	0.16
C_1	110.29	96.10	104.04
R^2	1	0.99	1

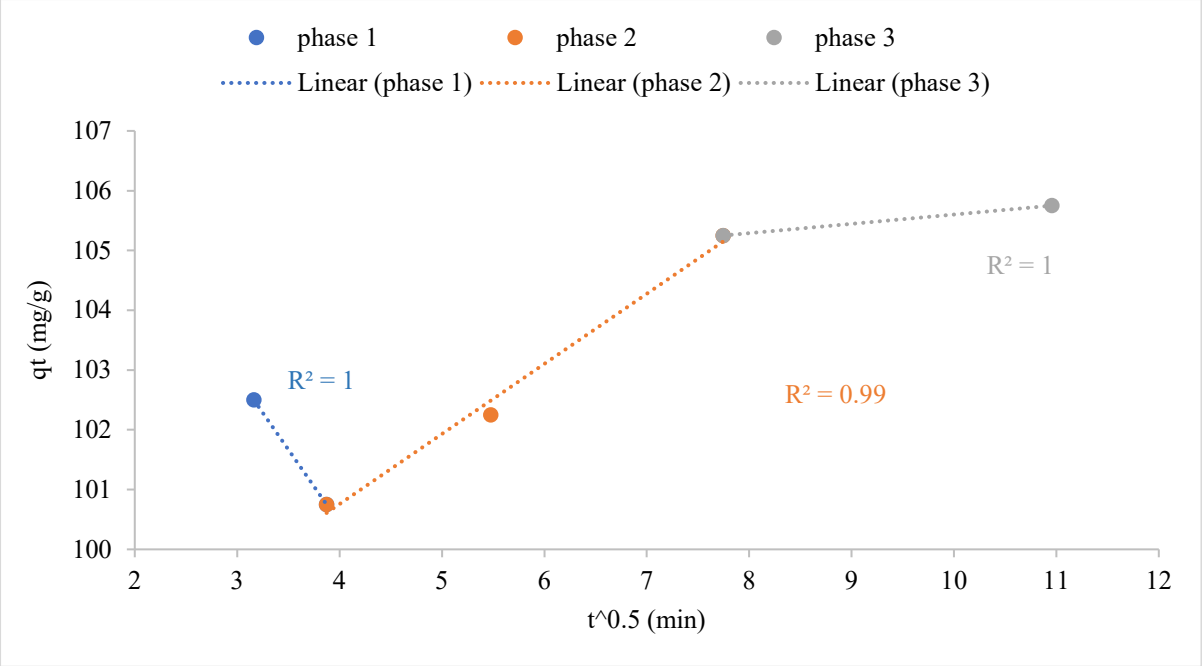

Figure 5.7: Intra-particle diffusion plot for oil adsorption onto the prepared composite.

5.7. Adsorption isotherms

The linear plots of the adsorption isotherms are presented in Figure 5.8, while the constant parameters for Langmuir and Freundlich isotherm models are presented in Table 5.7. Based on the results depicted in Figure 5.8, the experimental data fits the Freundlich isotherms well. This is evidenced by the high correlation coefficient (R^2=0.98) which indicates heterogeneity and multilayer adsorption. Furthermore, the Freundlich intensity parameter (1/n) values less than 1 confirm the favourability of the sorption processes (Munzhelele et al., 2021).

Table 5.7: Adsorption isotherm parameters for oil adsorption onto the composite

Freundlich Parameters	Values	Langmuir Parameters	Values
K_F (mg/g)	0.47	Q_m (mg/g)	0.28
N	0.31	K_L (L/mg)	-0.03
R^2	0.98	R^2	0.97

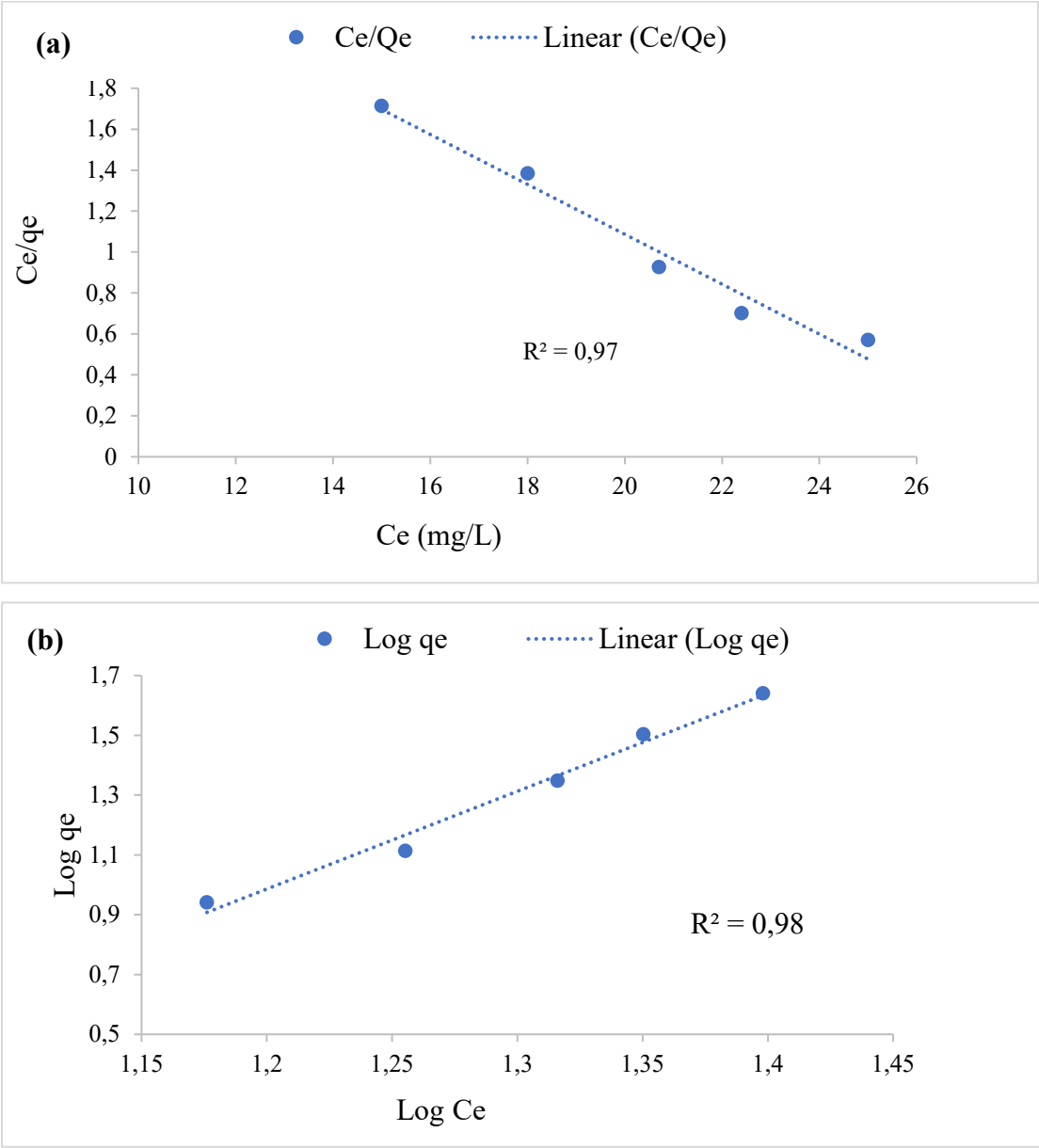

Figure 5.8: Linear plots for (a) Langmuir and (b) Freundlich for oil adsorption onto the prepared composite.

5.8. Regeneration studies

Figure 5.9 presents the reusability studies of the prepared composite. The oil removal percentage of composite generally decreases with each regeneration cycle reaching 27% by the 5th cycle (from 81% in the first cycle). The decrease in the reusability of the composite might be due to inadequate regeneration of the active sites on the surface of the composite adsorbent. These results indicates that the material can be regenerated albeit reaching a mere 27% at the 5th cycle.

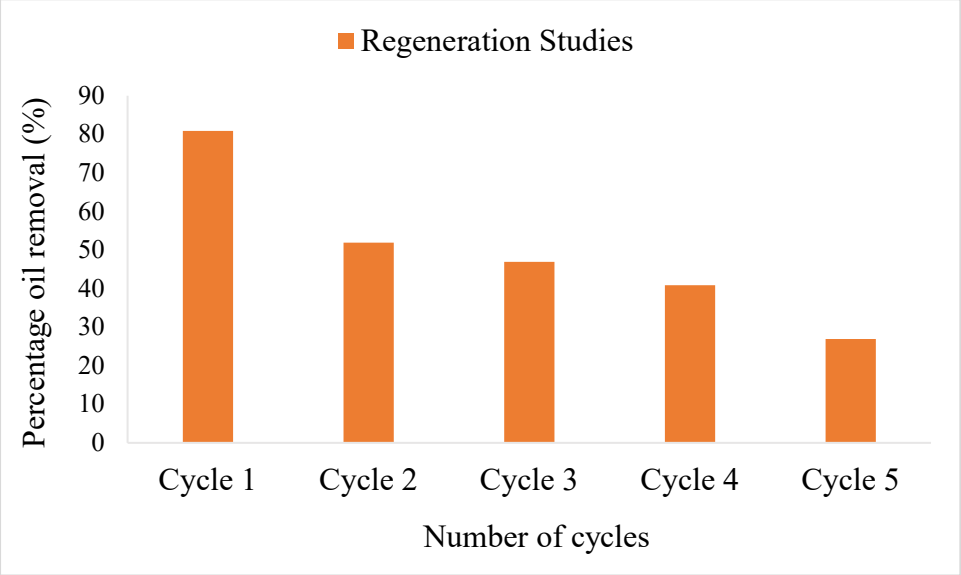

Figure 5.9: A recyclability study of the prepared composite.

5.9. Comparison to other adsorbents

Table 5.8 shows a comparative analysis of adsorption capacities of the synthesized composite adsorbent with other reported adsorbents in the literature. It is evident that the adsorption capacity of the synthesized composite is greater than that of Feldspar/banana peel composite and PTMA and ODTMA montmorillonite but lower than the acetylated coconut-husk derived biochar and organic/silver nanocomposite. However, it is a well-known that the adsorption capacity depends on the experimental conditions (Zhang et al., 2020). That being the case, the synthesized composite is an effective adsorbent for the treatment of oily wastewaters.

Table 5.8: Comparison of adsorption capacity for different adsorbents

Adsorbent	Type of oily water	Adsorption Capacity (mg/g)	Reference
Feldspar/banana peel composite	Crude oil produced water	360	(Dawodu et al., 2021)
Acetylated coconut-husk-derived biochar	Crude oil contaminated marine water	1680	(Agarry et al., 2020)
Organic/silver nanocomposite	Oil-in-water emulsion	6110	(Akpomie and Conradie, 2021)
PTMA and ODTMA montmorillonite	Surface oil spill	300	(Amir et al., 2013)
Acid-leached DE	Synthetic oily wastewater	124.16	This study
Amine-functionalized AC	Synthetic oily wastewater	167.96	This study
Acid-leached DE/amine-functionalized AC composite	Synthetic oily wastewater	416.17	This study

5.10. Summary

In this chapter, the acid-leached diatomaceous earth/amine-functionalized activated carbon composite was successfully prepared and tested evaluated for the treatment of oily wastewater. The BET surface area of the composite was found to be 2.06 m^2/g. It was demonstrated in this study that the composite could be applied as an effective adsorbent for oil adsorption with optimum conditions of 5250 mg/L initial oil concentration, 0.3 g adsorbent dosage, and 300 mins contact time yielding an oil removal percentage of 90.02% and maximum adsorption capacity of 416.67 mg/g. The adsorption kinetics data showed a best fit for pseudo second-

order model of reaction kinetics thus indicating that adsorption occurs via chemisorption. The adsorption isotherms data fits the Freundlich adsorption model better, thus indicating heterogeneity and multilayer adsorption. The regeneration studies revealed that the composite adsorbent has the potential to be reused for up to 5 adsorption-regeneration cycles using high purity ethanol as regenerant. The results attained from this study showed that the composite is a potential adsorbent for the removal of oil from oily wastewaters.

References

Abbas, M. 2020. Removal of brilliant green (BG) by activated carbon-derived from medlar nucleus (ACMN) – kinetic, isotherms and thermodynamic aspects of adsorption. *Adsorption Science and Technology,* 38, 464-482.

Abdel-Ghani, N. & El-Chaghaby, G. 2014. Biosorption for metal ions removal from aqueous solutions: A review of recent studies. *International Journal of Latest Research in Science and Technology,* 3, 24-42.

Abdulkareem, A., Popelka, A., Sobol˘ciak, P., Tanvir, A., Ouederni, M., AlMaadeed, M. A., Kasak, P., Adham, S. & Krupa, I. 2021. The separation of emulsified water/oil mixtures through adsorption on plasma-treated polyethylene powder. *Materials Science and Engineering,* 14(5), 1086.

Agarry, S. E., Oghenejoboh, K. M., Oghenejoboh, E. O., Owabor, C. N. & Ogunleye, O. O. 2020. Adsorptive remediation of crude oil contaminated marine water using chemically and thermally modified coconut (CoCos nucifera) husks. *Journal of Environmental Treatment Techniques,* 8, 694-707.

Ahmad, A. L., Sumathi, S. & Hameed, B. H. 2005. Adsorption of residue oil from palm oil mill effluent using powder and flake chitosan: Equilibrium and kinetic studies. *Water Research,* 39, 2483-2494.

Akpomie, K. G. & Conradie, J. 2021. Ultrasonic aided sorption of oil from oil-in-water emulsion onto oleophilic natural organic-silver nanocomposite. *Chemical Engineering Research and Design,* 165, 12-24.

Amir, D. Z., Bleiman, N. & Mishael, Y. G. 2013. Sepiolite as an effective natural porous adsorbent for oil-spill *Microporous and Mesoporous Material,* 169, 153-159.

Ani, J. U., Okoro, U. C., Aneke, L. E., Onukwuli, O. D., Obi, I. O., Akpomie, K. G. & Ofomatah, A. C. 2019. Application of response surface methodology for optimization of dissolved solids adsorption by activated coal. *Applied Water Science,* 9, 60.

Bandura, L., Woszuk, A., Kolodynska, D. & Franus, W. 2017. Application of mineral sorbents for removal of petroleum substances: A review. *Minerals,* 7(3), 37.

Comstock, S. E. H. & Boyer, T. H. 2014. Combined magnetic ion exchange and cation exchange for removal of doc and hardness. *Chemical Engineering Journal,* 241, 366-375.

Dawodu, F. A., Abonyi, C. J. & Akpomie, K. G. 2021. Feldspar-banana peel composite for efficient crude oil removal from solution. *Applied Water Science,* 11, 1-10

Dickhout, J. M., Moreno, J., Biesheuvel, P. M., Boels, L., Lammertink, R. G. H. & De Vos, W. M. 2017. Produced water treatment by membranes: A review from colloidal perspectives. *Journal of Colloid and Interface Science,* 487, 523-534.

Dickhout, J. M., Virga, E., Lammertink, R. G. H. & De Vos, W. M. 2019. Surfactant specific ionic strength effects on membrane fouling during produced water treatment. *Journal of Colloid and Interface Science,* 556, 12-23.

Ebelegi, A. N., Ayawei, N. & Wankasi, D. 2020. Interpretation of adsorption thermodynamics and kinetics. *Open Journal of Physical Chemistry,* 10, 166-182.

Firdous, S., Jin, W., Shahid, N., Bhatti, Z. A., Igbal, A., Mahmood, Q. & Ali, A. 2018. The perfomance of microbial fuel cells treating oil industrial wasterwater. *Environmental and Technology Innovation,* 10, 143-151.

Han, M., Zhang, J., Chu, W., Chen, J. & Zhou, G. 2019. Research progress and prospects of marine oily wastewater treatment: A review. *Water, Air, and Soil Pollution,* 11(12), 2517.

Ho, Y. 2006. Review of second-order models for adsorption systems. *Journal of Hazardous Materials,* 136, 681-689.

Huang, S., Ras, R. H. S. & Tian, X. 2018. Antifouling membranes for oily wastewater treatment: Interplay between wetting and membrane fouling. *Current Opinion in Colloid and Interface Science,* 36, 90-109.

Humbatova, S. I. & Hajiyev, N. Q.O. 2019. Oil factor in economic development. *Energies,* 12(8), 1573.

Ismail, M. S., Yahya, M. D., Auta, M. & Obayomi, K. S. 2022. Facile preparation of amine - functionalized corn husk derived activated carbon for effective removal of selected heavy metals from battery recycling wastewater. *Heliyon,* 8(5).

Izevbekhai, O. U., Gitari, M. W., Tavengwa, N., Ayinde, W. B. & Mudzielwana, R. 2020. Application of synthesized acetylated silica in the remediation of oily wastewater. *Journal of Taibah University for Science,* 14, 1033-1041.

Jamaly, S., Giwa, A & Hasan, S. W. 2015. Recent improvements in oily wastewater treatment: Progress, challenges, and future opportunities. *Journal of environmental sciences*, *37*, 15-30.

Kadir, S., Matali, S., Mohamad, N. F. & Rani, N. H. 2014. Preparation of activated carbon from oil palm empty fruit bunch (EFB) by stem activation using response surface methodology *international journal of Materials Science and Applications,* 3, 159-163.

kehinde, T. J. 2012. *Treatment of oilfield produced water with dissolved air flotation.* Master of Applied Science, Dalhousie University.

Li, M., Kuang, S., Kang, Y., Ma, H., Dong, J. & Guo, Z. 2022. Recent advances in application of iron-manganese oxide nanomaterials for removal of heavy metals in the aquatic environment. *Science of the Total Environment,* 819, 153157.

Li, Z., Wang, B., Qin, X., Wang, Y., Liu, Q., Shao, Q., Wang, N., Zhang, J., and, W. Z. & C., S. 2018. Superhydrophobic/superoleophilic polycarbonate/ carbon nanotubes porous monolith for selective oil adsorption from water. *ACS Sustainable Chemistry and Engineering,* 6, 13747-13755.

Lim, A., Chew, J. J., Ngu, L. H., Ismadji, S., Khaerudini, D. S. & Sunarso, J. 2020. Synthesis, characterization, adsorption isotherm, and kinetic study of oil palm trunk-derived activated carbon for tannin removal from aqueous solution. *American Chemical Society OMEGA,* 5, 28673-28683.

Makisha, N. 2020. Research of oily wastewater treatment by means of membrane methods. In IOP Conference Series: *Earth and Environmental Science,* 459(4), 042015.

Mohammed, D. & Tanweer, A. 2018. A review on utilization of wood biomass as a sustainable precursor for activated carbon production and application. *Renewable and Sustainable Energy Reviews,* 87, 1-21.

Moreira, F. C., Boaventura, R. A. R., Brillas, E. & Vilar, V. J. P. 2017. Electrochemical advanced oxidation processes: A review on their application to synthetic and real wastewaters. *Applied Catalysis B: Environmental,* 202, 217-261.

Mudzielwana, R., Gitari, M. W., Akinyemi, S. A. & Msagati, T. A. 2018. Performance of Mn 2+-modified bentonite clay for the removal of fluoride from aqueous solution *South African Journal of Chemistry,* 71, 15-23.

Munzhelele, E. P., Ayinde, W. B., Mudzielwana, R. & Gitari, W. M. 2021. Synthesis of fe doped poly p-phenylenediamine composite: Co-adsorption application on toxic metal ions (f− and as3+) and microbial disinfection in aqueous solution. *Toxics,* 9(4), 74.

Najaa Syuhada, M. T., Rozidaini, M. G. & Norhisyam, I. 2017. Response surface methodology optimization of oil removal using banana peel as biosorbent. *Malaysian Journal of Analytical Sciences,* 21, 1101-1110.

Rashid, J., Tehreem, F., Rehman, A. & Kumar, R. 2019. Synthesis using natural functionalization of activated carbon from pumpkin peels for decolourization of aqueous methylene blue. *Science of the Total Environment,* 671, 369-376.

Sohaimi, K. S. A., Ngadi, N., Mat, H., Inuwa, I. M. & Wong, S. 2017. Synthesis, characterization and application of textile sludge biochars for oil removal. *Journal of Environmental Chemical Engineering,* 5, 122-135.

Syuhada, N., Mohd Ghazi, R. & Ismail, N. 2017. Response surface methodology optimization of oil removal using banana peel as biosorbent. *Malaysian Journal of Analytical Science.,* 21, 1101-1110.

Weber, W. J. & Morris, J. C. 1963. Kinetics of adsorption on carbon from solution. *Journal of the Sanitary Engineering Division,* 81, 31-59.

Yang, L., May, P. W., Yin, L., Smith, J. A. & Rosser, K. N. 2007. Ultra fine carbon nitride nanocrystals synthesized by laser ablation in liquid solution. *Journal of Nanoparticle Research,* 9, 1181-1185.

Zhang, J., Xu, H., Guo, J., Chen, T. & Liu, H. 2020. Superhydrophobic polypyrrole-coated cigarette filters for effective oil/water separation. *Applied Sciences,* 10, 1985.

Zhao, C., Zhou, J., Yan, Y. a., Yang, L., Xing, G., Li, H., Wu, P., Wang, M. & H, Z. 2020. Application of coagulation/flocculation in oily wastewater treatment: A review. *Science of the Total Environment,* 765, 142795.

Zhao, M. Q., Huang, J. Q., Zhang, Q., Luo, W. L. & Wei, F. 2011. Improvement of oil adsorption performance by a sponge-like natural vermiculite-carbon nanotube hybrid. *Applied Clay Science* 53, 1-7.

Chapter 6: Conclusions and Recommendations

6.1. Conclusion

The aim of this study is to synthesize acid-leached diatomaceous-amine-functionalized activated carbon composite adsorbent for application in treatment of oily wastewater.

The specific objectives were:

- To prepare and characterize acid-leached diatomaceous earth for application in treatment of oily wastewater.
- To prepare and characterize amine-functionalized macadamia nutshell-derived activated carbon for the treatment of oily wastewater.
- To prepare and Characterize acid leached diatomaceous earth and amine-functionalized activated carbon composite adsorbent for application in treatment of oily wastewater and further evaluate the regeneration potential of the synthesized composite.

Below are the major conclusions drawn from the study based on the specific objectives of the study.

In terms of the first objective, it was found that acid activation of the raw diatomaceous earth successfully removed impurities and this was affirmed by an increase in the silica content coupled with a decrease in the amount of the carbonates and clay minerals. The removal of impurities led to improved pore characteristics and adsorption capacity of the acid-leached diatomaceous earth. Furthermore, results of the oil removal experimental revealed that acid-leached diatomaceous earth is a promising adsorbent for the treatment of oily wastewater.

As for the second objective, it was found that activated carbon can be extracted from macadamia nutshells. Furthermore, the macadamia nutshell-based activated carbon was successfully modified with hydroxylamine hydrochloride and evaluated for its effectiveness towards oil removal. It was found that the amine-functionalized activated carbon had high oil removal efficiency and high adsorption capacity. The results reported herein showed that the amine-functionalized activated carbon has the potential to be used as an adsorbent for the removal of oil from oily wastewater.

The third objective was addressed by blending synthesized acid-leached diatomaceous earth with amine-functionalized activated carbon to produce a composite adsorbent that is capable of treating wastewater. As part of the study, the regeneration potential of this composite

adsorbent was evaluated. It was noted that the adsorption capacity and oil removal efficiency when the acid-leached diatomaceous earth was coupled to amine-functionalized activated carbon. The recyclability part of the study showed that the composite adsorbent can be generated up to 5 times thus making the use of this adsorbent economically feasible. Most importantly, this study shows that adsorbents have potential to be applied in the remediation of oily wastewater treatment and removal of oil from water bodies.

6.2. Recommendations for future work

Based on the conclusions drawn from this study, the following recommendations are made for future studies:

- Test the feasibility of adsorbent in field applications
- Conduct the cost benefit analysis for the composite adsorbent.
- Assess the chemical stability of the material.